Broadening and Shift of Spectral Lines Due to the Presence of Foreign Gases*

SHANG-YI CH'EN† AND MAKOTO TAKEO‡

Department of Physics, University of Oregon, Eugene, Oregon

TABLE OF CONTENTS

I. INTRODUCTION

THE modification of the spectral lines of an emitting or absorbing particle due to collisions with other particles as exhibited by broadening, shift, asymmetry, and the occasional appearance of certain diffuse bands, has opened up a new way to study the perturbations of energy levels. The variation of interatomic and intermolecular forces as a function of interatomic distance as determined from these effects has been increasingly attracting the attention not only of theoretical and experimental physicists but also of those who are working on certain basic problems of chemistry, genetics and astrophysics.

The first review article on the causes of broadening of spectral lines was written by Weisskopf[1] in 1933. Margenau and Watson[2] made an extensive review of the theories and experimental observations on the pressure effects on spectral lines developed up to 1936. Schulz,[3] Budini,[4] and Unsöld[5] wrote corresponding reviews in later years. There has been a very considerable amount of work done within the past thirteen years, both theoretical and experimental, and the need of another review is quite obvious.

* Supported by the National Science Foundation, NSF-G1872.
† In memory of his father, T. W. Ch'en, July, 1884–July 20, 1956.
‡ Formerly at Department of Physics, Defense Academy, Yokosuka, Japan; now at Physics Department, Portland State College, Portland, Oregon.

[1] V. Weisskopf, Physik. Z. **34**, 1 (1933).
[2] H. Margenau and W. W. Watson, Revs. Modern Phys. **8**, 22 (1936).
[3] P. Schulz, Physik. Z. **39**, 412 (1938).
[4] P. Budini, Nuovo cimento **16**, 86 (1939).
[5] A. Unsöld, Vjschr. Astron. Ges. **78**, 213 (1943).

This review article is intended to constitute a sequel to Margenau and Watson's article, to bring it up to 1956. To restrict the length of this paper, only pressure effects due to neutral particles are discussed. The effects of electron and ion collisions, high-temperature broadening, and, consequently, observations with shock waves are postponed for consideration in a separate review. The modification of both atomic and molecular spectral lines in the visible, ultraviolet, infrared, and microwave regions is discussed. In Chapter III, the materials of Secs. B and C are purposely given separately from Sec. A for emphasis. During the course of the preparation of this article, Sobel'man and Robin and Robin[6] gave a review of the theories and a bibliography of the pressure broadening of atomic lines respectively. The present article is an entirely independent review covering also molecular lines and includes a review of experimental observations.

II. THEORY

Since Lorentz presented his theoretical treatment[7] of the problem of the broadening of spectral lines in 1906, a number of different approaches have appeared. The relations between them are sometimes difficult to see and it is not always clear whether they describe the same effect. It may be, therefore, of interest to review these treatments. However, those appearing in the review article published by Margenau and Watson[2] are mainly excluded.

A. CAUSES PRODUCING BROADENING AND SHIFT OF SPECTRAL LINES

Every influence on a radiating or absorbing atom (or molecule) affects its spectral lines in one way or another. The effect of its own thermal motion, which broadens the lines statistically, is known as the Doppler effect.[8,9] In the case of emission or resonance absorption the process of radiation damping,[9] or a finite width of each of the two energy levels associated with spectral lines, is responsible for the natural width.[10] If the atom (or molecule) is in a gas of the same or of different kind, the spectral lines are broadened and sometimes are shifted with asymmetry of the line shape. The line broadening due to the first two effects is independent of pressure, while that due to the last effect (pressure effect) depends on the density of the gas and is, under ordinary experimental conditions where the pressure is more than a few cm of Hg, much larger than the first two effects in the visible down to the microwave region. Therefore, the Doppler and radiation damping effects on line shapes will be entirely neglected in this discussion,[11] although for emission spectra in flames the Doppler effect should be added.[12]

The radiating or absorbing atom (or molecule) in a gas is exposed to the interaction with surrounding atoms (or molecules) which are moving under thermal motion. The essential cause of line broadening lies in the finite difference of interaction energies of the radiating atom (or molecule), in the initial and final states involved in the radiation process, with a colliding atom (or molecule). It is usually not easy to find the interaction energy over the whole range of the distance, including excited states. Thus, it is sometimes necessary to use the approximate Lennard-Jones potential energy,

$$V=-\alpha R^{-6}+\beta R^{-12},$$

which has been found to be useful in the kinetic theory of gases. When a more detailed discussion is required, the potential energy of the classical electrostatic interaction between atoms or molecules is expanded in a series in R^{-1}. This is equivalent to the procedure of expanding the two charge distributions in terms of the electric multipole moments in the expression of the electrostatic interaction. However, in this expansion care must be taken to determine whether or not the two charges overlap. Otherwise, the resulting expansion in series may diverge for all R.[13]

Referring to the coordinate systems, x_i, y_i, z_i, and x_j, y_j, z_j parallel to each other with z_i and z_j in the direction of R and with the origin at the nuclei of each charge distribution i or j, $V(R)$ is given by[14]

$$\begin{aligned}V(R)\sim&-\frac{1}{R^3}\sum_{ij}e_ie_j[2z_iz_j-x_ix_j-y_iy_j]\\&+\frac{3}{2}\frac{1}{R^4}\sum_{ij}e_ie_j[r_i^2z_j-z_ir_j^2\\&+(2x_ix_j+2y_iy_j-3z_iz_j)(z_i-z_j)]\\&+\frac{3}{4}\frac{1}{R^5}\sum_{ij}e_ie_j[r_i^2r_j^2-5z_i^2r_j^2-5r_i^2z_j^2\\&-15z_i^2z_j^2+2(4z_iz_j+x_ix_j+y_iy_j)^2]+\cdots\end{aligned}\quad(1)$$

for electrically neutral and tightly bound charge distributions at a large distance $R(R>r_i+r_j)$. If the two charges overlap, the integral over the charge distribution should be cut off at the distance where the two charges start to overlap, in order to obtain a convergent potential for all R.

---

[6] I. I. Sobel'man, Uspekhi Fiz. Nauk **54**, 551 (1954); S. Robin and J. Robin, J. phys. radium **17**, 143 (1956).
[7] H. A. Lorentz, Proc. Acad. Sci. Amsterdam **8**, 591 (1906).
[8] L. G. Henyey, Proc. Natl. Acad. Sci. **26**, 50 (1940).
[9] D. G. Kendall, Z. Astrophys. **16**, 308 (1938).
[10] V. Weisskopf and E. W. Wigner, Z. Physik **63**, 54 (1930); **65**, 18 (1931); F. Hoyt, Phys. Rev. **36**, 860 (1931); L. Spitzer, Jr., Phys. Rev. **55**, 361 (1939); Physica **7**, 133 (1940); E. Arnous and W. Heitler, Proc. Roy. Soc. (London) **A220**, 290 (1953).
[11] However, in the microwave region at a low pressure the Doppler effect will bother. Reduction of this effect in observations has been studied by M. W. P. Strandberg and H. Dreicer, Phys. Rev. **94**, 1393 (1954).
[12] S. S. Penner and R. W. Kavanagh, J. Opt. Soc. Am. **43**, 385 (1953); L. Huldt and E. Knall, Z. Naturforsch. **9a**, 663 (1954).
[13] F. C. Brooks, Phys. Rev. **86**, 92 (1952).
[14] H. Margenau, Phys. Rev. **38**, 747 (1931).

The recently developed expansion[15] of $V(R)$ has made it possible to systematize and simplify the study of the interaction of complex charge distributions even when they overlap. The expansion of $V(R)$ is in terms of spherical harmonics $Y_\lambda{}^\mu(\theta,\phi)$ corresponding to multipole moments of the charge distributions. If one refers to a spherical coordinate system with origin at the center of mass and the polar coordinate in the direction of R, the coordinates of charges e_i, belonging to one atom or molecule, are (r_i,θ_i,ϕ_i) and those of charges e_j, belonging to the other, are (r_j,θ_j,ϕ_j). For no overlapping of charge distributions, i.e., $R>r_i+r_j$, Carlson and Rushbrooke[15] gave the following expansion:

$$V(R)=\sum_{ij} e_ie_j \sum_{\lambda=0}^{\infty}\sum_{\lambda'=0}^{\infty} \frac{r_i{}^\lambda r_j{}^{\lambda'}}{R^{\lambda+\lambda'+1}} \frac{(-1)^{\lambda_L}4\pi(\lambda+\lambda')!}{[(2\lambda+1)(2\lambda'+1)]^{\frac{1}{2}}} \times \sum_{\mu=-\lambda_L}^{\mu=+\lambda_L} \frac{y_\lambda{}^\mu(\theta_i,\phi_i)y_{\lambda'}{}^{-\mu}(\theta_j,\phi_j)}{[(\lambda+\mu)!(\lambda-\mu)!(\lambda'+\mu)!(\lambda'-\mu)!]^{\frac{1}{2}}}. \quad (1')$$

Here λ_L is the lesser of λ and λ'. Buehler and Hirschfelder[15] have obtained the rather complicated expression for the case when the two charges overlap each other. Since this type of mathematical approach includes every case of charge distributions in a convergent form, it is of great value in the evaluation of Coulombic integrals in the quantum-mechanical treatment of short-range intermolecular forces.

The potential (1) or (1′) is considered as a perturbation upon the system and perturbation theory or the variational method may be employed to evaluate the resultant shift in energy levels, which is identified with the potential energy of the intermolecular force. If ions are not considered,[16] V starts with $1/R^3$ as in Eq. (1) in the approximation[17] of separate electronic, nuclear, and molecular motions. At low pressures (average R large), the predominant part of the interaction arises from the term of lowest power, and other higher terms may be neglected. On the other hand, at close distances interaction energies are quite complicated and will not be discussed here, although they are quite important.

In the discussion of long-range van der Waals' forces it is customary to consider four types of forces: (i) electrostatic forces such as those between electric dipoles, (ii) induction forces such as those between a polarizable nonpolar molecule, and an electric dipole, (iii) dispersion forces such as those between nonpolar molecules, and (iv) resonance forces realized by exchanges of excitation energy between molecules of the same kind. In the following paragraphs, however, the types of forces discussed in the several cases are only the more important ones.

1. Interaction between Atoms

a. Resonance Interaction between Identical Atoms

This is characteristic of the case when the interacting atoms, one of which is excited, are identical. Since they are identical, they can exchange the excitation energy (light quantum) with one another.[2,18] This resonance introduces twofold degeneracy (symmetric§ and antisymmetric) and a term,

$$V_{\rm res}=\gamma(e^2\hbar f_{0n}/4\pi m_e\omega_0)\frac{1}{R^3}, \quad (2)$$

in the interaction energy. The numerical factor γ takes the value -2 if the magnetic quantum number m of the excited atom is 0, 1 if $m=\pm1$. f_{0n} is the oscillator strength corresponding to the transition from the normal to the excited state n, ω_0 the angular frequency of the spectra line concerned, and m_e the electronic mass. This term is not additive,[2,19,20] which makes it difficult to calculate in the case of high pressure where multiple interactions are involved, and has not been treated rigorously, although various[21] attempts have been made. However, according to the sum rule, the average of the interaction energy over all states of different m's is zero. The root mean square value over magnetic quantum numbers m in the J representation for a binary case was given by Foley[22] to show its J dependence, but Eq. (2) will be in error for the case when multiplet separation is comparable or less than the perturbation energy.

It is easy to see how the resonance effect affects the radiation process.[23] When an excited atom passes by an unexcited atom of the same kind, there must be a finite probability that the energy of excitation will be transferred from the first to the second atom, without the intervention of radiation. This results in a reduction

[15] C. Carlson and G. S. Rushbrooke, Proc. Cambridge Phil. Soc. **46**, 626 (1950); R. J. Buehler and J. O. Hirschfelder, Phys. Rev. **83**, 628 (1951); **85**, 149 (1952).

[16] Stark effect broadening of spectral lines due to ions, and dipole and quadrupole gases are considered by H. Holtsmark, reference 69; M. Born, *Optik* (Verlag Julius Springer, Berlin, 1933), p. 444; R. Rompe and P. Schultz, Z. Physik **119**, 269 (1941); S. L. Mandelshtam and N. N. Sololev, J. Exptl. Theoret. Phys. **20**, 323 (1950); I. I. Sobel'man and L. A. Vainshtein, Doklady, Akad. Nauk S.S.S.R. **90**, No. 5, 757 (1953); and by E. F. M. v.d. Held, Z. Physik **70**, 508 (1931). Also see, for instance, reference 94, and R. G. Breene, Jr., Revs. Modern Phys. **29**, 96 (1957), Chap. II.

[17] Hirschfelder, Curtiss, and Bird, *Molecular Theory of Gases and Liquids* (John Wiley and Sons, Inc., New York, 1954), p. 920.

[18] G. W. King and J. H. Van Vleck, Phys. Rev. **55**, 1165 (1939).

§ Only the symmetric states with respect to the exchange of the atoms can combine optically with ground states.

[19] For information on the nonadditivity in first-order interactions for three helium atoms, see P. Rosen, J. Chem. Phys. **21**, 1007 (1953).

[20] H. Margenau, Revs. Modern Phys. **11**, 1 (1939).

[21] J. Holtsmark, Z. Physik **34**, 722 (1925); J. Frenkel, Z. Physik **59**, 198 (1930); L. Mensing, Z. Physik **61**, 655 (1930).

[22] H. M. Foley and D. M. Dennison, Phys. Rev. **61**, 386 (1942); H. M. Foley, Phys. Rev. **69**, 616 (1946).

[23] W. Furssow and A. Wlassow, Physik. Z. Sowjetunion **10**, 379 (1936); W. V. Houston, Phys. Rev. **54**, 884 (1938). Also see R. G. Breene, Jr., Revs. Modern Phys. **29**, 122 (1957), Chap. V.

of the lifetime of the excited atom and a corresponding broadening of the line emitted.

b. *Dispersion Interaction*

The charge distribution of atoms in the ground states is usually nondegenerate with respect to parity, without electric dipole moments.[24] Thus, the first-order dipole-dipole interaction vanishes as does the term $1/R^3$ in Eq. (1). This is true in the system of identical atoms in the ground states or of atoms of different kind. The second order perturbation theory gives the asymptotic potential energy[20] between two atoms in the states k and l as,

$$V_{\rm dis}=-\frac{1}{R^6}\frac{3}{2m_e^2}(\hbar e)^4 \sum_{(k\neq k',l\neq l')}^{k'l'} \times\frac{f_{kk'}f_{ll'}}{(E_{k'}-E_k)(F_{l'}-F_l)(E_{k'}+F_{l'}-E_k-E_l)} +0\left(\frac{1}{R^8}\right), \quad (3)$$

where $f_{kk'}$ is the oscillator strength corresponding to the transition kk' for the first atom, $f_{ll'}$ for the second. The E's and F's are the energies of the various states for the two atoms, respectively. It must be noted that the calculation was done by neglecting the electron-exchange effect, by assuming that atoms are non-degenerate, that they are quite far away from one another, and that their wave functions do not overlap. This last assumption clearly allows the additiveness[25] of the force. As will be seen easily, the value of Eq. (3) is usually negative, and numerically much larger for the excited state than for the ground state, except for the highly excited states. The defect of Eq. (3) is, however, that it requires a knowledge of every energy level of the atoms concerned, which is hard to obtain. The previous calculations were improved by Buckingham,[20,26] who applied the variational method to the ground states, made use of wave functions obtained by the method of self-consistent fields, and included the effect of electron exchange. This result provides a method for obtaining the dispersion energy from the observed polarizabilities α_1 and α_2 of the two atoms with N_1 and N_2 electrons, respectively:

$$V_{\rm dis}=-\frac{3}{2}\frac{a_0^{\frac{1}{2}}e^2}{R^6}\frac{\alpha_1\alpha_2}{(\alpha_1/N_1)^{\frac{1}{2}}+(\alpha_2/N_2)^{\frac{1}{2}}}. \quad (4)$$

a_0 is the radius of the first Bohr orbit. Massey and Burshop calculated the van der Waals constants for alkali metal-rare gas atom impact by this method and found reasonable agreement with those obtained by the molecular ray technique.[27]

The above formulas are not valid for degenerate states, which are always involved in the optical transition, although Eq. (3) may be thought of as an average over the degeneracy for such levels. Really, it is not easy to obtain the van der Waals constant for excited states and to compare the line broadening theory with observations. Recently, the authors[28] have calculated the van der Waals energy for the doublet P state and found that $^2P_{\frac{3}{2}}$ levels split according to the magnetic quantum number due to the electric quadrupole moment of the atom in the level. The ratio of magnitudes of van der Waals energies for $^2P_{\frac{3}{2}}{}^{|m|=\frac{3}{2}}$, $^2P_{\frac{3}{2}}{}^{|m|=\frac{1}{2}}$, and $^2P_{\frac{1}{2}}{}^{|m|=\frac{1}{2}}$, interacting with a spherically symmetric atom in the ground state, is 4:5:6. They claim that this split of the $^2P_{\frac{3}{2}}$ level is responsible for one aspect of fine structure pressure broadening.

Under ordinary experimental conditions, the resonance interaction can be neglected in the line broadening due to foreign gases, because the number of foreign atoms or molecules surrounding the optically active atom is far greater than the number of neighbors of its own kind.

c. *Energy State of Atoms at High Pressure*

There have been some calculations on the ground state of atoms under high pressure using as a model an atom enclosed in a box of a certain size which corresponds uniquely to the pressure.[29]

The present authors[28] applied perturbation theory to this model for the case of an alkali atom compressed by rare gas atoms and obtained the energy corresponding to the isolated nth state.

$$E=W_n+(n|V|n) +\sum_j{}' (n|V|j)(j|V|n)/(W_n-W_j), \quad (5)$$

where W_n is the eigenvalue of the unperturbed nth state. $\sum_j{}'$ implies the exclusion of the term $j=n$ from the summation. The matrix element is

$$(n,l,m,s|V|n',l',m',s') =\begin{cases}\alpha\displaystyle\int_{r_0}^{\infty}R_{nl}^*(r)R_{n'l}(r)r^2dr, & \text{if } l=l',\ m=m',\ s=s',\\ 0, & \text{otherwise,}\end{cases}$$

[24] L. I. Schiff, *Quantum Mechanics* (McGraw-Hill Book Company, Inc., New York, 1949), p. 158.

[25] Even though the wave functions do not overlap, the third-order energy is not additive. See B. M. Axilrod and E. Teller, J. Chem. Phys. **11**, 299 (1943); B. M. Axilrod, J. Chem. Phys. **17**, 1349 (1949); **19**, 719 (1951); **19**, 724 (1951).

[26] R. A. Buckingham, Proc. Roy. Soc. (London) **A160**, 113 (1937); Proc. Roy. Irish Acad. **45**, 31 (1938).

[27] N. S. W. Massey and R. H. S. Burshop, *Electronic and Ionic Impact Phenomena* (Clarendon Press, Oxford, 1952), p. 375.

[28] M. Takeo and S. Y. Ch'en, Phys. Rev. **93**, 420 (1954).

[29] Michels, deBoer, and Bijl, Physica **4**, 981 (1937); A. Sommerfeld and H. Welker, Ann. Physik (5) **32**, 56 (1938); S. R. deGroot and G. A. tenSeldam, Physica **12**, 669 (1946); **18**, 891, 905, and 909 (1952); T. L. Cottrell, Trans. Faradary Soc. **47**, 337 (1951).

where α stands for the dimension: $\alpha=1$ in atomic units of energy, decided upon by a comparison of the above calculation with the exact calculated value[29] for hydrogen. $R_{n1}(r)$ is the radial part of the wave function. r_0 is the radius of the sphere. The energy increases with decreasing r_0. The energy change is greater for the excited state than for the ground state at the same r_0. Since the pressure is given by $p=-dE/(4\pi r_0^2 dr)$, the corresponding hydrostatic pressure on the atom is easily calculated.

2. Interaction between Molecules

In order for an interaction to be effective for line broadening, the perturbation must be different for two levels in radiative transition. Any vibrational or rotational levels belonging to a specified electronic level have nearly the same second-order dispersion forces. Thus, in molecular spectra, the effect of dispersion forces can be neglected in many cases. Furthermore, it often happens that the separation of successive rotational levels is smaller than the thermal energy. For this reason, it must be noted that the ordinary second-order perturbation theory cannot be used in some cases.

Since molecules have more internal degrees of freedom than atoms, the calculation of multiple interactions is quite difficult. The following discussion is restricted to the binary interaction. Recently, however, Matossi[30] calculated the multiple interaction of identical polar molecules by considering the problem as the coupling of oscillators with essentially the same eigenfrequency ω_0 after the method of Holtsmark[21] for the atomic case. He showed that the multiple interaction gives rise to a splitting of the frequencies by an amount which depends on the distance and the orientation of the oscillating dipoles, thus resulting in distributed frequencies which can be considered as equivalent to line broadening. With a doubtful assumption that the frequencies are distributed according to the Gaussian error curve, he obtained a result that the half-width at half-intensity of the distributed frequencies is given by

$$\frac{1.18}{24\pi^{\frac{3}{2}}c^2}(8)^{\frac{1}{2}}\frac{\epsilon_e^2 N^{\frac{1}{2}}}{m r_0^{\frac{3}{2}}\omega_0}\ \text{cm}^{-1},$$

where r_0 is the molecular diameter, c the velocity of light, m the reduced mass of the molecules, ϵ_e the effective charge defined as the ratio of dipole moment to atomic distance, and N the number density of the molecules. This $\sqrt{N}$ dependence of half-width was used to explain several experimental results,[31] especially those for the infrared absorption of water.[32]

[30] F. Matossi, Phys. Rev. **76**, 1845 (1948).
[31] B. Trumpy, Z. Physik **34**, 715 (1925); **40**, 594 (1927); Hosche, Polanyi, and Vogt, Z. Physik **41**, 587 (1927).
[32] W. M. Elsasser, Harvard Meteorol. Stud. No. 6 (1942), p. 46; F. Matossi and E. Rauscher, Z. Physik **125**, 418 (1949).

a. Interaction between Symmetric Top Molecules (NH_3, PH_3, CH_3Cl, CHF_3, CH_3F, PF_3, CF_3Cl, $CHBr_3$ etc.)

The intermolecular forces (electrostatic) between symmetric top molecules carrying a permanent electric dipole μ along their figure axis can be easily obtained by using the expansion (1). Assuming the two molecules in the rotational states J (total angular momentum), M (equatorial), K (symmetric top molecule quantum number), and J', M', K', respectively, we find the required matrix elements[33] are

$$(J,K,M|\cos\theta|J,K,M)=KM/[J(J+1)],$$
$$(J,K,M|\sin\theta e^{\pm i\phi}|J,K,M\pm1)$$
$$=\mp K/[J(J+1)]\cdot[(J\pm M+1)(J\mp M)]^{\frac{1}{2}}. \quad (6)$$

Then, the formula (1) leads, in its asymptotic form,[34] to

$$(J,K,M_jJ',K',M_j'|V_{\text{st}}|J,K,M_i,J',K',M_i')$$
$$=\frac{\mu\mu'}{R^3}\frac{KK'}{J(J+1)J'(J'+1)}$$
$$\times[-2M_iM_i'\delta(M_j,M_i)\delta(M_j',M_i')$$
$$+\tfrac{1}{2}\{(J-M_i+1)(J+M_i)(J'-M_i')$$
$$\times(J'+M_i'+1)\}^{\frac{1}{2}}\delta(M_j,M_i-1)\delta(M_j',M_i'+1)$$
$$+\tfrac{1}{2}\{(J+M_i+1)(J-M_i)(J'+M_i')$$
$$\times(J'-M_i'+1)\}^{\frac{1}{2}}\delta(M_j,M_i+1)\delta(M_j',M_i'-1)]. \quad (7)$$

Again, the sum rule shows that the average value over i and j vanishes. The mean absolute value may be approximated by its root-mean-square value,[34]

$$\langle V_{\text{st}}^2\rangle^{\frac{1}{2}}(J,K;J',K')$$
$$=\left(\frac{2}{3}\right)^{\frac{1}{2}}\frac{KK'}{[J(J+1)J'(J'+1)]^{\frac{1}{2}}}\frac{\mu\mu'}{R^3}. \quad (8)$$

This can be used for two molecules of the same or different kind.

Since the selection rule for optical transition is $\Delta J=\pm1$, a molecule in the rotational state J shows, in addition to the above, a resonance interaction with another identical molecule with $J'=J\pm1$, in whatever vibrational states they may be. It must be noted that both the initial and final levels of an optical transition undergoes resonance if the above condition is satisfied. The calculation of this interaction requires the matrix elements,[33]

[33] R. De L. Kronig and I. Rabi, Phys. Rev. **29**, 262 (1927).
[34] H. Margenau and D. J. Warren, Phys. Rev. **51**, 748 (1937).

$$
\begin{aligned}
&(J,K,M|\cos\theta|J+1,K,M)\\
&\quad=\{[(J+1)^2-K^2][(J+1)^2-M^2]\}^{\frac{1}{2}}/\\
&\qquad\qquad\{(J+1)[(2J+1)(2J+3)]^{\frac{1}{2}}\},\\
&(J,K,M|\cos\theta|J-1,K,M)\\
&\quad=-[(J^2-K^2)(J^2-M^2)]^{\frac{1}{2}}/\\
&\qquad\qquad\{J[2J-1)(2J+1)]^{\frac{1}{2}}\},\\
&(J,K,M|\sin\theta e^{\pm i\phi}|J+1,K,M\pm1)\\
&\quad=\{[(J+1)^2-K^2](J\pm M+1)(J\pm M+2)\}^{\frac{1}{2}}/\\
&\qquad\qquad\{(J+1)[(2J+1)(2J+3)]^{\frac{1}{2}}\},\\
&(J,K,M|\sin\theta e^{\pm i\phi}|J-1,K,M\pm1)\\
&\quad=\{(J^2-K^2)(J\mp M+1)(J\mp M)\}^{\frac{1}{2}}/\\
&\qquad\qquad\{J[(2J-1)(2J+1)]^{\frac{1}{2}}\}.
\end{aligned}
\tag{9}
$$

From Eq. (1) the resonance energy between the molecule with J and $J-1$, respectively, is then given by

$$
\begin{aligned}
&V_{\rm res}(J\to J-1)\\
&=\pm\frac{\{(J^2-K^2)(J^2-K'^2)\}^{\frac{1}{2}}}{J^2(2J-1)(2J+1)}[\{(J-M+1)(J-M)\\
&\quad\times(J-M')(J+1-M')\}^{\frac{1}{2}}\delta(M,M+1)\\
&\quad\times\delta(M',M'-1)+\{(J+M+1)(J+M)\\
&\quad\times(J+M')(J+1+M')\}^{\frac{1}{2}}\delta(M,M-1)\\
&\quad\times\delta(M',M'+1)-2[(J^2-M^2)(J^2-M'^2)^{\frac{1}{2}}\\
&\qquad\qquad\times\delta(M,M)\delta(M',M')].
\end{aligned}
\tag{10}
$$

The average value vanishes. Its root-mean-square value,

$$
\langle V_{\rm res}^2\rangle^{\frac{1}{2}}(J,K;J-1,K')=\left(\frac{2}{3}\right)^{\frac{1}{2}}\frac{\{(J^2-K^2)(J^2-K'^2)\}^{\frac{1}{2}}}{J\{(2J-1)(2J+1)\}^{\frac{1}{2}}}\frac{\mu^2}{R^3},
\tag{11}
$$

may be used as the average value. The resonance interaction energy between the two molecules with J and $J+1$ is obtained by replacing J by $J+1$ in these expressions.

Vibrational resonances may be neglected in microwave spectra because few vibrationally excited molecules are present. If second-order effects are negligible, the interaction energy between symmetric tops may be given, then, by the sum of the above three equations. However, the distribution of the value of J depends on the statistical energy distribution, approximately Maxwell-Boltzmann's, and molecules with J value of maximum population will encounter most frequently molecules of $J\pm1$. In some molecular lines specified by J of small population, the resonance is less effective than the nonresonance, Eq. (7). This is usually realized in the infrared line broadening such as that of HCN.

In line broadening, only interactions relating to the states which can optically combine with one another are influential. Thus, in the inversion spectrum of ammonia, which is emitted by the transition between the states $+$ and $-$, denoting the symmetry of the wave function with respect to inversion, the antisymmetrical interaction energy is most effective.[35]

b. Interaction between Linear Molecules

(i) Linear Molecules with Dipole Moment μ. (N_2O, HCN, ICl, ClCN, BrCN, ICN, OCS, etc.).—The diagonal elements of the dipole interaction vanish because the dipole is pictured as rotating about an axis perpendicular to its electric moment. Other elements are

$$
\begin{aligned}
&(JMJ'M'|V|jmj'm')\\
&\quad=(\mu\mu'/2R^3)\{A(-M)A(M')\delta(m,M-1)\\
&\qquad\times\delta(m',M'+1)+A(M)A(-M')\delta(m,M+1)\\
&\qquad\times\delta(m',M'-1)-2B(M)B(M')\\
&\qquad\qquad\times\delta(m,M)\delta(m',M')\},
\end{aligned}
\tag{12}
$$

where

$$
\begin{aligned}
A(\pm M)&=\left[\frac{(J\pm M+2)(J\pm M+1)}{(2J+3)(2J+1)}\right]^{\frac{1}{2}}\delta(j,J+1)\\
&\quad-\left[\frac{(J\mp M+1)(J\mp M)}{(2J+1)(2J-1)}\right]^{\frac{1}{2}}\delta(j,J-1),\\
B(M)&=\left[\frac{(J+M+1)(J-M+1)}{(2J+3)(2J+1)}\right]^{\frac{1}{2}}\delta(j,J+1)\\
&\quad+\left[\frac{(J+M)(J-M)}{(2J+1)(2J-1)}\right]^{\frac{1}{2}}\delta(j,J-1).
\end{aligned}
$$

These are easily obtained from Eqs. (1) and (9) by putting $K=0$.

Clearly, if the two molecules are of the same kind, the interaction becomes first order or second order according to whether there is rotational resonance or not. When a linear molecule with value J encounters another with $J\pm1$, the root-mean-square direction-averaged energy is[20]

$$
\langle V_{\rm res}^2\rangle^{\frac{1}{2}}(J\to J-1)=\left(\frac{2}{3}\right)^{\frac{1}{2}}\frac{J}{\{(2J-1)(2J+1)\}^{\frac{1}{2}}}\frac{\mu^2}{R^3}.
\tag{13}
$$

For the case $(J\to J+1)$, J is replaced by $J+1$ in this expression. For nonresonating collision, London[20,36] calculated the second-order perturbation energy. Denoting by I the moment of inertia of the molecule concerned, one finds

$$
V_{\rm dis,\,Av}=\frac{2\mu^4 I}{3\hbar^2R^6}\frac{J(J+1)+J'(J'+1)}{(J+J')(J+J'+2)(J-J'-1)(J-J'+1)}.
\tag{14}
$$

[35] H. Margenau, Phys. Rev. **76**, 1423 (1949).
[36] F. London, Z. Physik **63**, 245 (1930).

The value of this energy is positive (repulsive) or negative (attractive) according to the J' of the colliding molecule. Clearly, for $J-J'=\pm 1$ (resonance), Eq. (14) has no meaning.

The ordinary linear molecule has a moment of inertia, I, around 10^{-39} g cm^2. Thus, from $\hbar^2 J(J+1)/2I = kT$, $J\sim 20$ is most common at room temperature. The thermal energy is usually larger than the difference of successive rotational levels, $\hbar^2 J/I$, especially for lower rotational levels. In this case, where second-order perturbation theory cannot be used, London[26] applied the variational method. Since lower rotational levels are degenerate in the order of thermal energy, the first-order dipole interaction must appear even in the nonresonating case, such as the first-order Stark effect in the hydrogen atom. Hence the eigenvalue is proportional to R^{-3} instead of R^{-6} as in Eq. (14). Keeping this in mind and using the perturbation method, Mizushima[37] took for simplicity the root mean square of the matrix element (12) over M and M':

$$(JJ'|V|jj') = \left(\frac{2}{3}\right)^{\frac{1}{2}} \frac{\mu\mu'}{R^3}\{(2J+1)(2J'+1)\}^{-\frac{1}{2}} \times\{(J+1)^{\frac{1}{2}}\delta(j,J+1)+J^{\frac{1}{2}}\delta(j,J-1)\} \times\{(J'+1)^{\frac{1}{2}}\delta(j',J'+1)+J'^{\frac{1}{2}}\delta(j',J'-1)\}. \quad (15)$$

Since the rotational quantum number of most colliding molecules is very large, Eq. (15) may be approximated by

$$(JJ'|V|jj') = 3^{-\frac{1}{2}}(\mu\mu'/R^3)(2J+1)^{-\frac{1}{2}} \times\{(J+1)^{\frac{1}{2}}\delta(j,J+1)+J^{\frac{1}{2}}\delta(j,J-1)\} \times\{\delta(j',J'+1)+\delta(j',J'-1)\}. \quad (16)$$

By neglecting energy differences among unperturbed states to get the first-order energy, and considering the fact that the matrix (16) is finite since it is mostly concerned with smaller J's, the energy difference in the transition $J-1\rightarrow J$ was taken as

$$0.2\mu\mu'/JR^3, \quad (17)$$

averaged over J'. But the neglect of the diagonal terms might be very serious, especially for molecules with very small I, in which case the spacing of rotational levels would be rather large. This thermal effect, however, suggests that the R^{-6} law, Eq. (14), goes over to the R^{-3} law, Eq. (17), for small R and, consequently, produces large interactions in the lower rotational levels.

(*ii*) *Nonpolar Linear Molecules.* (O_2, N_2, CO_2, CS_2, *etc.*).—In the interaction between nonpolar molecues, the quadrupole moment interaction may be important in addition to the rotational resonance, if possible, and London's dispersion. This term corresponds to the third one in the expansion (1). The diagonal matrix element is[38]

$$V_{QQ} = \frac{6}{R^5}QQ'[\{K(K+1)-3M^2\}/(2K+3)(2K-1)] \cdot[\{K'(K'+1)-3M'^2\}/(2K'+3)(2K'-1)], \quad (18)$$

where Q is the quadrupole moment.

If a mo.ecule such as oxygen is considered, Eq. (18) must be revised. Since the electronic ground state of the oxygen molecule is $^3\Sigma$, it has three states, $J=K+1$, K, $K-1$, for each K except for $K=0$ and 1. Using the wave function[39] for these states of oxygen, one obtains the diagonal elements. The factor which comes from one molecule is

$$K\{(K+1)(K+2)-3M^2\}/\{(2K+1)(K+1)(2K+3)\} \quad \text{for} \quad J=K+1, \quad (19)$$

$$\{K(K+1)-3\}\{K(K+1)-3M^2\}/\{K(K+1)(2K+3)(2K-1)\} \quad \text{for} \quad J=K, \quad (20)$$

$$(K+1)\{K(K-1)-3M^2\}/\{K(2K+1)(2K-1)\} \quad \text{for} \quad J=K-1. \quad (21)$$

Again, this interaction is proportional to R^{-5}. Since the mean K is very large at room temperature, the above three terms may be replaced by a single expression,

$$(K^2-3M^2)/4K^2. \quad (22)$$

Equation (22) may be used for the colliding molecule (primed). Thus, for instance, the energy difference of the radiating molecule with K, M in the transition $K+1\rightarrow K$, perturbed by a molecule with K', M', is given by

$$\frac{6}{R^5}QQ'\{(K'^2-M'^2)/4K'^2\}\cdot\{\text{Eq. (19)–Eq. (20)}\}. \quad (23)$$

The last factor in this formula gives the K dependence. For the transition $K-1\rightarrow K$, this factor is replaced by {Eq. (21)–Eq. (20)}.

c. Interaction of a Molecule with a Polarizable Atom

This is a calculation of the induction force. Margenau[40] calculated the interaction energy between a polarizable molecule without μ and a molecule with μ to be given classically without J dependence. Suppose that an axial symmetric molecule has a dipole moment in the direction of z and a quadrupole moment Q, and a polarizable isotropic atom is at a distance R from the molecule, and in the direction θ from the z axis. The electrostatic potential at the atom is

$$U = -\frac{\mu}{R^2}\cos\theta+\frac{1}{2}\left(\frac{3\cos^2\theta-1}{R^3}\right)Q, \quad (24)$$

[37] M. Mizushima, Phys. Rev. **83**, 94 (1951); **84**, 363 (1951).

[38] F. London, Z. physik. Chem. (B) **11**, 222 (1930).

[39] E. U. Condon and G. H. Shortley, *The Theory of Atomic Spectra* (Cambridge University Press, New York, 1935), p. 76.

[40] H. Margenau, Phys. Rev. **49**, 596 (1936).

where the quadrupole moment is

$$Q=Q_{zz}-Q_{xx}=\int_{\text{mole}}\rho(z^2-x^2)dv. \tag{25}$$

The origin of coordinates must be chosen at the center of rotation of the molecule. Then, since the field at the polarizable atom is $-\Delta U$, the interaction energy is given by

$$V=-\tfrac{1}{2}\alpha(\Delta U)^2, \tag{26}$$

where α is the polarizability of the perturbing atom. The energy change will be obtained by applying perturbation theory with the wave function of the molecule. As stated before under Sec. *a*, for the inversion spectra of ammonia the antisymmetrical interaction term in Eq. (26),

$$-6\alpha\mu Q/R^7\cos^3\theta \tag{27}$$

is the most effective for the pressure broadening of the line.[41]

d. Dipole-Quadrupole Interaction

The electrostatic potential energy for an interaction between a molecule with a dipole moment μ_1 and a colliding molecule with a quadrupole moment Q_2 is given by

$$V_{\mu Q}=-\frac{3}{4}\frac{\mu_1 Q_2}{R^4}[\cos\theta_1(1-3\cos^2\theta_2)+2\cos\theta_2\sin\theta_2\sin\theta_1\cos(\phi_1-\phi_2)], \tag{28}$$

where the angles are defined in the same way as in Eq. (1′). With the above expression, Smith and Howard[42] have explained the pressure broadening of the ammonia inversion spectra by foreign nonpolar linear molecules, and determined reasonable values of their quadrupole moments. Smith, Lackner, and Volkor[43] introduced an interaction of this type in addition to the dipole-dipole interaction of Sec. *b*.1 to explain the J and T dependence of the self-pressure broadening of the linear molecules OCS and BrCN.

B. IMPACT THEORY

1. Classical Collision Damping Theory

The shape of spectral lines may be expressed by an intensity distribution function $I(\omega)$ as a function of angular frequency ω. However, in the line broadening problem it is not interesting to find the absolute intensity; rather, attention is paid to the half-width, $\Delta\omega_{\frac{1}{2}}$, intensity maximum frequency, ω_m, and asymmetry of the function associated with a natural frequency ω_0.

$I(\omega)d\omega$ is proportional to the intensity at frequency between ω and $\omega+d\omega$ withdrawn from a light wave of uniform color distribution as it passes an infinitely thin sheet of absorbing molecules. The constant of proportionality is given by the normalization condition,

$$\int_0^\infty I(\omega)d\omega=1. \tag{29}$$

$I(\omega)$ is also proportional to the intensity of emission at ω by a thin layer of the molecules under similar conditions.[2,44] The half-width $\Delta\omega_{\frac{1}{2}}$ is the entire frequency range in which $I(\omega)$ is larger than or equal to half its maximum. Thus, if $I(\omega)$ is symmetrical about its maximum frequency ω_m,

$$I(\omega_m\pm\tfrac{1}{2}\Delta\omega_{\frac{1}{2}})=\tfrac{1}{2}I(\omega_m). \tag{30}$$

Experimentally, it is customary to express ω_m in terms of the shift, $\Delta\omega=|\omega_m-\omega_0|$, of the maximum frequency of the broadened line from its natural frequency ω_0. The effect is referred to as a violet shift or red shift,[2] depending upon the sign of $\omega_m-\omega_0$.

In the case of absorption due to a thin sheet of molecules, the quantity $I(\omega)$ is proportional to the absorption coefficient α at ω and, in practice, the measurement of the line contour $I(\omega)$ itself is the determination of $\alpha=f(\omega)$.

In classical theory, the absorption process is rather obvious. The active atom is replaced by a harmonic oscillator of natural frequency ω_0. Denoting the angular frequency of the incident light wave by ω, we find the equation of motion of the oscillating charge e with mass m under the influence of an electric field $E\cos\omega t$ to be

$$m\left(\frac{d^2x}{dt^2}+\omega_0^2x\right)=eE\cos\omega t, \tag{31}$$

with solution[45]

$$x=\Re\left\{\frac{eEe^{i\omega t}}{m(\omega_0^2-\omega^2)}+C_1e^{i\omega_0 t}+C_2e^{-i\omega_0 t}\right\}. \tag{32}$$

Suppose that a collision takes place at time $t-\theta$. Then, the amplitudes C_1 and C_2 may be affected by the collision. If the collision takes place over an interval of time which is short compared to the period of the oscillation in the impressed field (adiabatic assumption),[45] the transient amplitudes C_1 and C_2 come into play only through their discontinuities at collision and may be determined by the values of x and dx/dt just after the collision. Furthermore, the collision may be assumed to be so strong that the molecule has no memory regarding its orientation or other distribution properties

[41] P. W. Anderson, Phys. Rev. **80**, 511 (1950).
[42] W. V. Smith and R. Howard, Phys. Rev. **79**, 132 (1950).
[43] Smith, Lackner, and Volkor, J. Chem. Phys. **23**, 389 (1955).
[44] J. H. Van Vleck and H. Margenau, Phys. Rev. **76**, 1211 (1949).
[45] J. H. Van Vleck and V. F. Weisskopf, Revs. Modern Phys. **17**, 227 (1945).

before collision (strong collision). This assumption led Lorentz[7] to assume, in addition, that the mean distribution of the oscillators just after collision was not polarized because of the random nature of collisions.

However, since the oscillators are imbedded in an impressed radiation field, there must be an easy direction for them to orient to after collisions and their mean distribution, given by Boltzmann statistics, should be polarized. The Hamiltonian function for this system is

$$H(t)=\frac{p^2}{2m}+\tfrac{1}{2}m(\omega_0 x)^2-exE\cos\omega t, \quad p=m\frac{dx}{dt}.$$

Then, according to Boltzmann statistics, the average value of x after collision must be given by

$$\bar{x}=\frac{\int_{-\infty}^{\infty}\int_{-\infty}^{\infty} x\exp[-H(t-\theta)/kT]dxdp}{\int_{-\infty}^{\infty}\int_{-\infty}^{\infty}\exp[-H(t-\theta)/kT]dxdp}=\frac{2Ee\cos\omega(t-\theta)}{m\omega_0^2}, \quad (33a)$$

and

$$\bar{p}=0, \quad \text{at} \quad t_0=t-\theta. \quad (33b)$$

$\bar{x}$ and $\bar{p}$ determine the values of C_1 and C_2, and, finally, give

$$x=\Re\left[\frac{eE\exp[i\omega t]}{m(\omega_0^2-\omega^2)}\left\{1-\frac{1}{2}\left(1+\frac{\omega}{\omega_0}\right)\exp[i(\omega_0-\omega)\theta]-\frac{1}{2}\left(1-\frac{\omega}{\omega_0}\right)exp[-i(\omega_0+\omega)\theta]\right\}+\frac{eE\exp[i\omega(t-\theta)]}{2m\omega_0^2}\times(\exp[i\omega_0\theta]+\exp[-i\omega_0\theta])\right].$$

This x must be averaged over θ. In the case of random collisions, the probability that the last collision having taken place before t lies in the time interval between $t-\theta-d\theta$ and $t-\theta$ is $e^{-\theta/\tau}d\theta/\tau$, τ being the mean free time. Averaging over this distribution of θ from $\theta=0$ to ∞, we find x takes the form

$$x=\Re\left[\frac{eE\,exp[i\omega t]}{m(\omega_0^2-\omega^2)}\left\{1-\frac{(\omega_0+\omega)(\omega/\omega_0^2)\tau}{2[(1/\tau)-i(\omega_0-\omega)]}+\frac{(\omega_0-\omega)(\omega/\omega_0^2)\tau}{2[(1/\tau)+i(\omega_0+\omega)]}\right\}\right]. \quad (34)$$

Writing the square-bracketed term of (35) in the form $Ee^{i\omega t}(x'-ix'')$, we obtain the absorption coefficient[46] α as a function of ω:

$$\alpha=4\pi N^a\omega ex''/c=\frac{2\pi N^a e^2}{mc}\left(\frac{\omega}{\omega_0}\right)^2\times\left(\frac{1/\tau}{(\omega_0-\omega)^2+(1/\tau^2)}+\frac{1/\tau}{(\omega_0+\omega)^2+(1/\tau^2)}\right). \quad (35)$$

This is the absorption line shape. N^a is the number density of absorbing oscillators with natural frequency ω_0. For $\omega_0-\omega\ll\omega_0$, the second term is negligibly small under ordinary conditions, as in the case of atomic spectra or of sharp lines, while in the microwave region, where the width and the frequency are sometimes comparable in order of magnitude, it cannot be overlooked. The Lorentz assumption gives the same formula except for the sign of the second term. Therefore, it predicts a zero effect at low frequency, while it is nearly the same numerically as (35) for high frequencies. If the frequency of oscillation is extremely high, the phase may oscillate rapidly during a collision and thermal equilibrium may not be created after collision. Then, the Lorentz treatment may give a correct answer.

Recently, Bruin[47] reconsidered the collision broadening theory in analogy with the network theory to represent spectral lines graphically in the complex plane.

Equation (35) can be transformed easily into a quantum-mechanical expression if one makes use of the fact that each transition $i\rightarrow j$ could be identified with a virtual classical oscillator and applies the rule (see Born,[48] p. 468) of multiplying a classical quantity e^2/m by the oscillator strength

$$f_{ij}=\frac{2m}{3\hbar e^2}\omega_{ij}|\mu_{ij}|^2.$$

Here μ_{ij} is the dipole moment matrix element related with the radiation process $i\rightarrow j$; ω_{ij} is the frequency of the radiation. If the incident radiation is weak enough to produce thermal equilibrium, the number densities of the two levels, N_i and N_j, are determined by the Boltzmann distribution law. Since Eq. (35) holds for any possible transition, true absorption or induced emission, and $\omega_{ij}=-\omega_{ji}$, one has

$$\alpha_{ij}(\omega)=\frac{4\pi(N_i^e-N_j^e)}{3\hbar c}\omega_{ij}|\mu_{ij}|^2\left(\frac{\omega}{\omega_{ij}}\right)^2\times\left(\frac{1/\tau}{(\omega_{ij}-\omega)^2+(1/\tau^2)}+\frac{1/\tau}{(\omega_{ij}+\omega)^2+(1/\tau^2)}\right), \quad (36a)$$

where the superscripts imply thermal equilibrium, and

[46] J. A. Stratton, *Electromagnetic Theory* (McGraw-Hill Book Company, Inc., New York, 1941), p. 323.

[47] F. Bruin, thesis, Amsterdam (1956).

[48] Max Born, *Optik* (Verlag Julius Springer, Berlin, 1933), p. 441.

$$N_i^e - N_j^e = N_i^e[1-\exp(-\hbar\omega_{ij}/kT)]$$
$$\simeq \begin{cases} \dfrac{\hbar\omega_{ij}}{kT} N_i^e, & \text{for microwaves.} \\ N_i^e, & \text{for the visible region.} \end{cases}$$

For plane polarized radiation, Eq. (36a) should be multiplied by 3. The transition $j \to i$ involved in Eq. (36a) corresponds to stimulated emission.

Later, Van Vleck and Margenau[44] showed explicitly that the shape of spectral lines for a classical harmonic oscillator and also a Debye slow rotator are the same in absorption and spontaneous emission,[49] provided the energy density obeys the Rayleigh-Jeans law. They showed also that the Lorentz formula is obtained by adding the work done on the molecule by the electromagnetic wave between collisions and at collision. Karplus and Schwinger[50] have given a quantum-mechanical derivation of the Van Vleck-Weisskopf absorption formula (35) and extended it to higher power levels of the exciting radiation, where transitions among the molecular states are included at a rate that is not negligible compared with the collision rate. This treatment invalidates the assumption of thermal equilibrium, although the conditions assumed hardly exist in the visible region.[1] They found that the broadening of the absorption line at high power levels is not to be attributed to any intrinsic modification of the line shape, but rather to a frequency dependent alteration of the populations of the two levels. The net rate of absorption is the difference between the rates of true absorption and stimulated emission, with the common transition probability for the two processes possessing the characteristic frequency dependence $1/[(\omega_{ij}-\omega)^2+(1/\tau^2)]$. The frequency dependence of the population difference may be written

$$\bar{\rho}_{ii} - \bar{\rho}_{jj} = \frac{1/\tau}{(1/\tau)+w}(\rho_i^e - \rho_j^e),$$

where

$$w = \frac{1}{\hbar^2}|V_{ij}|^2 \frac{1/\tau}{(\omega_{ij}-\omega)^2+(1/\tau^2)}.$$

$\bar{\rho}_{ii}$ is the mean density of the level i over the collision time θ, and ρ_i^e is that of the isolated molecule at temperature T. V_{ij} is the matrix element of the energy in the external radiation field. Denoting the electric field by $E\cos\omega t$ and the induced dipole moment by μ, one finds $V_{ij}=\mu_{ij}E$. Then, the power absorbed per unit volume is

$$P_a = \tfrac{1}{2}\omega\hbar\omega(\bar{\rho}_{ii}-\bar{\rho}_{jj})N^a,$$

where the transition probability for absorption or stimulated emission has been placed equal to $(1/2)w$, since both processes contribute equally to the rate at which radiative transitions tend to decrease the population difference. If P denotes the radiation power incident on the gas per unit time per unit area, $P=E^2c/8\pi$, c being the velocity of light. Hence,

$$P_a = \frac{4\pi\omega P}{c\hbar}|\mu_{ij}|^2 \frac{(1/\tau)(N_i^e - N_j^e)}{(\omega_{ij}-\omega)^2+(1/\tau^2)+\dfrac{8\pi P}{c\hbar^2}|\mu_{ij}|^2}. \quad (36b)$$

Thus, as P increases, the value of P_a saturates. In the limit of complete saturation one has

$$P_a = \frac{\hbar\omega}{2\tau}(N_i^e - N_j^e) \simeq \frac{\hbar^2\omega}{2\tau}\frac{\omega_{ij}N_j^e}{kT}.$$

This saturation effect, Eq. (36b), has been experimentally confirmed with ammonia in the microwave region.[51]

The half-width of the line shape may be given by

$$\Delta\omega_{\frac{1}{2}} = \frac{2}{\tau} = 2\pi\rho^2\bar{v}N \quad (37)$$

for the case of resonance absorption in Eq. (35). In this ρ is the optical collision diameter, related to the force law at collision, $\bar{v}$, the rms velocity of impact, and N the number of colliding atoms per unit volume. The line shift, in this approximation, is obviously zero. The linear dependence of the half-width on N is characteristic of this treatment. The collision mechanism replaced by the assumption of strong collision has lost the chance to include the force law precisely in the theory. However, the magnitude of the optical collision diameter corresponds to that of the intermolecular force concerned. The optical collision diameter[48] is usually greater by a factor two or three, sometimes by a factor one hundred, than the gas-kinetic one which is related to momentum transfer. (See Table III.) This discrepancy may be partly attributed to the inclusion of excited states in optical collision diameters, but it makes the theoretical treatment easier, since in such cases the flying path of perturbers is approximated by a straight line.

2. Classical Fourier Integral Theory

Assume a radiating classical oscillator with natural frequency ω_0. Although the frequency of the oscillator would be ω_0 again after completion of an adiabatic collision, the change of the oscillation during collision would be so appreciable that the phase would be quite

[49] About the line shape modified by self-absorption, if any, in emission, see R. D. Cowan and G. H. Dieke, Revs. Modern Phys. **20**, 418 (1948). Especially, in arc this effect should be taken into consideration; see H. Edels and J. D. Craggs, Proc. Phys. Soc. (London) **A64**, 562 (1951), or in flame; see Huldt and Knoll (reference 12).

[50] R. Karplus and J. Schwinger, Phys. Rev. **73**, 1020 (1948). Also, see P. I. Richards and H. S. Snyder, Phys. Rev. **73**, 269 (1948).

[51] T. A. Pond and W. F. Cannon, Phys. Rev. **72**, 121 (1947); B. Bleaney and R. P. Penrose, Proc. Phys. Soc. (London) **60**, 83 (1948); R. L. Carter and W. V. Smith, Phys. Rev. **73**, 1053 (1948); Townes, reference 179.

different from what the oscillator would have if the collision had not taken place. The phase shift of the oscillator is given by

$$\Theta=\int_{\Delta\tau}\Delta\omega(\tau)d\tau, \tag{38}$$

where $\Delta\tau$ is the collision duration and $\Delta\omega(\tau)$ the difference between the frequencies between and at collisions. Since an adiabatic collision and no change of amplitude are assumed, it may affect the radiation only through Θ, regardless of the manner by which it is produced. The strong collision assumed in the previous section is equivalent to the assumption that Θ is arbitrarily large. But a number of small phases could add up to a large phase shift and affect a spectral line. The main purpose of the modified theory described here, however, is to account for the magnitude of $\Delta\omega(\tau)$ resulting from disturbances at collision.

If the frequency of the oscillator changes with time under the influence of colliding molecules, the oscillation may be expressed by

$$x(t)=x_0\exp\left[-i\int_0^t\omega(t')dt'\right]. \tag{39}$$

The Fourier analysis of this disturbed oscillation may give information on $I(\omega)$. According to classical mechanics, the power radiated by a charge e oscillating in one direction is $(2/3)e^2c^{-3}(d^2x/dt^2)^2$. Hence, taking Fourier components of the displacement (39) and multiplying it by ω^2 to obtain acceleration, the power emitted in the spectral ω and $\omega+d\omega$ is

$$I(\omega)d\omega=\frac{e^2\omega^4}{3\pi c^3}x_0^2\left|\int_{-\infty}^{\infty}dt\times\exp\left\{-i\int_0^t\omega(t')dt'+i\omega t\right\}\right|^2d\omega. \tag{40}$$

This formula is what Weisskopf[1] obtained by the WKB method and later by many people in a more general way.[52,53]

To reduce the general formula (40) to a more comprehensive form approximations may be made. For instance, if the Lorentz view is followed, the oscillation stops completely at strong collision, and the wave train emitted is finite in its length, say, from $t=0$ to θ. Then, the limits of integration are from 0 to θ. After averaging $I(\omega)$ over the distribution of θ as before, the formula (35) is obtained, except for unimportant factors (see Born,[48] p. 437). This is true also if the recalculation is carried out by assuming the Rayleigh-Jeans law and the equipartition value for the statistical average of the square of the amplitude of a harmonic oscillator. Since there is no impressed field, the consideration of Boltzmann statistics is unnecessary.

The phase shift Θ may be supposed to operate only as a temporary interrupter of the radiation process. Although the distribution of the magnitude of Θ is continuous, Lenz,[54] Weisskopf,[1] and others[55] assumed that the effective phase shift must be greater than some critical value—unity in Weisskopf's treatment, $\pi/2$ or 1.1 in others. The Lorentz view requires that the line intensity be lowered inversely proportionally to the number of collisions per unit time; the improved view does not mean the complete stoppage of the emission of radiation, which agrees with many experiments.

Although, by critical values of effective phase shift, early investigators determined theoretically the collision diameter, the cut-off distance of the radiation process, there was no definite meaning attached to the magnitude of the effective phase shift. Reinsberg, Lindholm[56] and Foley[22] improved this point, including every magnitude of phase shift. Rewriting the formula (40), Foley obtained

$$I(\omega)=\frac{e^2\omega^4}{3\pi c^3}x_0^2\int_{-\infty}^{\infty}dt_1\int_{-\infty}^{\infty}dt_2\times\exp\left[-i\int_{t_2}^{t_1}\omega(t')dt'+i\omega(t_1-t_2)\right]. \tag{41}$$

The substitution $t_1-t_2=\tau$, $t_2=t_0$ leads to

$$I(\omega)=\frac{2e^2\omega^4}{3\pi c^3}x_0^2\Re\int_0^{\infty}d\tau\int_{-\infty}^{\infty}dt_0\times\exp\left[-i\int_{t_0}^{t_0+\tau}\omega(t')dt'+i\omega\tau\right]. \tag{42}$$

Denoting the natural frequency of the oscillator by ω_0, and putting

$$\Delta\omega(t')=\omega(t')-\omega_0,\quad \Delta\omega=\omega-\omega_0, \tag{43}$$

where $\Delta\omega$ is measured from the unshifted line maximum, we find the intensity distribution is given by

$$I(\omega)=\frac{2e^2\omega^4}{3\pi c^3}x_0^2\Re\int_0^{\infty}d\tau\int_{-\infty}^{\infty}dt_0\times\exp\left[-i\int_{t_0}^{t_0+\tau}\Delta\omega(t')dt'+i\Delta\omega\tau\right]. \tag{44}$$

This formula may be thought of as the Fourier ampli-

[52] P. W. Anderson, Phys. Rev. **76**, 647 (1949). Furthermore, the fact that most of the optical collisions take place without momentum transfer may allow this assumption.

[53] H. Margenau and R. Meyerott, Astrophys. J. **121**, 194 (1955).

[54] W. Lenz, Z. Physik **80**, 423 (1933).

[55] H. Kallman and F. London, Z. physik. Chem. **B2**, 207 (1929); H. Kuhn and F. London, Phil. Mag. (7) **18**, 983 (1934); G. Burkhardt, Z. Physik **115**, 592 (1940).

[56] C. Reinsberg, Z. Physik **111**, 95 (1938); E. Lindholm, Arkiv Mat. Astron. Fys. **28B**, 1 (1942).

tude of the function

$$\varphi(\tau)=\int_{-\infty}^{\infty}dt_0\exp\left[-i\int_{t_0}^{t_0+\tau}\Delta\omega(t')dt'\right], \quad (45)$$

which is the average value of the phase difference occurring between the time $t_0+\tau$ and t_0 over the complete interval of t_0, that is, the radiation process. Recently the general formula (44) has been used to obtain a line shape at ordinary pressures.

If we assume an adiabatic collision, only the phase shift at collision is important. Since the collision duration is infinitely short, each collision is binary and independent. Therefore, the phase difference appearing in the above integral is approximated by the sum of such phase shifts taking place in the time interval.

$$\exp\left(-i\int_{t_0}^{t_0+\tau}\Delta\omega(t')dt'\right)=\exp(-i\sum_{i=0}^{n}\Theta_i). \quad (46)$$

This must be averaged over the distribution of n. If the mean free time between random collisions is τ_0, the probability that n collisions take place in the interval τ is $(\tau/\tau_0)^n(e^{-\tau/\tau_0}/n!)$. In this form of interpretation of the above integral (45), the average over t_0 may be converted to a spatial average. If we consider one oscillator for the complete interval t_0 we obtain the same result as that found by considering a great number of oscillators in a short time interval. If the latter view is followed, the average over t_0 may turn out to be the average of Θ_i over its distribution. Two types of averaging processes are involved, and the order in which they are carried out does not affect the result.[37] Denoting the probability of occurrence of a phase shift Θ within an interval between Θ and $\Theta+d\Theta$ by $\rho(\Theta)d\Theta$, we can write the above integral (45) as

$$\sum_{n=0}^{\infty}(\tau/\tau_0)^n\left(\frac{e^{-\tau/\tau_0}}{n!}\right)\prod_{i=1}^{n}\int_{-\infty}^{\infty}d\Theta_i\rho(\Theta_i)e^{-i\Theta i}, \quad (47)$$

since the phase shift distribution from $-\infty$ to ∞. The $\rho(\Theta)$ may be understood as the collision parameter producing a phase shift Θ, if we assume straight paths for colliding molecules. Since the value of the integral with respect to Θ_i is the same for any suffix i, it may be written $A-iB$.

$$A=\int_{-\infty}^{\infty}d\Theta\rho(\Theta)\cos\Theta, \quad B=\int_{-\infty}^{\infty}d\Theta\rho(\Theta)\sin\Theta. \quad (48)$$

Hence, (45) is reduced to

$$\varphi(\tau)=\exp\left[\frac{A-iB}{\tau_0}\tau-\frac{\tau}{\tau_0}\right]. \quad (49)$$

Thus, the intensity formula turns out to be

$$I(\Delta\omega)=\frac{2\omega^4}{3\pi c^3}(ex_0)^2\frac{(1-A)/\tau_0}{\{(1-A)/\tau_0\}^2+\{B/\tau_0-\Delta\omega\}^2}. \quad (50)$$

The correlation function method,[6,52] when one does not assume a distribution of n, gives the same result as above for Eq. (44).

According to Eq. (50), the intensity maximum occurs at $\Delta\omega=B/\tau_0$, so that if B is positive the line center shifts to the blue, and, if negative, to the red. The half-width is given by $2(1-A)/\tau_0$ with no assymmetry. According to the definitions of A and B, and noting that the distribution function $\rho(\Theta)$ is normalized, we observe that the half-width and line shift are given by

$$\Delta\omega_{\frac{1}{2}}=2\int\rho(\Theta)(1-\cos\Theta)d\Theta/\tau_0,$$

and

$$\Delta\omega_m=\int\rho(\Theta)\sin\Theta d\Theta/\tau_0. \quad (51)$$

Since $\sin\Theta$ is an odd function, and if positive as well as negative values of Θ are equally probable, the shift of the maximum frequency is zero, as in the case of resonance broadening. The function $\rho(\Theta)d(\Theta)/\tau_0$ can be interpreted as the number of collisions per unit time with phase shift between Θ and $\Theta+d\Theta$. Thus, both the width and shift are proportional to density, the number of molecules per unit volume.

There are many cases where the molecular energy under the influence of another molecule at a distance R is expressed by

$$(E_0+\hbar\gamma/R^p)_i,$$

where i refers to the initial as well as to the final state of the radiative transition concerned. Hence,

$$\Delta\omega(t')=\Delta\gamma/R(t')^p, \quad (52)$$

$\Delta\gamma$ being the difference of the force constants for the two states. If the path of a colliding molecule with relative velocity v is straight, as is probable in the case of no complete interruption of the radiation process,[52] $R=(\rho^2+v^2t'^2)^{\frac{1}{2}}$ with impact parameter ρ and time t'. With the help of Eq. (52) the phase shift, Eq. (38), is, under the binary interaction, given by[56a]

$$\Theta=\int_{-\infty}^{\infty}\Delta\gamma/(\rho^2+v^2t'^2)^{p/2}dt'$$

$$=\left(\frac{\Delta\gamma}{v\rho^{p-1}}\right)\pi\Gamma(p-1)2^{2-p}\left[\Gamma\left(\frac{p}{2}\right)\right]^{-2}. \quad (53)$$

The extension of integration limits to infinity may not be inconsistent with the assumption of adiabatic collision.

The number of collisions with relative velocity between v and $v+dv$ and impact parameter between ρ and $\rho+d\rho$ can be obtained easily by the kinetic theory of gases:

$$\rho(\Theta)d\Theta/\tau_0=8\pi^{\frac{1}{2}}(m/2kT)^{\frac{3}{2}}\exp(-mv^2/2kT)v^3dv\rho d\rho gN,$$

[56a] D. B. Dettaan, *Nouvelles Tables d'Intégrales I éfines* (P. Engels, Libraire Editeur, Leide, 1867), p. 69.

where m is the reduced mass, and N the number of molecules per unit volume. The term g refers to the fact that the force law depends on the various states of colliding molecules and is the probability of a molecule being in a particular rotational state; it must be summed over all states.

Thus, in the case of the force law of inverse pth power, the half-width and line shift are

$$\Delta\omega_{\frac{1}{2}}=2\pi^{(p+3)/(2p-2)}(kT/2m)^{(p-3)/(2p-2)}\times\Gamma\left(\frac{2p-3}{p-1}\right)\Gamma\left(\frac{p-3}{p-1}\right)\times\left[\Gamma(p-1)\Big/\left\{\Gamma\left(\frac{p}{2}\right)\right\}^2\right]^{2/(p-1)}\times\sin\left\{\frac{p-3}{2p-2}\pi\right\}\langle|\Delta\gamma|^{2/(p-1)}\rangle N, \quad (54a)$$

$$\Delta\omega_m=\tfrac{1}{2}\tan\left(\frac{\pi}{p-1}\right)\Delta\omega_{\frac{1}{2}}\langle\Delta\gamma/|\Delta\gamma|\rangle. \quad (54b)$$

In order that these expressions be convergent, p must be larger than 2. The bracket $\langle\ \rangle$ implies an average over g. The value of $\langle|\Delta\gamma|^{2/(p-1)}\rangle$ may be sometimes approximated by the mean square value. For some special values of p, the equation gives

$$\Delta\omega_{\frac{1}{2}}=2\pi^2\langle|\Delta\gamma|\rangle N, \quad \text{for } p=3, \quad (55)$$

$$\Delta\omega_{\frac{1}{2}}=13.4(kT/2m)^{1/4}\langle|\Delta\gamma|^{1/2}\rangle N, \quad \text{for } p=5, \quad (56)$$

$$\Delta\omega_{\frac{1}{2}}=12.9(kT/2m)^{3/10}\langle|\Delta\gamma|^{2/5}\rangle N, \quad \text{for } p=6, \quad (57)$$

respectively. Lindholm[57] derived a formula essentially equivalent to Eq. (57).

It is interesting to consider the range of values of phase shifts Θ which affect the line shape the most. Under the force law, Eq. (52), $\rho(\Theta)=C\Theta^{-1/(p-1)}$ in Eq. (51). Then, when the sign of Θ is positive at all collisions, the integrand of $\Delta\omega_m$ in Eq. (51) oscillates between positive and negative with slowly varying amplitude in the range of $\Theta>1$. Hence, the integrand in this range, corresponding to strong phase shifts, averages nearly to zero and contributes very little to the value of $\Delta\omega_m$. Therefore, the line shift should come from the range of $\Theta<1$. This range is the one completely neglected, by Weisskopf[1] and others,[54,55] as ineffective on line shape. On the other hand, the greater part of the value of $\Delta\omega_{\frac{1}{2}}$ in Eq. (51) comes from the range of $\Theta>1$, since the integrand of $\Delta\omega_{\frac{1}{2}}$ is always positive. Thus the older view of Weisskopf[1] and others[54,55] on line broadening using the idea of critical effective phase shifts can be well understood. However, the result, obtained here, that the strong phase shift averages to zero, still leaves some ambiguity in the theory. An analysis[58] shows that the statistical theory in Section C is better for such collisions. Actually, the Fourier integral theory is good for a line shape near its center.[54]

If the sign of $\Delta\gamma$ is common to all collisions, Eq. (54) gives Foley's relation

$$\Delta\omega_{\frac{1}{2}}/|\Delta\omega_m|=2\cot\left(\frac{\pi}{p-1}\right). \quad (58)$$

The above condition is valid for heavier atoms perturbed by foreign gases where van der Waals forces are important. Although the observed values of line shifts and widths in atomic lines perturbed by foreign gases give widely distributed values for the ratio, Foley[22] shows that p in (58) is nearly 6, assuming the predominance of only one type of force. (See Table III.) However, in most cases of molecular spectra the above condition does not hold and Eq. (58) cannot be used.

Since the interaction forces which are predominant for molecules at low pressures are rather well known, the test of Eqs. (54a) and (54b) has been made with good over-all agreement with observations. For atomic lines the test can hardly be made directly, except for the linearity relationship to N as well as the test of (58). The tests for both microwave and atomic lines require quite different approaches, and may call for separate experimental justifications.

3. Quantum-Mechanical Fourier Integral Theory

In the standard Fourier integral theory, as shown in the previous section, the inclusion of all phase shifts at collisions removed the ambiguous collision diameter and gave rise to a line shift. However, its basic assumption is that the collision is adiabatic and does not change the amplitude of the oscillator in a particular direction.

If molecules have rotational levels whose spacing is small in comparison with the thermal energy, transitions between levels (reorientation of the molecule) may be induced even by adiabatic collisions (infinitely short collision duration) and the amplitude will change. As has been considered by Spitzer,[59] Van Vleck and Weisskopf,[45] Fröhlich,[60] and later under more refined assumptions for low frequency limiting cases by Gross,[61] this effect places the results of the old Lorentz theory in contradiction to the theory of dielectric relaxation developed by Debye[62] and others,[63] as shown in Sec. B1. The relaxation theory of dielectrics treats broadening as the limiting case of a spectral line of zero frequency,

[57] E. Lindholm, Arkiv Mat. Astron. Fys. **32A**, 17 (1945).

[58] T. Holstein, Phys. Rev. **79**, 744 (1950). Also, see reference 37.

[59] L. Spitzer, Jr., Phys. Rev. **58**, 348 (1940).

[60] H. Fröhlich, Nature **157**, 478 (1946); *Theory of Dielectrics* (Oxford University Press, New York, 1949). This model for one degree of freedom was extended to the case of two degrees of freedom by R. Huby, Rept. Brit. Elect. Allied Industr. Research Assoc. [reference L/T 179 (1947)].

[61] F. P. Gross, Phys. Rev. **97**, 395 (1955).

[62] P. Debye, *Polar Molecules* (Chemical Catalog Company, New York, 1929), Chap. V.

[63] W. Kauzman, Revs. Modern Phys. **14**, 12 (1942).

in which case the standard Fourier integral theory also does not give any pressure effect. Thus, it is necessary to develop a generalized Fourier integral theory.

The starting point is given by the radiation theory of quantum mechanics. This method was followed by Lindhold,[57] Foley,[22] Anderson,[52,64] Mizushima,[37] Karplus and Schwinger,[50] Leslie,[65] and Bloom and Margenau.[66] It is customary to treat the intermolecular motion classically. Since the range of the intermolecular force, which is important to line broadening in the valid range of the Fourier integral theory, is several times larger than the wave packet associated with a moving molecule, the packet may be considered as a point without a large error, except for very light molecules such as helium. The coordinates of a colliding molecule are known functions of time, and the molecular interaction is expressed in terms of a definite time. Thus, the following discussions are limited to the classical region well outside of an absorber. First a general formula will be obtained, and then it will be applied to the low-pressure case when multiple collisions can be neglected.

The Hamiltonian of a molecule undergoing perturbations $C(t)$ due to collisions and $F(t)$ due to light waves will be

$$H(t)=H_0+C(t)+F(t), \tag{59}$$

where H_0 is the Hamiltonian of an unperturbed molecule in a stationary state denoted by φ_m. This state is usually highly degenerate, but has a discrete energy. Thus one can know which spectral line is under consideration. While Mizushima[37] solved the Schrödinger equation with this H under the assumption of adiabatic hypothesis (no transition between atomic states due to collision) following Foley's method, Bloom and Margenau[66] divided the transitions concerned into two parts, one due to collisions and another due to the radiation field. They considered only the transitions relating to the radiation process. The wave function of the molecule perturbed by collisions will be expressed in terms of φ_m by

$$\Phi_i(t)=\sum_m U_{mi}(t)\varphi_m, \tag{60}$$

which satisfies the Schrödinger equation $i\hbar\partial\Phi_i/\partial t=[H_0+C(t)]\Phi_i$, with an initial condition $\Phi_i(t_0)=\varphi_i$, i.e. $U(t_0)=1$. Since this Φ_i forms a complete orthogonal set at every instant, the solution of the Schrödinger equation with the Hamiltonian H (59) can be expanded as $\Psi=\sum_i a_i(t)\Phi_i(t)$. In this $a_i(t)$ is the probability amplitude of the collision-smeared state Φ_i. The density of the ith level at t is $\rho_i(t)=a_i^*(t)a_i(t)$. This transition probability amplitude is induced by the light wave and is related to the radiation problem.

The amplitudes are subject to the equation[67]

$$i\hbar da_k/dt=\sum_i F_{ki}a_i, \tag{61}$$

with

$$F_{ki}=\int\Phi_k^*F\Phi_i dv.$$

The increasing rate of the population in the kth level due to absorption depends on the value of $|F_{ki}|^2$ and the population in the ith level. However, there must be induced radiations, which are connected to the transition $k\rightarrow i$ leading to the decrease of $\rho_k(t)$. Thus,

$$\rho_k(t)=\rho_k(t_0)+\sum_i\rho_i(t_0)\left|(i\hbar)^{-1}\int_{t_0}^{t}F_{ki}dt\right|^2 -\sum_i\rho_k(t_0)\left|(i\hbar)^{-1}\int_{t_0}^{t}F_{ki}dt\right|^2_0.$$

Bloom and Margenau[66] solved Eq. (61) rigorously and obtained the $\rho_k(t)$ up to second order in F_{ki}, which is the same as above.

The F_{ki} can be expressed in the stationary states base φ.

$$F_{ki}=\sum_{ml}U_{mk}^*U_{li}\int\varphi_m^*F\varphi_l dv.$$

The explicit form of the field perturbation in the dipole approximation is $F(t)=-\mathbf{E}\cdot\boldsymbol{\mu}\cos(\omega t+\alpha)$. When one sets $\mathbf{E}\cdot\boldsymbol{\mu}=E\mu\cos\theta$ and averages over θ and over the random phase angle α, one obtains

$$\rho_k(\infty)-\rho_k=\frac{E^2}{12\hbar^2}\sum_i(\rho_i-\rho_k)\left\{\left|\int_{-\infty}^{\infty}dt\mu_{ki}(t)e^{i\omega t}\right|^2 +\left|\int_{-\infty}^{\infty}dt\mu_{ki}(t)e^{-i\omega t}\right|^2\right\}, \tag{62}$$

where

$$\mu_{ki}(t)=\sum_{ml}U_{mk}^*(t)U_{li}(t)\int\varphi_m^*\mu(t_0)\varphi_l dv. \tag{63}$$

Hence, the intensity distribution may be expressed by

$$I(\omega)=\hbar\omega(\rho_k(\infty)-\rho_k)=\frac{2\pi\omega I_0(\omega)}{3\hbar c}\sum_i(\rho_i-\rho_k) \times\left\{\left|\int_{-\infty}^{\infty}dt\mu_{ki}(t)e^{i\omega t}\right|^2+\left|\int_{-\infty}^{\infty}dt\mu_{ki}(t)e^{-i\omega t}\right|^2\right\}, \tag{64}$$

where $I_0(\omega)$ represents the incident light beam. Equation (64) has been also obtained by the calculation of work done by the light wave.[66] This result suggests a possible process of separation of $I(\omega)$ into lines $I_{ki}(\omega)$.

[64] P. W. Anderson, dissertation, Harvard University, 1949 (unpublished).
[65] D. C. M. Leslie, Phil. Mag. **42**, 37 (1951).
[66] S. Bloom and H. Margenau, Phys. Rev. **90**, 791 (1953).
[67] L. I. Schift, *Quantum Mechanics* (McGraw-Hill Book Company, Inc., New York, 1949), pp. 190–193.

When $C(t)$ is absent, $\mu_{ki}(t)=\mu_{ki}(0)\exp(i\omega_{ki}t)$, where $\omega_{ki}=(E_k-E_i)/\hbar$. Therefore, one may take it as an approximate solution in the case of the weak collision perturbation. Hence, the first integrand in Eq. (64) has approximately with exponential factor $\exp i(\omega_{ki}+\omega)t$, the second the factor $\exp i(\omega_{ki}-\omega)t$. If $E_k>E_i$ the second of these produces resonance and the first can be neglected; otherwise their role is reversed. In that case,

$$\rho_i\left|\int_{-\infty}^{\infty}dt\mu_{ki}(t)e^{-i\omega t}\right|^2 \tag{65}$$

represents absorption, and

$$-\rho_k\left|\int_{-\infty}^{\infty}dt\mu_{ki}(t)e^{-i\omega t}\right|^2 \tag{66}$$

represents induced emission.

The problem is reduced, then, to obtain the dipole moment $\mu_{ki}(t)$. It is well known that it is possible to rewrite Eq. (63) in the vector form,[68]

$$\mu(t)=U^{-1}(t)\mu(t_0)U(t), \tag{67}$$

where $U(t)$ is unitary and satisfies the equations

$$i\hbar dU/dt=(H_0+C(t))U, \tag{68}$$

and

$$U(t_0)=1.$$

If one sets $U(t)=\exp(H_0t/i\hbar)T(t)$, where $T(t)$ is unitary, the differential equations lead to

$$i\hbar dT/dt=C'(t)T(t), \tag{69}$$

where

$$C'(t)=\exp\left(-\frac{H_0t}{i\hbar}\right)C(t)\exp\left(\frac{H_0t}{i\hbar}\right).$$

The matrix element of $C'(t)$ is given by

$$C_{mm'}'(t)=C(t)_{mm'}\exp[(E_{m'}-E_m)t/i\hbar]. \tag{70}$$

Then,

$$\mu_{ki}(t)=\sum_{ml}(T(t)_{km}^{-1})\exp(-i\omega_{ml}t)\mu_{ml}(t_0)(T(t)_{li}). \tag{71}$$

The diagonal elements of $T(t)$ give the phase shifts of $\mu(t)$ due to collision interaction $C(t)$, while the off-diagonal elements—or their squared absolute values—gives the transition probabilities due to this interaction.

Because $C(t)$ and H_0 do not commute, $C'(t)$ defined above does not commute with itself at all times. However, in cases where $C(t)$ is either diagonal already, or can be made so in a simple manner such as replacing the so-called van der Waals forces, a second-order phenomenon, by a first-order effective Hamiltonian, Eq. (69) integrates easily.

$$T_{kk}(t)=\exp\left[\frac{1}{i\hbar}\int^t C_{kk}(t')dt'\right]. \tag{72}$$

[68] M. Born and P. Jordan, *Elementare Quantenmechanik* (Verlag Julius Springer, Berlin, 1930), p. 327.

Thus, (71) leads to

$$\mu_{ki}(t)=\mu_{ki}(t_0)\exp\left\{-i\omega_{ki}t-\frac{1}{i\hbar}\times\left(\int^t C_{kk}(t')dt'-\int^t C_{ii}(t')dt'\right)\right\}. \tag{73}$$

The substitution from (73) into (65) gives the classical Fourier integral formula (40) for absorption, if we assume that ρ_k (66) is negligibly small. In Eq. (73) the term,

$$\frac{1}{\hbar}\left(\int^t C_{kk}(t')dt'-\int^t C_{ii}(t')dt'\right),$$

is equivalent to the phase shift, Eq. (53), at a collision.

For a binary case, if one assumes a straight path for a colliding molecule, Eq. (72) leads to

$$T_{kk}(\rho)=\exp\left[-i\int_{-\infty}^{\infty}C_{kk}([\rho^2+v^2t'^2]^{\frac{1}{2}})/\hbar dt'\right], \tag{74}$$

where ρ is the impact parameter. Of course, T may be a function of angles, in addition to ρ, required to specify one type of the collision. However, because of the random collision the effect of collisions may be isotropic, so that a collision can be represented by ρ on the average. Hence, Eq. (73) reduces Eq. (65) to the standard Fourier integral theory. From the interaction Hamiltonian $C(t)$, $\Delta\gamma$ defined by Eq. (52) can be obtained. Thus $\Delta\omega_{\frac{1}{2}}$ or $\Delta\omega_m$ can be evaluated by Eq. (54). Since $C(t)$ is generated by a classical thermal motion of a perturber, it cannot be greater than the thermal energy per particle of order kT. Thus any broadening, such that $\hbar\Delta\omega>kT$, is out of the present treatment.

This procedure is generalized to include nondiagonal terms as follows. By a unitary transformation A, $C'(t)$ is diagonalized.

$$AC'(t)A^{-1}=V_{ij}\delta_{ij}. \tag{75}$$

Transforming by A, Eq. (69) becomes

$$i\hbar A\frac{dT}{dt}A^{-1}=V_{ij}\delta_{ij}AT(t)A^{-1}.$$

If dA/dt is neglected by the adiabatic assumption (very slow thermal motion), we obtain

$$T(t)=A^{-1}\left\{\exp\frac{1}{i\hbar}\int^t V_{ij}dt\right\}\delta_{ij}A. \tag{76}$$

From Eqs. (65), (71), and (76), the intensity distribution can be obtained.

Sometimes the transformation A in Eq. (75) may be

difficult to obtain. In this case, by introducing higher order terms into $C(t)$ and ignoring the noncommuting property of $C'(t)$ with itself, the solution of Eq. (69) will be approximated by Eq. (72) or, for independent binary collisions, by Eq. (74). If the value of the integral,

$$\int_{-\infty}^{\infty} C'_{mm'}((\rho^2+v^2t'^2)^{\frac{1}{2}})/\hbar dt' = P_{mm'}(\rho), \tag{77}$$

is small (weak collisions), Eq. (74) can be expanded as

$$T_{mm'}(\rho)=\delta_{mm'}-iP_{mm'}(\rho)+P_{mm'}{}^2(\rho)/2-\cdots. \tag{78}$$

This gives a method of successive approximations.[52]

Since collisions are independent, $T(\rho)$ operates independently on the degenerate levels (m, m', m'', m''') belonging to the initial (k) and final (i) eigenvalues. If n collisions have taken place during a time interval τ, from Eq. (67) $\mu_{ik}(t_0)$ transforms to

$$\mu_{ik}'(t_0+\tau)=T_i^{-1}(\rho_n)T_i^{-1}(\rho_{n-1})\cdots \times T_i^{-1}(\rho_1)\mu_{ik}'(t_0)T_k(\rho_1)\cdots T_k(\rho_n),$$

where $\mu'=\exp(-H_0t/i\hbar)\mu\exp(H_0t/i\hbar)$. It is easy to introduce the degeneracy into this expression:

$$\mu_{ik}'(t_0+\tau)_{m'm} = \sum_{m''m'''}\{\prod_j T_i^{-1}(\rho_j)\}_{m'm''}\mu_{ik}'(t_0)_{m''m'''} \times\{\prod_j T_k(\rho_j)\}_{m'''m}. \tag{79}$$

Because the effect of collisions is isotropic, $\mu_{ik}'(t_0+\tau)$ and $\mu_{ik}'(t_0)$ have exactly the same transformation properties under rotation. Hence, this can be written as

$$\mu_{ik}'(t_0+\tau)_{m'm}=\mu_{ik}'(t_0)_{m'm}F(\tau) \tag{80}$$

with a scalar function $F(\tau)$.

If we follow the same procedure as followed in the derivation of Eq. (42), Eq. (65) can lead to

$$I_{ki}(\omega)=\rho_i\int d\tau e^{i(\omega-\omega_{ki})\tau}\varphi_{ki}(\tau), \tag{81}$$

with

$$\varphi_{ki}(\tau)=\langle\sum_{m'}\mu_{ki}'^*(t_0)_{mm'}\mu_{ik}(t_0+\tau)_{m'm}\rangle_{\text{Av over } t_0}. \tag{81a}$$

Equation (45) and Eq. (81a) are equivalent. If an elementary time interval $d\tau$ is chosen long compared to the duration of one collision which will be represented by $T(\rho)$, one has

$$\delta\varphi_{ki}(\tau)=\varphi_{ki}(\tau+d\tau)-\varphi_{ki}(\tau)=\langle\sum_{m'm''m'''}\mu_{ki}'^*(t_0)_{mm'}[T_i^{-1}(\rho)_{m'm''}\mu_{ik}'(t_0)_{m''m'''}T_k(\rho)_{m'''m}-\mu_{ki}'(t_0)_{m'm}]\rangle F(\tau). \tag{82}$$

On the other hand, Eq. (80) gives

$$\delta\varphi_{ki}(\tau)=\langle\sum_{m'}\mu_{ki}'^*(t_0)_{mm'}\mu_{ik}'(t_0)_{m'm}\rangle dF(\tau). \tag{83}$$

Therefore, it follows that

$$\frac{dF(\tau)}{d\tau}=\left\langle\frac{\sum_{m'm''m'''}\mu_{ki}'^*(t_0)_{mm'}T_i^{-1}(\rho)_{m'm''}\mu_{ik}'(t_0)_{m''m'''}T_k(\rho)_{m'''m}}{\sum_{m'}\mu_{ki}'^*(t_0)_{mm'}\mu_{ik}'(t_0)_{m'm}}-1\right\rangle F(\tau).$$

The average over t_0 is replaced by an average over ρ. The probability that a collision of the type ρ occurs in $d\tau$ is given by $Nvd\tau 2\pi\rho d\rho$, where N is the number density of perturbers and v the mean velocity. Therefore,

$$dF(\tau)/d\tau=-Nvd\tau F(\tau)\int 2\pi\rho d\rho S(\rho), \tag{84}$$

where

$$S(\rho)=1-\frac{\sum_{m'm''m'''}\mu_{ki}'^*(t_0)_{mm'}T_i^{-1}(\rho)_{m'm''}\mu_{ik}'(t_0)_{m''m'''}T_k(\rho)_{m'''m}}{\sum_{m'}\mu_{ki}'^*(t_0)_{mm'}\mu_{ik}'(t_0)_{m'm}}.$$

Hence the correlation function φ_{ki} is given by

$$\varphi_{ki}(\tau)=\sum_{m'}\mu_{ki}'^*(t_0)_{mm'}\mu_{ik}'(t_0)\exp(-Nv\sigma\tau),$$

where σ denotes the complex cross section defined by the integral in Eq. (84). It is obvious from the discussion in the previous section that the line shift in frequency and the half-width follow from the imaginary and the real parts of $Nv(1-\sigma)$, respectively.

The cross section σ is given by the average of the partial cross section $\sigma(J_2)$ due to the different state J_2 of perturbers labeled 2.

$$\sigma=\sum_{J_2}B(J_2)\sigma(J_2). \tag{85}$$

$B(J_2)$ is the Boltzmann distribution function for the colliding molecule in the state J_2. It has been assumed in Eq. (85) that no transitions occurs in molecule (2)

quantum numbers, except perhaps for the degenerate ones, or that transitions in molecules (2) can occur only simultaneously with those of molecule (1), so that T_i and T_k are still essentially diagonal in molecule (1) and (2) (resonance cases). Since the interaction Hamiltonian $C'(t)$ depends on J_2, $\sigma(J_2)$ is averaged over the degenerate substate M_2 (possibly magnetic quantum number) belonging to J_2:

$$S(\rho,J_2)=1-\frac{\sum_{M_2m'm''m'''}\mu_{ki}'^*(t_0)_{mm'}T_i^{-1}(\rho)_{m'm''}{}^{J_2}\mu_{ik}'(t_0)_{m''m'''}T_k(\rho)_{m'''m}{}^{J_2}}{(2J_2+1)\sum_{m'}\mu_{ki}'^*(t_0)_{mm'}\mu_{ik}'(t_0)_{m'm}}. \tag{86}$$

To evaluate this expression S, the expansion (78) may be used. It is found that the zeroth order in $P(\rho)$ of S vanishes. The first-order terms are, after having averaged over the degenerate index m, which will be denoted by m_k and m_i for the absorber in the state k and i, respectively.

$$S_1(\rho,J_2)=i\left[\sum_{m_kM_2}\frac{(k,m_k,J_2,M_2|P|k,m_k,J_2,M_2)}{(2J_k+1)(2J_2+1)}-\sum_{m_iM_2}\frac{(i,m_i,J_2,M_2|P|i,m_i,J_2,M_2)}{(2J_i+1)(2J_2+1)}\right]. \tag{87}$$

Since this is imaginary, S_1 contributes to the line shift. On the other hand, the first term which gives a contribution to the line breadth is one of the two possible second-order terms called by Anderson $(S_2)_{\text{outer}}$.[52]

$$S_2(\rho,J_2)_{\text{outer}}=\tfrac{1}{2}\left[\sum_{m_kM_2}\frac{(k,m_k,J_2,M_2|P^2|k,m_k,J_2,M_2)}{(2J_k+1)(2J_2+1)}+\sum_{m_iM_2}\frac{(i,m_i,J_2,M_2|P^2|i,m_i,J_2,M_2)}{(2J_i+1)(2J_2+1)}\right]. \tag{88}$$

m_k is the degenerate index of an absorber in the state k and $2J_k+1$ is the degeneracy of the state. Another second-order term $S_2(\rho,J_2)_{\text{middle}}$, which arises from the cross term, $\mu_{ki}'^*(t_0)_{mm'}P_i^{-1}(\rho)_{m'm''}{}^{J_2}\mu_{ik}'(t_0)_{m''m'''}P_k(\rho)_{m'''m}{}^{J_2}$ when Eq. (78) is introduced into Eq. (86), is quite complex and difficult to evaluate. But, when the absorber has a permanent electric dipole moment, $S_2(\rho,J_2)_{\text{middle}}$ vanishes. When ρ is small, Eq. (78) cannot be used. In this strong collision, S has its maximum value of $S=1$ (real).

A typical matrix element necessary to evaluate Eqs. (87) and (88) is given by

$$(\alpha|P|\beta)=(k,m_k,J_2,M_2|P|k',m_k',J_2',M_2')=\frac{1}{\hbar}\int_{-\infty}^{\infty}\exp(i\omega_{\alpha\beta}t)(\alpha|C(t)|\beta)dt, \tag{89}$$

where

$$\omega_{\alpha\beta}=\frac{E(\alpha)-E(\beta)}{\hbar}=\frac{E(k)+E(J_2)-E(k')-E(J_2')}{\hbar}.$$

$E(k)$ is the energy of the absorbing molecule in the initial state. Clearly from Eq. (89) those $(\alpha|P|\beta)$ where $\omega_{\alpha\beta}=0$ (resonant collision) make a significant contribution to S.

C. STATISTICAL THEORY

1. Classical Statistical Theory

As will be discussed later, many experimental results are inconsistent even with the linear dependence of half-width on density obtained by the phase shift approximation. This discrepancy seems to be more prominent at higher densities, where multiple interactions[30] may dominate binary ones.

To a first approximation molecules can be regarded as at rest, and the frequency emitted by an active molecule at each position x is simply given by $(V_b(x)-V_a(x))/\hbar$, $V_b(x)$ and $V_a(x)$ being potential energies of the molecule concerned in the initial and final states respectively at a point x in configuration space. The intensity within a certain frequency interval $d\omega$ is, therefore, proportional to the probability of those configurations of perturbers which yield the value $V(x)$. This consideration was put into the treatment first by Holtsmark[69] and others[70,53] in connection with the Stark effect in ionized or dipole gases and later by Kuhn[71] and Margenau.[2,72,73]

The potential $V(x)$ of the radiating molecule is the sum of the energy in the isolated state E_0 and perturbation energies due to all other molecules. Thus, it is a function of the position of all perturbing molecules. If we assume additiveness of perturbation energies, we find

$$V(x)=E_0+\sum\hbar\gamma R_i^{-p}U(\xi_i),$$

where R_i is the distance of the ith perturber from the radiating molecule, ξ_i denotes a set of angle and spin variables, and γ is the force constant. As a rule the perturbation energies are much larger for excited states than for normal states. The frequency difference $\Delta\omega$ from the natural frequency will not be given by Eq. (52), but rather will be given approximately by

$$\Delta\omega=\sum_i\gamma R_i^{-p}U(\xi_i), \tag{90}$$

[69] H. Holtsmark, Ann. Physik **58**, 577 (1919); Physik. Z. **20**, 162 (1919); **25**, 73 (1924).
[70] L. Spitzer, Jr., Phys. Rev. **55**, 699 (1939).
[71] H. Kuhn, Phil. Mag. **18**, 987 (1934); Phys. Rev. **52**, 133 (1937).
[72] H. Margenau, Phys. Rev. **40**, 387 (1932); **48**, 755 (1935).
[73] H. Margenau, Phys. Rev. **82**, 156 (1951).

using only γ's for excited states. The variation of intensity with $\Delta\omega$ is determined by the probability $I(\Delta\omega)$ that, in the presence of n perturbing molecules, the potential energy

$$\sum_{i=j}^{n} \gamma R_i^{-p} U(\xi_i)$$

shall have the value $\Delta\omega$. This probability is easily calculated by the use of Markoff's method,[74] or the result may be obtained by the assumption that the probability is proportional to the time interval during which $\Delta\omega$ is radiated. Since perturbers are considered as at rest, the radiation may be expressed by

$$\exp(i \sum_{i=1}^{n} \gamma R_i^{-p} U(\xi_i) t). \tag{91}$$

Then, the Fourier component with respect to t will give the relative intensity as a function of $\Delta\omega$

$$I(\Delta\omega)=\frac{1}{2\pi}\int_{-\infty}^{\infty} \exp(i \sum_{i=1}^{n} \gamma R_i^{-p} U(\xi_i) t - i\Delta\omega t) dt. \tag{92}$$

This has been analytically obtained[75] from Eq. (81) for a limiting case consistent with the above assumption. This must be averaged over the distribution of R_i and ξ_i.

As Margenau[73] assumed, $U(\xi)$ leads very often only to different numerical factors, -1 or $+1$ being equally probable, according to values of ξ. Thus, the probability densities with respect to R_i and ξ_i are given by

$$p(R_i)dR_i=\frac{3R_i^2 dR_i}{R_0^3}, \quad p(\xi_i)d\xi_i=\tfrac{1}{2}d\xi,$$

where $4\pi R_0^3/3$ is the volume occupied by the gas. Then,

$$I(\Delta\omega)=\frac{1}{2\pi}\int_{-\infty}^{\infty} e^{-i\Delta\omega t} A_n(t) dt, \tag{93}$$

with

$$A_n(t)=\left\{\int_{-1}^{1} p(\xi)d\xi \int_0^R p(R)dR \exp[i\gamma R^{-p} U(\xi) t]\right\}^n.$$

The evaluation is rather straightforward and the final result is

$$I(\Delta\omega)=\frac{1}{\pi}\int_0^{\infty} \exp(-N g_p t^{3/p}) \cos\Delta\omega t dt, \quad p>\tfrac{3}{2}, \tag{94}$$

where N is the number density of perturbers and

$$g_p=\frac{4\pi}{3}\gamma^{3/p} \sin\left[\left(1-\frac{3}{p}\right)\frac{\pi}{2}\right]\Gamma\left(1-\frac{3}{p}\right).$$

It is easily seen that, because of the above assumption as to $U(\xi)$, the intensity distribution given by (93) is symmetrical about the natural frequency. The intensity at the center, where $\Delta\omega=0$, is

$$I(0)=\left(\frac{p}{3\pi}\right)\Gamma\left(\frac{p}{3}\right)\Big/(N g_p)^{p/3},$$

which decreases with $N^{-p/3}$ in the normalized $I(\Delta\omega)$. It suggests that, in contrast to Eq. (54a), the half-width increases roughly with $N^{p/3}$. For large values of $\Delta\omega$, $I(\Delta\omega)$ becomes proportional to $\Delta\omega^{-1-3/p}$. Hence, the intensity at the wing of its distribution changes as $\Delta\omega^{-1-3/p}$. If only binary interactions are considered, this also leads to $\Delta\omega^{-1-3/p}$, as can be seen easily by putting $N=1$ in Eq. (94). This is in agreement with expectation, since the large interaction energies, corresponding to very short interacting distances, are predominantly caused by single impacts of the molecules. According to Holstein's analysis,[58] for large values of $\Delta\omega$, the Fourier integral formula (40) can be transformed to the statistical one. Thus a line shape at the wing is approximated by the statistical theory rather than by the phase shift approximation.

There are other types of forces which do not change sign with ξ, as in the interaction between nonpolar spherically symmetric molecules. Then $U(\xi)=1$ and the intensity $I(\Delta\omega)$ appears only on one side of the natural frequency. Equation (93) leads to

$$I(\Delta\omega)=\frac{1}{\pi}\int_0^{\infty} \exp(-N g' t^{3/p}) \cdot \cos(\Delta\omega t + N g'' t^{3/p}) dt, \tag{95}$$

where

$$g'+ig''=i\frac{4\pi}{3}\gamma^{3/p}\int_0^{\infty} \rho^{-3/p} e^{i\rho} d\rho.$$

For van der Waals forces, for which $p=6$, $\gamma<0$ and $g'=g''$,

$$I(\Delta\omega)=\begin{cases} 0, & \text{if } \Delta\omega<0, \\ \dfrac{2\pi}{3}|\gamma|^{\frac{1}{2}} N \Delta\omega^{-\frac{1}{2}} \exp\left(-\dfrac{4\pi}{9}|\gamma| N^2/\Delta\omega\right), & \text{if } \Delta\omega>0, \end{cases} \tag{96}$$

as was derived by Margenau,[2,72] and the shift and half-width changes as

$$\Delta\omega_m=-(\tfrac{2}{3}\pi)^3|\gamma|N^2, \quad \text{(red shift)} \tag{97}$$

$$\Delta\omega_{\frac{1}{2}}=0.822\pi^3|\gamma|N^2. \tag{98}$$

This yields a method for obtaining the van der Waals coefficient for excited states. Since Eq. (96) involves the assumption that a force varying as R^{-6} is valid all the way into the origin of R, Eq. (96) may be in error for large $\Delta\omega$, which corresponds to close encounters. But for large $\Delta\omega$, Eq. (96) gives

$$I(\Delta\omega)\sim\Delta\omega^{-\frac{3}{2}}. \tag{99}$$

[74] S. Chandrasekhar, Revs. Modern Phys. **15**, 1 (1943).
[75] P. W. Anderson, Phys. Rev. **86**, 809 (1952).

This is Kuhn's relation for the wing of the broadened line, as supported by his observation[76] of the broadened wing of Hg 2357 by A and Hg, and by the observations of Ruhmkorf[77] using N_2, O_2, CO_2, and A as perturbers and of Minkowski[77] with NaD lines perturbed by A. This was also confirmed with D lines in an acetylene flame by Huldt and Knall.[12] However, an experimental line shape at the wing seems sometimes to be more complicated.[78,79]

The validity of Eq. (99) has been discussed by Lindholm,[57] Holstein,[58] and Anderson.[75] The latter two obtained for the wing,

$$I(\omega)=\frac{4\pi N\gamma^{3/p}}{p\Delta\omega^{1+3/p}}\times\left\{1-\frac{p}{36}\left(1+\frac{1}{2p}\right)\left(1-\frac{1}{p^2}\right)\frac{v^2}{\Delta\omega^{2-2/p}\gamma^{2/p}}\right\}, \quad (100)$$

for the interaction energy of the type $\Delta\omega=\gamma/R^p$. Thus Eq. (99) is valid when $\Delta\omega\gg v^{p/(p-1)}\gamma^{-1/(p-1)}$. On the other hand, the impact theory is good[59] when $\Delta\omega\ll v^{p/(p-1)}\gamma^{-1/(p-1)}$ (near the unperturbed line). This condition for the validity of the statistical theory may be rewritten, as obtained rather rigorously by Margenau,[80] as $T\Delta\omega\gg 1$, where T is about equal to ρ/v, ρ being the impact parameter for the collision, since $\Delta\omega_{\frac{1}{2}}$ (statistical)$\simeq\gamma N^{p/3}\sim\gamma/\rho^p$.

The recent experimental results[81–86] at pressures of several hundreds of atmospheres reveal the insufficiency of the above theory. Equation (90) does not predict the reversal of the direction of line shift at high pressure which is found in some cases (see Fig. 3). Bergeon, Robin, and Vodar[87] presented a qualitative discussion suggesting that the repulsive force, which would be dominant at high pressures, must be included in the calculation of Margenau's formula (93), in addition to the long-range force given by Eq. (90). They employed the Lennard-Jones formulas for the interaction energy and calculated the line shape numerically, assuming the additiveness of the energy and its applicability to both normal and excited energy levels. Though better broadened line contours than otherwise were obtained, the forces at small distances are not clear without detailed discussion. In any case, it is likely that they are not additive.[88] However, potential curves at very close distance have been devised[89] to explain the absorption bands (see III.C) appearing on the violet side of spectral lines.

Furthermore, recent observations on certain steller absorption line broadening[90] and on shock phenomena[91] have made clear some insufficiencies of the statistical theory of Holtsmark[69] which attributes the broadening to the Stark effect. The Debye-Hückel effect was introduced to account for the discrepancies, but this resulted in corrections which are too small.[53,92] Following the suggestion of Baranger,[93] an extensive study has been made quantum-mechanically on electron impact line broadening, showing that for the Lyman α line, where there is a linear Stark effect, the ion broadening is the dominant effect,[94] but that for the anomalous $3d\rightarrow 2p$ line of HeI, which has a small Stark shift, the electrons can make important contributions.[95]

Generally speaking, pressure broadening changes from collision type to statistical type with increasing pressure.[58,59,71] However, as shown in Part III, the transition from one type to the other is not clear. The "modulation index," which corresponds to the ratio of the maximum frequency shift to the number of collisions per second, has been proposed[96] to determine the predominance of one type or the other under certain conditions. Lindholm,[57] Holstein,[97] and others worked out the transition, as detailed in II.D, including the line shape at the violet wing.

2. Quantum-Mechanical Justification of Statistical Theory

Jablonski[98] has given a theory of the pressure-broadened atomic line shape with a very close analogy to the theory of intensity distribution in molecular spectra. He calculated the stationary states of interatomic motion under the influence of an interaction between a radiating atom and a colliding one.

For simplicity, consider the wave function φ of a single pair of atoms consisting of a radiator and a perturber in a spherical box of radius R_0, with the radiator at its center and with the boundary condition $\varphi(R_0)=0$. In the Lorentz approximation, where molecular rotation

[76] H. Kuhn, Proc. Roy. Soc. (London) **A158**, 212 (1937); **158**, 230 (1937).
[77] H. A. Ruhmkorf, Ann. Physik **31**, 21 (1938); R. Minkowski, Z. Physik **93**, 731 (1935).
[78] S. Y. Ch'en and C. S. Chang, Phys. Rev. **75**, 81 (1949).
[79] Ch'en, Bennett, and Jefimenko. J. Opt. Soc. Am. **45**, 182 (1956).
[80] H. Margenau, RM-1670-AEC, April 3 (1956).
[81] S. Y. Ch'en, thesis, California Institute of Technology (1940), p. 35.
[82] Robin, Robin, and Vodar, Compt. rend. **232**, 1754 (1951).
[83] S. Robin, thesis, Paris, (1951); J. chim. Phys. **49**, 1 (1952).
[84] J. Robin and S. Robin, Compt. rend. **233**, 928 (1951).
[85] J. Robin and S. Robin, Compt. rend. **233**, 1019 (1951); J. Robin, thesis, Paris (1953).
[86] (a) J. Robin, Compt. rend. **238**, 1491 (1954); (b) A. Michel and H. De Kluiver, Physica **22**, 919 (1956).
[87] Bergeon, Robin, and Vodar, Compt. rend. **235**, 360 (1952); R. Bergeon, *ibid.* **238**, 2507 (1954); R. Bergeon and B. Vodar, *ibid.* **240**, 172 (1955).
[88] L. Jansen and Z. I. Slawsky, J. Chem. Phys. **22**, 1701 (1954); R. T. McGinnies and L. Jansen, Phys. Rev. **101**, 1301 (1956).
[89] H. Kuhn, Z. Physik **72**, 462 (1931); and see reference 146, 147, and 149.
[90] A. B. Underhill, Astrophys. J. **116**, 446 (1953); G. L. Odgers, Astrophys. J. **116**, 444 (1953).
[91] A. Kantrowitz, Phys. Rev. **90**, 368 (1953).
[92] F. N. Edmonds, Astrophys. J. **123**, 45 (1956).
[93] M. Baranger, Phys. Rev. **91**, 436 (1953).
[94] Kivel, Bloom, and Margenau, Phys. Rev. **98**, 495 (1955); H. Margenau and B. Kivel, Phys. Rev. **98**, 1822 (1955).
[95] B. Kivel, Phys. Rev. **98**, 1055 (1955).
[96] H. Margenau and S. Bloom, Phys. Rev. **79**, 213 (1950).
[97] G. N. Plass and D. Warner, Phys. Rev. **86**, 138 (1952).
[98] A. Jablonski, Acta Phys. Polon. **6**, 371 (1937); **7**, 196 (1938); Physica **8**, 541 (1940); Phys. Rev. **68**, 78 (1945).

can be neglected, the relevant part of φ is only the radial wave function φ_{vl}, where v and l are a set of radial and angular momentum quantum numbers for the relative motion of the two atoms. Since the intermolecular forces are different for upper and lower states, which are designated by $'$ and $''$, respectively, the solutions of two different radial wave equations:

$$d\varphi_{v'l'}/dR+\frac{2m}{\hbar^2}\left(W_{v'l'}-V'(R)-\hbar^2\frac{l'(l'+1)}{2mR^2}\right)\varphi_{v'l'}=0, \quad (101)$$

and

$$d\varphi_{v''l''}/dR+\frac{2m}{\hbar^2}\left(W_{v''l''}-V''(R)-\hbar^2\frac{l''(l''+1)}{2mR^2}\right)\varphi_{v''l''}=0,$$

are required. m denotes the reduced mass of the pair, W_{vl} the relative energy of the motion, and $V(R)$ the mutual potential energy.

It is easily shown that the two sets of rotational wave functions for upper and lower states are orthogonal. Hence, only transitions with $l'=l''$ are allowed. If we denote the atomic transition amplitude by $\mathfrak{M}_0$, we may write the total transition amplitude as

$$D_{v'v''l}=\mathfrak{M}_0\int\varphi_{v'l}{}^*\varphi_{v''l}dv. \quad (102)$$

Here we have assumed the classical Franck-Condon principle.[99] Clearly the matrix element $D_{v'v''l}$ depends on l through the solution φ_{vl} of (101). For large l's in comparison with the difference of $V'(R)$ and $V''(R)$, both sets $\varphi_{v'l}$ and $\varphi_{v''l}$ become practically identical and hence orthogonal. Therefore, no transitions $v'\rightarrow v''$ with $v'\neq v''$ will occur between states of sufficiently large l's, and there will be no appreciable change of translational energy. Thus, this region of large l's corresponds to Lorentz' impact parameters larger than the critical optical collision diameter. However, for smaller values of l, the dependence of $D_{v'v''l}$ on l becomes very marked. Classically speaking, the effect on spectral lines produced by collisions depends very markedly on impact parameter. Thus, one is not justified in assuming that all collisions with impact parameter smaller than a certain optical collision diameter are equally effective.[1,54,55]

The solution of Eq. (101) with WKB approximation is

$$\varphi_{vl}=\left(\frac{2p(\infty)}{R_0p(R)}\right)^{\frac{1}{2}}\cos\left[\frac{1}{\hbar}\int_{R_t}^{R}p(x)dx+\delta\right], \quad (103)$$

where $p(x)=[2m(W_{vl}-V(x)-\hbar^2l(l+1)/x^2)]^{\frac{1}{2}}$ is the radial component of relative momentum of the two atoms. $p(\infty)$, which is the value of $p(x)$ at $x=\infty$, together with R_0 in Eq. (103), is determined by normalization. The above solution is valid only for $R>R_t$, where R_t is the distance of classical turning point given by $p(R_t)=0$. δ is a phase constant which is adjusted according to the solution for $R<R_t$. The transition amplitude is

$$D_{v'v''l}=\frac{\mathfrak{M}_0}{R_0}\int_{R_t}^{R_0}\left(\frac{p'(\infty)p''(\infty)}{p'(R)p''(R)}\right)^{\frac{1}{2}}\times\cos\left(\int_{R_t}^{R}\frac{p'(x)-p''(x)}{\hbar}dx+\delta'-\delta''\right)dR. \quad (104)$$

Obviously, the largest contribution to the value of this integral comes from the region $R\sim R_c$ for which $p'(R)=p''(R)$. Thus, the relative momentum $p(R)$ of the nuclei of the two atoms does not change in the transition $v'\leftrightarrow v''$, consistent with the classical conservation law of momentum. It may be interpreted, therefore, that the transition $v'\leftrightarrow v''$ occurs at $R=R_c$. Then, the energy change of nuclear motion involved in the transition is given by the condition $p'(R_c)=p''(R_c)$, i.e.,

$$W_{v'l}-W_{v''l}=V'(R_c)-V''(R_c). \quad (105)$$

This energy must be transferred to the radiation, resulting in the frequency shift $\Delta\omega$. Thus, $\Delta\omega$ may be expressed as a function of R_c. Then, if $D_{v'v''l}$ of Eq. (104) is known as a function of R_c, the probability of the frequency shift $\Delta\omega$ will result.

To obtain the function $D_{v'v''l}(\Delta\omega)$, Jablonski first expanded the integrand of Eq. (104) near $R=R_c$ and took only the first nonvanishing two terms. This procedure depends primarily on the assumption that the integrand of Eq. (104) slowly oscillates near $R=R_c$. This assumption is clearly equivalent to the assumption made by Kuhn and London.[55]

In the calculation of $I(\Delta\omega)$ for absorption of a particular atomic line, the probability $D^2{}_{v'v''l}$ must be averaged over all initial and final states, $v''l$ and $v'l$. Thus, after some reductions, the asymptotic form is

$$I(\Delta\omega)=\frac{3R_c{}^2(1-V''(R_c)/W_{v''l})^{\frac{1}{2}}}{R_0{}^3|\hbar d\Delta\omega/dR|_{R=R_c}}, \quad (106)$$

where $\hbar\Delta\omega=V'(R_c)-V''(R_c)$. This can be rewritten as

$$I(\Delta\omega)d\omega=CR_c{}^2dR_c,$$

where C is some constant. This is clearly an expression of Kuhn's idea.[71] The relation, like Eq. (106), for emission is obtained by replacing $''$ by $'$.

If n free perturbers exist in the box and the interaction is additive, the total wave function $\varphi_{vl}{}^t$ and the total energy will be such that

$$\varphi_{vl}{}^t=\prod_i^n\varphi_{vl,i}, \quad W_{vl}{}^t=\sum_i^n W_{vl,i},$$

[99] G. Herzberg, *Molecular Spectra and Molecular Structure* (D. Van Nostand Company, Inc., New York, 1951).

with

$$V'(R_c)^t - V''(R_c)^t = \hbar\Delta\omega. \tag{107}$$

Again, $'$ designates the upper state. Then, since $n=(4\pi/3)R_0^3N$, where N is the number density of perturbers, and since the energy is additive,

$$I^t(\Delta\omega)=\sum_i a_i 4\pi N f^2(\Delta\omega)\frac{(1-V''(R_c)/W_{v''l})}{|\hbar d\Delta\omega/dR_c|} \tag{108}$$

where a_i assures the different probability arising from the different type of potential energy $V(R)$, if any. $f(\Delta\omega)$ is R_c expressed as a function of $\Delta\omega$ obtained from Eq. (107). Strictly speaking, $I^t(\Delta\omega)$ must be averaged over all W_{vl} occurring in the gas under consideration, but, since the factor in brackets constitutes a small correction only, at least in a certain range of frequency, it is permissible to put $W_{vl}=\frac{3}{2}kT$. Thus, the dependence on temperature of $I^t(\Delta\omega)$ is very slight, as experimentally observed, except for the part of the line arising from transitions in the repulsive branches of the potential curves, particularly at the points at which $V(R_c)=W_{vl}$. Apart from the above factor, Eq. (108) is identical with the equation obtained from the statistical theory.[2,72]

Since the WKB method is valid when the potential energy $V(R)$ changes so slowly that the momentum of the particle is sensibly constant over many wavelengths of φ_{vl}, Eq. (108) cannot be used for light perturbers or light radiators such as helium.

D. THEORY AT GENERAL PRESSURES

There have been many attempts[2,57,58,75,96,97] to span a bridge between the impact theory and the statistical theory, especially to find a theory valid at intermediate pressures, so that the broadening behavior, including the line shape, over the whole range of pressures is described. In practice, however, more stress was put on the line shape at the wings with conditions such as in Eq. (100) because of the mathematical difficulties involved.

Recently Anderson and Talman[100] extended the use[75] of the general Fourier integral formula, (40), in a more general way. Equation (40) was obtained under the assumption of classical paths of perturbers and the adiabatic assumption. It goes over to the expression in either the impact theory or the statistical theory depending on the additional assumptions made simply for an easier mathematical treatment. One of these made here is about the frequency perturbation: $\Delta\omega=-(\gamma/R^p)$ as in Eq. (90). Since this interaction energy is usually additive and if we assume that the motions of perturbers are independent, the correlation function (45) can be rewritten.

$$\varphi(\tau)=\left\langle \exp\left[-i\int_0^\tau \Delta\omega(R)dt'\right]\right\rangle^n. \tag{109}$$

[100] P. W. Anderson and J. D. Talman, Bell Telephone Laboratories, Murray Hill, New Jersey (1956).

n is the total number of perturbers. As in Eq. (46), the average may be understood as over the configuration space. Since collisions are isotropic and independent, we assume without loss of generality that all collisions take place from the direction of x. Referring to generalized coordinates ρ, x_0, the impact parameter and the position on the trajectory at $t'=0$ respectively, one finds that the volume, V, of our system is represented by

$$V=2\pi\int\rho d\rho\int dx_0. \tag{110}$$

If we assume, in addition, that the perturbers describe straight line paths and all travel with velocity $\bar{v}$; $R^2=(x_0+\bar{v}t')^2+\rho^2$. Thus,

$$\begin{aligned}\varphi(\tau)&=\left\{\frac{1}{V}\int dV\exp\left[-i\int_0^\tau\Delta\omega(R)dt'\right]\right\}^n,\\ &=\left\{1-\frac{2\pi}{V}\int_0^\infty\rho d\rho\int_{-\infty}^\infty dx_0\right.\\ &\quad\left.\times\left[1-\exp\left(-i\int_0^\tau\Delta\omega\{[(x_0+\bar{v}t')^2+\rho^2]^{\frac{1}{2}}\}dt'\right)\right]\right\}^n,\\ &\equiv\left[1-\frac{V'(\tau)}{V}\right]^n, \text{ say.}\end{aligned} \tag{111}$$

Then, by making V and $n\to\infty$, while the number density of perturber $N=n/V$ is kept constant, we have

$$\varphi(\tau)=\exp[-NV'(\tau)]. \tag{112}$$

This is the basic formula.

For small values of $\bar{v}$, Eq. (112) yields the statistical distribution which is exact if the perturbers are stationary. With $\bar{v}=0$ in Eq. (112), we obtain

$$V'(\tau)=4\pi\int_0^\infty R^2\{1-\exp[-i\Delta\omega(R)\tau]\}dR, \tag{113}$$

noticing that $\rho^2+x_0^2=R^2$ and $2\pi\rho d\rho dx_0=4\pi R^2dR$. A simple calculation will show that Eq. (113) gives Margenau's equation (93). Equation (113) is valid not only as $v\to0$ but as $\tau\to0$. If one refers to Eq. (112), it becomes clear that when N is large $\varphi(\tau)$ is only large for small τ so that the above is indeed also the high pressure limit.

For large $\bar{v}$ and low density Eq. (112) should approach the impact theory. Putting $u=x_0+\bar{v}\tau$, one finds that $V'(\tau)$ becomes

$$\begin{aligned}V'(\tau)=2\pi&\int_0^\infty\rho d\rho\int_{-\infty}^\infty dx_0\\ &\times\left\{1-\exp\left[-i\int_{x_0}^{x_0+\bar{v}\tau}\Delta\omega((\rho^2+u^2)^{\frac{1}{2}})\frac{1}{\bar{v}}du\right]\right\}.\end{aligned}$$

The integrand in the x_0 integration is small whenever the exponent

$$\frac{1}{\bar{v}}\int_{x_0}^{x_0+\bar{v}\tau}\Delta\omega((\rho^2+u^2)^{\frac{1}{2}})du$$

is small, that is, when $x_0\ll-\bar{v}\tau$ or $x_0\gg 0$, since the appreciable values of this integral lie in the range of $-\bar{v}\tau<x_0<0$.|| Hence,

$$V'(\tau)\sim 2\pi\int_0^\infty \rho d\rho\int_{-\bar{v}\tau}^0 dx_0 \times\left\{1-\exp\left[-i\int_{-\infty}^{\infty}\Delta\omega((\rho^2+u^2)^{\frac{1}{2}})\frac{1}{\bar{v}}du\right]\right\}, \quad (114)$$

$$=2\pi\bar{v}\tau\int_0^\infty \rho d\rho(1-e^{-i\Theta(\rho)}),$$

with

$$\Theta(\rho)=\int_{-\infty}^{\infty}\Delta\omega((\rho^2+u^2)^{\frac{1}{2}})\frac{1}{\bar{v}}du.$$

Referring to Eq. (53), we note that $\Theta(\rho)$ is a phase shift at a collision. It is clear now that Eq. (114), with Eq. (112), gives Foley's expression (50).

Equations (113) and (114) are the two limits of V' for large and small t. To study the intermediate region we choose a dimensionless form. For the frequency perturbation $\Delta\omega=-\gamma/R^p$, we define $R_0=(\gamma/\bar{v})^{1/(p-1)}$. With new variables such that $\rho=R_0r$, $x=R_0z$, $N=h/R_0^3$, $\Delta\omega=\bar{v}\Delta\omega'/R_0$, $t=R_0u/\bar{v}$ and $\tau=R_0y/\bar{v}$, Eq. (112) becomes

$$\varphi(R_0y/\bar{v})=e^{-h\psi(y)}, \quad (115)$$

with

$$\psi(y)=2\pi\int_0^\infty rdr\int_{\infty-}^{\infty}dz(1-e^{i\Theta}), \quad (116)$$

$$\Theta(y)=\int_0^y[(z+u)^2+r^2]^{-p/2}du. \quad (117)$$

Hence, from Eq. (44) or (81), we have

$$I(\bar{v}\Delta\omega'/R_0)=\frac{R_0}{2\pi\bar{v}}\int_{-\infty}^{\infty}\exp[i\Delta\omega'y-h\psi(y)]dy, \quad (118)$$

neglecting less important factors. $I(\Delta\omega')$ is determined by one parameter only, $h=NR_0^3=N(\gamma/\bar{v})^{3/(p-1)}$, and hence it is the magnitude of this parameter which determines the validity of the statistical or impact theories. Lenz's[54] method is equivalent to the approximation in Eq. (117) of replacing $\Theta(y)$ by its tangent at $y=0$ and is in disagreement with the statistical theory. Here notice that $y=\bar{v}\tau/R_0$. Lindholm's[57] method, which was carried out for a perturbation proportional to $1/R^6$ with a simplified model of collisions during which the frequency was constant, is equivalent to the approximation of replacing $\Theta(y)$ by a straight line which cuts the curve $\Theta(y)$ at $y=0$ and large. Thus, Lindholm obtained a result in agreement also with the statistical theory in its extremities, which could, however, be wrong in intermediate cases.

The problem of calculating a line shape has been reduced to that of calculating the dimensionless function (116). However, $\psi(y)$ cannot be obtained explicitly and is difficult to compute numerically. Anderson and Talman used the method to calculate the behavior of $\psi(y)$ for very small values of y and for large values of y and then to interpolate between the two.

They gave, for the case $p=6$, and small y

$$\psi(y)=i^{-1/2}\frac{4\pi}{3}\Gamma(\tfrac{1}{2})y^{1/2}+i^{-1/6}\frac{5\pi}{18}\Gamma(\tfrac{5}{6})y^{13/6}, \quad (119)$$

and for large y

$$\psi(y)=\frac{2\pi}{5}i^{-2/5}\left(\frac{3\pi}{8}\right)^{-3/5}\Gamma(\tfrac{2}{5})y+1.91+2.63i. \quad (120)$$

The asymptotic behaviors of the two match very well so that these may be used to approximate $\psi(y)$. Equations (119) and (120) will give numerically a line shape at any pressure for $p=6$, but no general analytic expression for the line shape can be obtained.

We shall be interested in the asymptotic behavior of $I(\omega)$ for: (a) large positive $\Delta\omega$, (b) $\Delta\omega$ near zero, and (c) large negative $\Delta\omega$, when h is large. Cases (a) and (b) cannot be properly treated by the statistical theory, as discussed before. For large values of h, Eq. (118) is large only for $|y|$ small, since the real part of $\psi(y)$ is a monotonically increasing function of $|y|$. Hence, $\psi(y)$ may be replaced by its expansion near the origin.

$$\psi(y)=\frac{4\pi}{3}\Gamma\left(1-\frac{3}{p}\right)\left(\frac{y}{i}\right)^{3/p} -\frac{(p-1)\pi}{18}\Gamma\left(1-\frac{1}{p}\right)\left(\frac{y}{i}\right)^{2+(1/p)}. \quad (121)$$

This is a general expression for Eq. (119). Therefore, we have

$$I(\bar{v}\Delta\omega'/R_0)=\frac{R_0}{2\pi\bar{v}}\int_{-\infty}^{\infty}\exp[\phi(\Delta\omega',y)]dy, \quad (122)$$

where

$$\phi(\Delta\omega',y)=i\Delta\omega'y-h\frac{4\pi}{3}\Gamma\left(1-\frac{3}{p}\right)\left(\frac{y}{i}\right)^{3/p} +h\frac{(p-1)\pi}{18}\Gamma\left(1-\frac{1}{p}\right)\left(\frac{y}{i}\right)^{2+(1/p)}. \quad (123)$$

In case (a), $\Delta\omega'\gg h$. The function $\exp(i\Delta\omega'y)$ is a rapidly oscillating function and e^{ϕ} oscillates rapidly except at points y_0 such that $d\psi/dy=i\Delta\omega$. Namely, the

|| This corresponds to the physical interpretation that only those which pass by the absorber within the time $0<t'<\tau$ affect the line shape.

neighborhoods of the points satisfying the equation,

$$\phi'(\Delta\omega',y_0)=i\Delta\omega'-\frac{4\pi}{p}\frac{h}{i}\Gamma\left(1-\frac{3}{p}\right)\left(\frac{y_0}{i}\right)^{(3/p)-1}$$
$$+\left(2+\frac{1}{p}\right)\frac{h}{i}\frac{(p-1)\pi}{18}\Gamma\left(1-\frac{1}{p}\right)\left(\frac{y_0}{i}\right)^{1+(1/p)}=0, \quad (124)$$

can contribute appreciably to the integral (122). When $p>3$, this is satisfied by y/i a large positive number, the third term being appreciable, or by y/i a small negative number, the second term being appreciable. From the branch cut of the integral (122), the first choice must be made and

$$y_0\sim i\left[\frac{18p\Delta\omega'}{h(p-1)(2p+1)\pi}\Big/\Gamma\left(1-\frac{1}{p}\right)\right]^{p/(p+1)}. \quad (125)$$

To integrate Eq. (122) around this point, ϕ may be expanded into Taylor series

$$\phi=\phi(\Delta\omega',y_0)+\tfrac{1}{2}\phi''(\Delta\omega',y_0)(y-y_0)^2+\cdots.$$

Thus, we have

$$I(\bar{v}\Delta\omega'/R_0)\sim\frac{R_0}{2\pi\bar{v}}\exp[\phi(\Delta\omega',y_0)]$$
$$\times\int_{-\infty}^{\infty}\exp[\tfrac{1}{2}\phi''(\Delta\omega,y_0)(y-y_0)^2]dy$$
$$=\frac{R_0}{\bar{v}}(-2\pi\phi'')^{-\frac{1}{2}}e^{\phi}. \quad (126)$$

This, with Eq. (125), gives the asymptotic behavior of $I(\Delta\omega')$. However, for $\Delta\omega'\gg h$, the intensity will be so low that it cannot be observed.

In case (b) ($\Delta\omega'$ small), on the other hand, it is of greater interest. The same method[101] as above will be applied. Since $\Delta\omega'\sim 0$, we have, from Eq. (124),

$$y_0=i\left\{\frac{72\Gamma[1-(3/p)]}{(p-1)(2p+1)\Gamma[1-(1/p)]}\right\}^{p/2(p-1)}. \quad (127)$$

Hence, Eq. (126) gives

$$I(\bar{v}\Delta\omega'/R_0)=\left(\frac{1}{16\pi^2h\Gamma[1-(3/p)]}\frac{p^2}{p-1}\right)^{\frac{1}{2}}$$
$$\times\left(\frac{(p-1)(2p+1)\Gamma[1-(1/p)]}{72\Gamma[1-(3/p)]}\right)^{(3-2p/4(p-1))}$$
$$\times\exp\left[-2h\left(\frac{p-1}{2p+1}\right)\frac{4\pi}{3}\Gamma\left(1-\frac{3}{p}\right)\left(\frac{72\Gamma[1-(3/p)]}{(2p+1)(p-1)\Gamma[1-(1/p)]}\right)^{3/(2p-2)}\right] \quad (128)$$
$$\times\exp\left[-\Delta\omega'\left(\frac{72\Gamma[1-(3/p)]}{(p-1)(2p+1)\Gamma[1-(1/p)]}\right)^{p/(2p-2)}\right].$$

Thus, at the position of the unperturbed frequency, the intensity falls off exponentially with both increasing h and increasing $\Delta\omega$. Both of these results disagree with Lindholm's result[57] such as const.$\times\Delta\omega^{-7/3}$ on this (violet) wing. However, the difference is very small[97] within the range of validity of the statistical theory. Actually, Huldt and Knall[12] observed that the intensity at the violet wing falls off as $\Delta\omega^{-2.35}$ which is very close to Lindholm's result.

For the red wing, $\Delta\omega'\ll 0$, Anderson and Talman obtained Eq. (100), the same result as obtained by Holstein, for large h. They showed that it is also valid for all h.

For $\Delta\omega'$ and h both small, the integrand in Eq. (118) is independent of $\Delta\omega'$ for $y<1$ since $\exp i\Delta\omega' y$ varies very little in this range. Therefore, the line shape should come from large y, say, Eq. (120) for $p=6$.

$$I(\bar{v}\Delta\omega'/R_0)=\frac{R_0}{2\pi\bar{v}}\int_{-\infty}^{\infty}\exp(i\Delta\omega' y-h\sigma y-hC)dy, \quad (129)$$

where

$$\sigma=\sigma_0 i^{-2/5}, \quad \sigma_0=\frac{2\pi}{5}\left(\frac{3\pi}{8}\right)^{-3/5}\Gamma(\tfrac{2}{5}),$$
$$C=1.91+2.63i.$$

Thus, we have

$$I(\bar{v}\Delta\omega'/R_0)=e^{-1.91h}\left[\frac{\sigma_0 h\cos(\pi/5)\cos 2.63h-\sin 2.63h[\Delta\omega'-\sigma_0 h\sin(\pi/5)]}{[\Delta\omega'-\sigma_0 h\sin(\pi/5)]^2+h^2\sigma_0^2\cos^2(\pi/5)}\right]. \quad (130)$$

[101] This method is called the method of steepest descents. See G. N. Watson, *Theory of Bessel Functions* (Cambridge University Press, New York, 1944), p. 235, or P. M. Morse and H. Feshbach, *Method of Theoretical Physics* (McGraw-Hill Book Company, Inc., New York, 1953), p. 440.

Therefore, the impact theory is valid only if the asymmetry term is small, namely, if $\Delta\omega'-\sigma_0 h\sin(\pi/5)$ is small for small h, as obtained by Spitzer.[54] Hence, the impact theory is applicable in the region near the peak. However, the center of the line at moderate pressures must be discussed by a numerical integration of Eq. (118) using Eqs. (119) and (120) for $\psi(y)$. Because of the fact that the line shapes thus calculated are almost indistinguishable from Lindholm's lines, for the central portion of the line the small y may reasonably correspond to the statistical theory and the large y to the impact theory.

It may be noticed that the above theory is exact when its basic assumptions about intermolecular forces are correct. Thus, in view of the fact that the intermolecular forces assumed above are not entirely realistic, although they have been used widely in theories, recalculation must be made. In this sense, the results[58] might be much improved, especially on the violet wing, if Eq. (118) is numerically integrated for the Lennard-Jones potential.

E. FINE STRUCTURE PRESSURE BROADENING AT ATOMIC LINES

Many experimental results have shown that the pressure-broadening scheme is different for different multiplet components. Half-widths, shifts, and asymmetries are definitely dependent on J, the inner quantum number.

1. Identical Atoms (See III B.a)

If Furssow and Wlassow's view[23] on resonance broadening (II. A. 1.a) is followed, the problem is reduced to the calculation of the dependence on J of the probability of energy transfer per collision between excited and unexcited identical atoms. This transfer would work as a radiation damping of the radiating atom and gives a broadened line of the dispersion type. Following Foley's calculation,[22] and making use of Eq. (55), we find the result for half-width to be

$$\Delta\omega_{\frac{1}{2}}=4\sqrt{3}\pi^4 N\frac{\hbar e^2}{m_e\Delta W_{JJ'}}\left(\frac{2J+1}{2J'+1}\right)^{\frac{1}{2}}f_{JJ'}, \quad (131)$$

with

$$f_{JJ'}=\frac{2m_e}{3\hbar^2}\frac{\Delta W_{JJ'}}{2J+1}\sum_{m'}|(J',m'|x|J,m)|^2.$$

Here $\Delta W_{JJ'}$ is the difference of the energies in the ground and excited states with inner quantum numbers J and J', respectively. $(J',m'|x|J,m)$ is the matrix element for dipole radiation, the square of which must be summed over all magnetic quantum numbers m' at the excited state for absorption. N is the number density of perturbers. For alkali doublets, the ratio of the half-width of the $J'=\frac{3}{2}$ and $J'=\frac{1}{2}$ component is approximately $\sqrt{2}$, when we neglect the difference of $\Delta W_{JJ'}$ for the two. Lindholm[102] calculated also quantum-mechanically the widths of Rb doublet components with the result of the ratio 1.6.

[102] E. Lindholm, Naturwissenschaften **30**, 533 (1942).

2. Perturbation Due to Foreign Atoms[28] (See III B.b)

If we assume the perturbers are spherically symmetric, we find the dispersion force is different for alkali atoms in the states $J=\frac{3}{2}$ and $\frac{1}{2}$ to the extent that the levels for $J=\frac{3}{2}$ split, according as $|m|=\frac{3}{2}$ and $\frac{1}{2}$. Therefore, the half-width for the $^2P_{\frac{3}{2}}$ component of the alkali resonance doublet is larger than that for the $^2P_{\frac{1}{2}}$ component. Using the value of dispersion energy given in (II. A. 1.b) and Foley's relation (58) with $p=6$, we find the half-width for the $^2P_{\frac{3}{2}}$ component is roughly 1.12 times larger than that of the $^2P_{\frac{1}{2}}$ component. But since the van der Waals force averaged over m for the two states is the same, no appreciable difference in shift is predicted. The difference of relative shift may come from the repulsive part of the interaction energy. Since the energy separation of the states $^2P_{\frac{3}{2}}{}^{|m|=\frac{3}{2}}$ and $^2P_{\frac{3}{2}}{}^{|m|=\frac{1}{2}}$ is dependent on the separation of the two atoms, greater asymmetry results for the $^2P_{\frac{3}{2}}$ component.

If the foreign gas pressure is high, perturbers may be arranged spherically symmetrically around the radiating alkali atom. Then the quadrupole moment of the atom in $J=\frac{3}{2}$ has no effect on the van der Waals force. Thus, the difference in half-width of the doublet components decreases as pressure increases, although at the wing of the line contour the above effect may still take place.

However, at high pressure, the repulsive part of the interaction energy may be predominant. Then, the energy may be found from the expression (5). The wave function is

$$\varphi=\varphi_n+\sum_j{}'\frac{(j|V|n)}{W_n-W_j}\varphi_j. \quad (132)$$

Starting from this wave function, one calculates the spin orbit energy, neglecting the atomic core effect,

$$\begin{cases} \frac{1}{2}l\zeta_{nl} & \text{if} \quad j=l+\frac{1}{2}, \\ -\frac{1}{2}(l+1)\zeta_{nl} & \text{if} \quad j=l-\frac{1}{2}, \end{cases}$$

$$\zeta_{nl}=d_{nl,\,nl}-(\hbar^2/|\Delta W|m_e^2c^2)\int_{r_0}^{\infty}|R_{nl}|^2\frac{e^2}{r}dr, \quad (133)$$

where $d_{nl,\,nl}$ is the unperturbed ζ_{nl} and r_0 is given by the pressure equation $p=-dE/4\pi r_0^2 dr_0$ with E from Eq. (5). The separation of the doublet decreases at higher pressure and one concludes that the shift of the $^2P_{\frac{3}{2}}$ component is smaller than that of the $^2P_{\frac{1}{2}}$, with no appreciable difference in half-width and asymmetry. At very high pressure, the relative magnitudes of the shifts would be reversed because of the distortion of the atomic core and its smaller screening effect on the nuclear charge.[28]

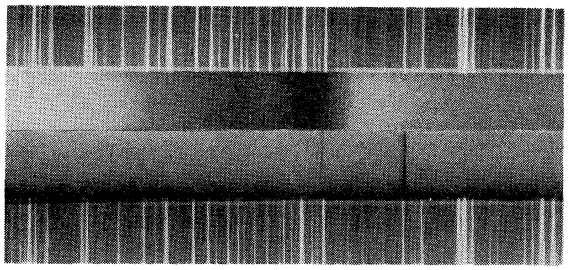

FIG. 1. The red shift and broadening of the blue doublet of Cs produced by argon (after Ch'en and Parker[103]).

Upper spectrum: Argon pressure = 128 atmospheres
Temperature = 262°C
Lower spectrum: Argon pressure = 1.09 atmospheres
Temperature = 150°C.

III. EXPERIMENTAL OBSERVATIONS

A. PRESSURE SHIFT AND BROADENING OF ATOMIC LINES

A review of the essentials of the experimental observarions published during the past twenty years on the effects of foreign gases at high pressures on atomic lines is given in the following five subsections. So far, except for Hg and Ag, all observations have been made upon the absorption lines of alkali atoms. The applied pressures of foreign gases have been increased to the order of a thousand atmospheres. For illustration, Fig. 1 is a picture showing the red shift and broadening of the blue doublet of cesium produced by argon, Cs(2)/A¶, at 128 atmospheres (262°C). Figure 2 is a plot of the line contours of the same doublet produced by argon and helium respectively.[103]

Customarily, the observations in absorption are carried out with a light source of continuous spectrum, as treated in the previous chapter. However, Kastha,[104] using a mercury lamp as a line source, observed how the Hg 2537 A line shape was modified after it has passed through an absorption cell of mercury vapor at about 100°C. He repeated the same observation with the sodium D line from a sodium lamp through a sodium vapor cell at 200–300°C. It was found that every line appeared separated into two components. Using the vapor pressure-temperature formula, one observes that the separation is linearly proportional to the pressure, and the two components extend to the position at which there was originally no appreciable intensity in the incident light. The change of frequency of the transmitted line may be caused by the absorbing and reemitting mechanism in the absorbing vapor. The intensity diminished with increase in pressure.

Furthermore, the broadening of certain lines caused by pressures of neutral particles can be observed in emission at electrical discharges, provided that those lines, for instance, mercury infrared line[105] (10140 A) or neon (5852 A)[106] are insensitive to the Stark broadening at low current.

1. The Shift of Low Member Lines

A resume of data for the shift** of the *first member* of the principal series (resonance lines) of a number of alkalis produced by *argon* is plotted in Fig. 3. The results for the Na−D lines were taken from Kleman and Lindholm's observations[107] and from Figs. 2 and 3 of Margenau and Watson's paper.[108] Their corrections for "thermal transpiration" are omitted and the shifts are converted into cm^{-1}. Hull's[109] and Ch'en's[110] results are used for the K and Rb resonance lines, respectively. Robin and Robin's[85] results are not drawn on the same scale but are attached as an insert, because (1) their data cover such a wide range of relative density that they could not be included in the figure without seriously reducing the size of the curve as presented, and (2) the precision of their results is rather low, the reciprocal dispersion being 160 A/mm at 7800 A and the errors of measurement being ±5 to ±25 A. For comparison, two of their readings are listed for r.d.†† = 100.

It is to be noted that for small values of r.d., below about 10, the shift increases approximately linearly with r.d. (at a rate of −0.32 cm^{-1}/r.d.). This linear dependence is predicted by the impact theory. For values of r.d. above 19 the curve deviates from linearity and then becomes linear again with about twice the

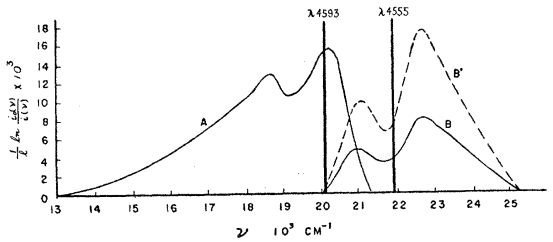

FIG. 2. The broadening and shift of the blue Cs doublet produced by argon and helium. Vertical lines: Position for unperturbed doublet. Curve A: for Cs(2)/A, $P = 127$ atmos; $T = 536$°K. Curve B: for Cs(2)/He, $P = 54.1$ atmos; $T = 519$°K. Curve B': for Cs(2)/He, $P = 54.1$ atmos; $T = 519$°K, plotted to the same atomic absorption coefficient scale as for Curve A. (After Ch'en and Parker[103]).

¶ Cs(2)/A is a notation to indicate the "second" member of the principal series of "cesium" under foreign gas pressure of "argon." This notation will be used very frequently hereafter.

[103] S. Y. Ch'en and W. J. Parker, J. Opt. Soc. Am. **45**, 22 (1955).

[104] G. S. Kastha, Indian J. Phys. **23**, 247 (1949); **27**, 67 (1953).

[105] R. Rompe and Schulz, Z. Physik **108**, 654 (1938); **110**, 223 (1938); P. Schulz, Physik. Z. **38**, 899 (1938).

[106] K. Lang, Acta Phys. Austriaca **5**, 376 (1951); Sitzber. IIa, **161**, 65 (1952).

** The notation for the sign of shift will be adopted as follows: If the shift is given in wavelength, "+" refers to red shift, and "−" refers to violet shift. If the shift is given in wave numbers, "+" refers to violet, and "−" refers to red shift. However, when a comparison of the amount of shift is described, its "absolute value" is always implied.

[107] B. Kleman and E. Lindholm, Arkiv Mat. Astron. Phys. **32B**, No. 4, Paper 10 (1946).

[108] H. Margenau and W. W. Watson, Phys. Rev. **44**, 92 (1933).

[109] G. F. Hull, Jr., Phys. Rev. **50**, 1148 (1936).

[110] S. Y. Ch'en, Phys. Rev. **58**, 1051 (1940).

†† Relative density will be hereafter abbreviated as r.d., the unit being the density of the same quantity of a foreign gas as that used in the experiment but at 0°C and 1 atmosphere.

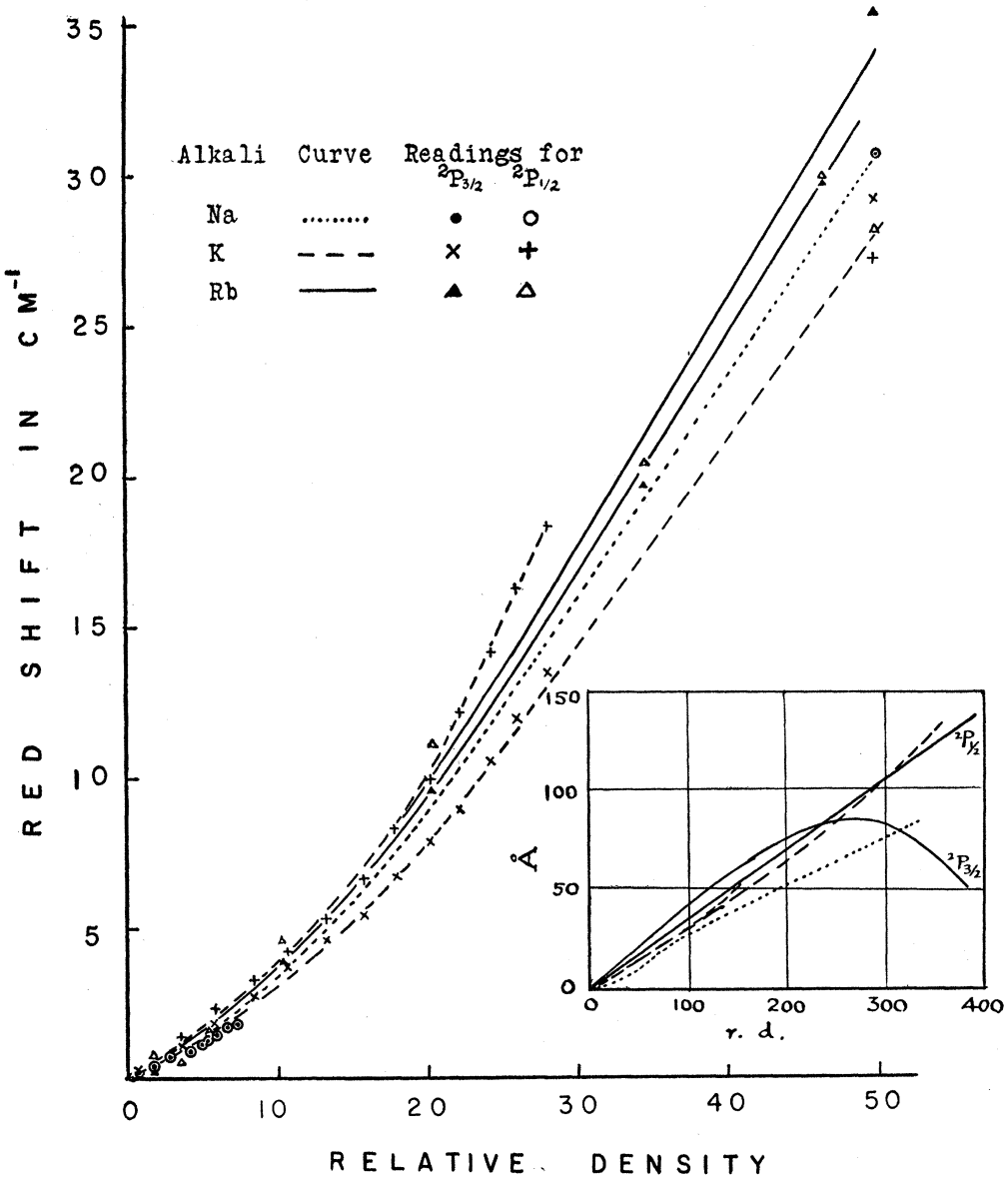

FIG. 3. The shift of the resonance lines of alkali metals produced by argon. Note: The ordinate for the main curve is shift in cm^{-1}, while that for the insert is shift in A. The abscissas are the relative densities of argon.

former slope (-0.71 cm^{-1}/r.d.) for r.d. above 25. Since it is almost impossible at present to get a correct idea of the atomic interaction forces for the excited states involved, a test of the theories as described in Part II can hardly be made. But, according to Margenau's rough approximation, the transition point is assumed to take place where the linear collision theory, Eq. (57), would give the same value for $\Delta\nu_m$ as is given by the quadratic statistical theory, Eq. (97), under the dispersion interaction alone, namely

$$N=\frac{12.88}{0.822\pi^3}\left(\frac{kT}{2m}\right)^{3/10}|\gamma|^{-3/5}. \tag{134}$$

γ can be evaluated through Eq. (3). The transition point N should be somewhere near 20 atmospheres for these cases as observed, and should move toward higher r.d. for smaller γ.

However, the shift does not show a quadratic relationship with r.d. when the pressure is high. According to the results of Robin and Robin the shift is essentially linear up to about r.d. 400 for all observed lines except the $^2P_{\frac{3}{2}}$ component of Rb. In the latter case the shift increases linearly for values of r.d. below 150, becomes a maximum at r.d. about 260, and then decreases for values of r.d. above this figure.

The shape of the shift *vs* r.d. curve for Hg λ2537

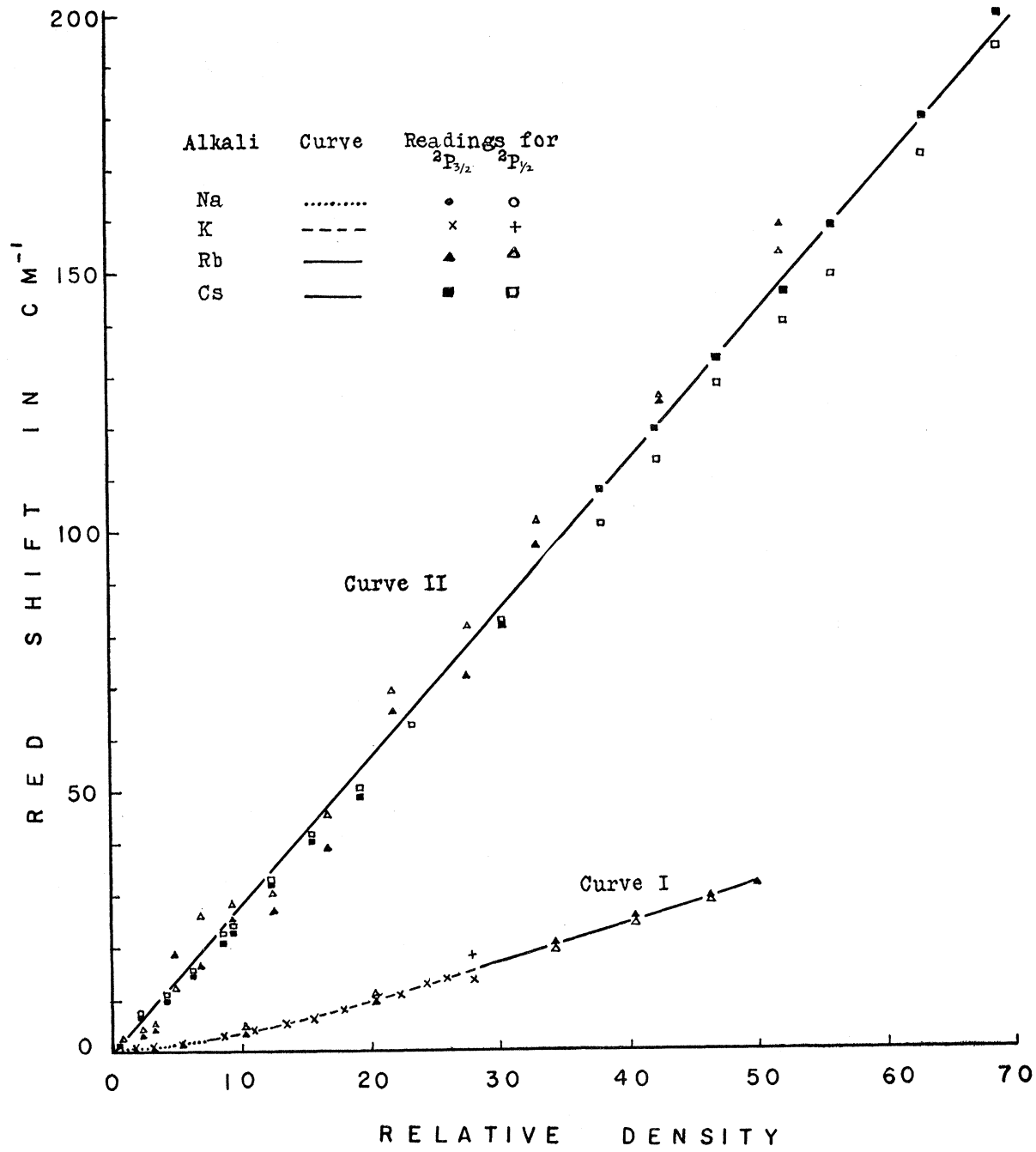

FIG. 4. Curve II is a plot of the shift of the second doublet of the absorption series of alkali metals (Rb and Cs) produced by argon; Curve I the corresponding curve for the first doublet plotted for comparison.

produced by argon is essentially the same as that for the resonance lines of the alkalis, except that the shift is about half as large in cm^{-1}, or twenty times smaller in A. The shift is -0.127 cm^{-1}/r.d.[111] for r.d.<50, and -0.323 cm^{-1}/r.d.[92] for $200<$r.d.<300. This relatively smaller shift for Hg λ2537 may be attributed to the small f value of the line in comparison with the f value of the alkali resonance lines.

The shift of Ag 3280, 3382 is -0.284 cm^{-1}/r.d. for r.d.<18.9,[112] and that of Pb 2833 is -0.5 cm^{-1}/r.d. for r.d.<8.[110]

A similar set of results for the shift of the second doublet of the absorption series of alkalis produced by

[111] Füchtbauer, Joos, and Dinkelacker, Ann. Physik **71**, 204 (1923).

[112] E. D. Clayton and S. Y. Ch'en, Phys. Rev. **85**, 68 (1952).

TABLE I. The mean shift of various low member lines per unit relative density, r.d., of various foreign gases under different ranges of r.d. values.

Absorption line/foreign gas	Mean shift/r.d. for low r.d. range $\langle\Delta\nu'\rangle$	Mean shift/r.d. for high r.d. range $\langle\Delta\nu''\rangle$	Ratio $\langle\Delta\nu''/\Delta\nu'\rangle$	Reference
(1) Na, K, Rb/A	(i) for resonance lines, $\langle\Delta\nu\rangle_1$			a
	-0.32 cm^{-1} (for r.d. <10)	-0.71 cm^{-1} ($25<$r.d.<200)	2.22	See Fig. 3
	(ii) for the second member of absorption series, $\langle\Delta\nu_2\rangle$			
	-2.81 cm^{-1} (for r.d. <70)	-6.03 cm^{-2} ($120<$r.d.<300)	2.14	Fig. 4
Ratio $\langle\Delta\nu\rangle_2/\langle\Delta\nu\rangle_1$	8.80	8.50		
(2) Hg 2537/A	-0.149 cm^{-1} (for r.d. <50)	-0.323 cm^{-1} ($200<$r.d.<300)	2.54	b
Ag 3280/A 3382/A	-0.28 cm^{-1} (for r.d. <19)			c
Pb 2833/A	-0.5 cm^{-1} (for r.d. <8)			
(3) Na, K, Rb/N_2	(i) for resonance lines, $\langle\Delta\nu_1\rangle$		2.5	See Fig. 5
	-0.27 cm^{-1} (for r.d. <15)	-0.67 cm^{-1} ($20<$r.d.<50)		
	(ii) for the second member of absorption series, $\langle\Delta\nu_2\rangle$			
K, Rb, Cs/N_2	-0.53 cm^{-1} (for r.d. <8)			
Ratio $\langle\Delta\nu\rangle_2/\langle\Delta\nu\rangle_1$	2.0			
Hg/N_2	-0.124 cm^{-1}/r.d. (for r.d. <50)	-0.139 cm^{-1} (r.d. 100)		b
(4) Rb, Cs/He	(i) for Rb resonance lines, $\langle\Delta\nu\rangle_1$			d
	$+0.24$ cm^{-1} ($^2P_{\frac{3}{2}}$)			
	$+0.13$ cm^{-1} ($^2P_{\frac{1}{2}}$) (for r.d. <50)			See Fig. 6
	(ii) for the second member of Rb, $\langle\Delta\nu_2\rangle$			e
	$+1.3$ cm^{-1} ($^2P_{\frac{3}{2}}$) (for r.d. <12)	$+3.6$(?) cm^{-1} ($^2P_{\frac{3}{2}}$) ($25<$r.d.<50)	2.8(?) ($^2P_{\frac{3}{2}}$)	
	$+0.53$ cm^{-1} ($^2P_{\frac{1}{2}}$) (for r.d. <12)	$+2.4$ cm^{-1} ($^2P_{\frac{1}{2}}$) ($25<$r.d.<50)	4.5($^2P_{\frac{1}{2}}$)	
Ratio $\langle\Delta\nu\rangle_2/\langle\Delta\nu\rangle_1$	5.4 ($^2P_{\frac{3}{2}}$) 4.1?($^2P_{\frac{1}{2}}$)			
	(iii) for the second member of Cs			f
	$+1.4$ cm^{-1} (?) (for $^2P_{\frac{3}{2}}$, r.d. <8)	$+3.51$ cm^{-1} (for $^2P_{\frac{3}{2}}$, $9<$r.d.<40)	2.5(?)	
	$+0.583$ cm^{-1} (for $^2P_{\frac{1}{2}}$, r.d. <12)	$+4.65$ (?) cm^{-1} (for $^2P_{\frac{1}{2}}$, $18<$r.d.<40)	7.9(?)	
(5) Hg 2537/He	$+0.079$ cm^{-1} (r.d. $=0$ to 500)			g

[a] See references 82, 85, 107–110.
[b] See references 84, 111.
[c] See reference 112.
[d] See reference 110.
[e] See reference 113.
[f] See reference 103.
[g] See reference 86.

argon is shown in Fig. 4. The results are taken from those of Ch'en and his associates.[103,113] The slope of the curve is -2.81 cm^{-1}/r.d. Robin and Robin[85] observed the shift of the second doublet of the principal series of Rb perturbed by argon for r.d. up to 300 with somewhat lower precision (± 2 to ± 10 A). The two components of the doublet fused into a single band as a result of broadening at pressures higher than r.d. 70. Their curve for r.d. less than 70 agrees very well with Ch'en's result. At r.d. about 90 the slope of the curve is practically doubled (-6.03 cm^{-1}/r.d. for $120<$r.d.<300).

It is apparent at once that for the first two doublets of the alkali absorption series, the shift (in cm^{-1}) is chiefly dependent on the member of the series and on the nature of the foreign gas but is essentially the same for all alkalis (with exceptions at high pressures, r.d.>200, at which the anomaly for the $^2P_{\frac{3}{2}}$ component of the Rb resonance lines is observed). As shown in Table I, the slope of the curve for the second doublet is about 8.6 times greater than that for the first doublet. The curves for argon are very straight up to r.d. 10 and 70 for the first and second doublets respectively (and up to r.d. 50 for Hg 2537). Above these respective r.d. the curves reach slopes something more than double the value for low r.d.

The experimental observations as described in the previous paragraph indicate that the force laws for the

[113] S. Y. Ch'en and D. A. Kohler, Phys. Rev. **90**, 1019 (1953).

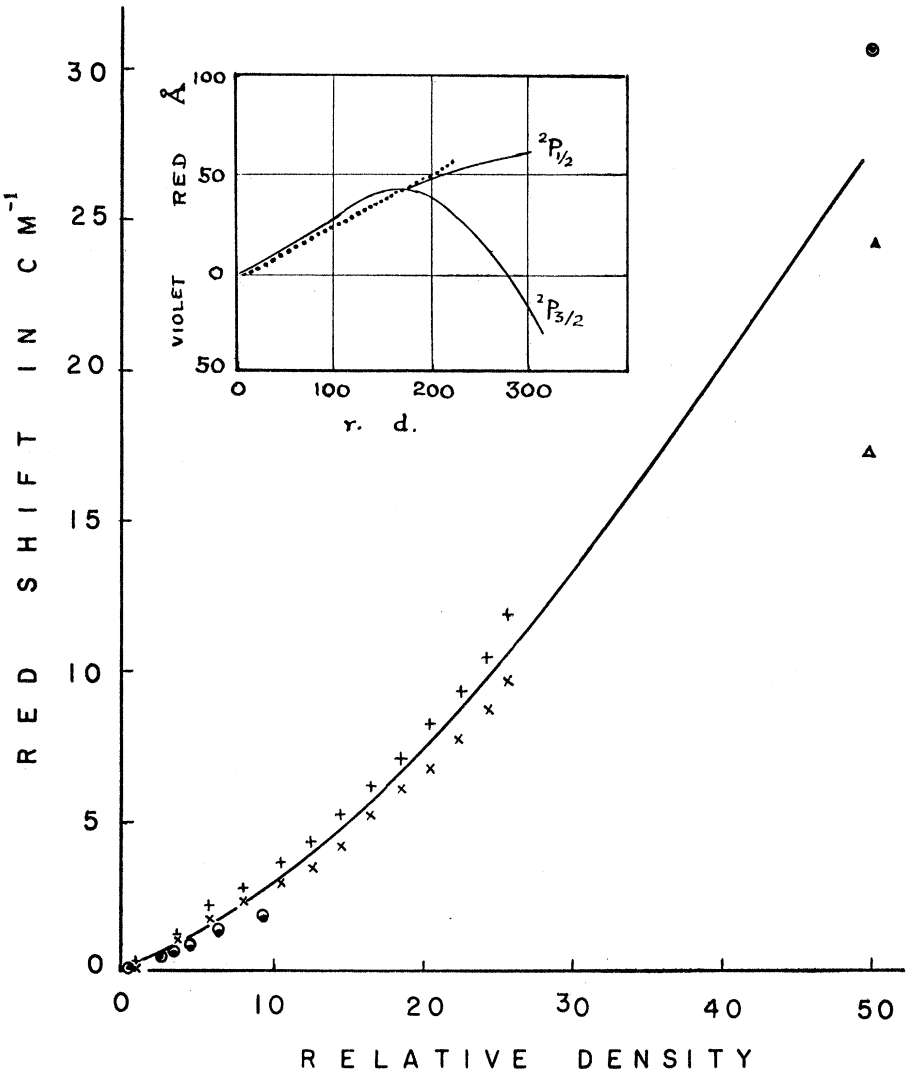

FIG. 5. The shift of the resonance lines of alkali atoms produced by nitrogen, plotted in the same way as in Fig. 3.

excited states of the two series lines are different. Because of the fact that the shift of the second member is greater than that of the first member, the γ value for the excited state of the second member should be greater. According to Eq. (134) the transition point for the second member would be smaller if the same type of dispersion forces are assumed for both members.

Quite plentiful data are also available for *nitrogen* and helium. As shown in Fig. 5, N_2 also produces a red shift and the curve swings up slightly at r.d. around 20. The shift for N_2 is a little less than that for argon. The points for the Na—D lines are taken from Margenau and Watson[108] and those for the K resonance lines from Hull.[109] The points in the figure for r.d. 50 were obtained by interpolation from Robin's result,[84] which is again shown as an insert. It is not easy to observe the pressure effect of N_2 or H_2 when the pressure is higher than 30 atmospheres because the alkali will start to react with the gas.[110] Data for the second member of the principal series can be obtained from Watson and Margenau's[114] result for K, from Ch'en and Pao's[115] result for Rb, and from Füchtbauer and Gössler's[116] result for Cs. The shift of the second member [-0.60 and -0.45 cm^{-1}/r.d. for K(2)/N_2 and Rb(2)/N_2, respectively] is twice that for the first member of the principal series. All authors reported that the shift of the third member is less than that of the second member by about 40% for Na, 30% for K, and 60% for Cs. According to Robin's result, as shown in the inserts of Fig. 5, as the pressure of N_2 increases the shorter wavelength ($^2P_{\frac{3}{2}}$) component of the Rb reso-

[114] W. W. Watson and H. Margenau, Phys. Rev. 44, 748 (1933).
[115] S. Y. Ch'en and C. S. Pao, Phys. Rev. 58, 1058 (1940).
[116] C. Füchtbauer and F. Gössler, Z. Physik 87, 89 (1934).

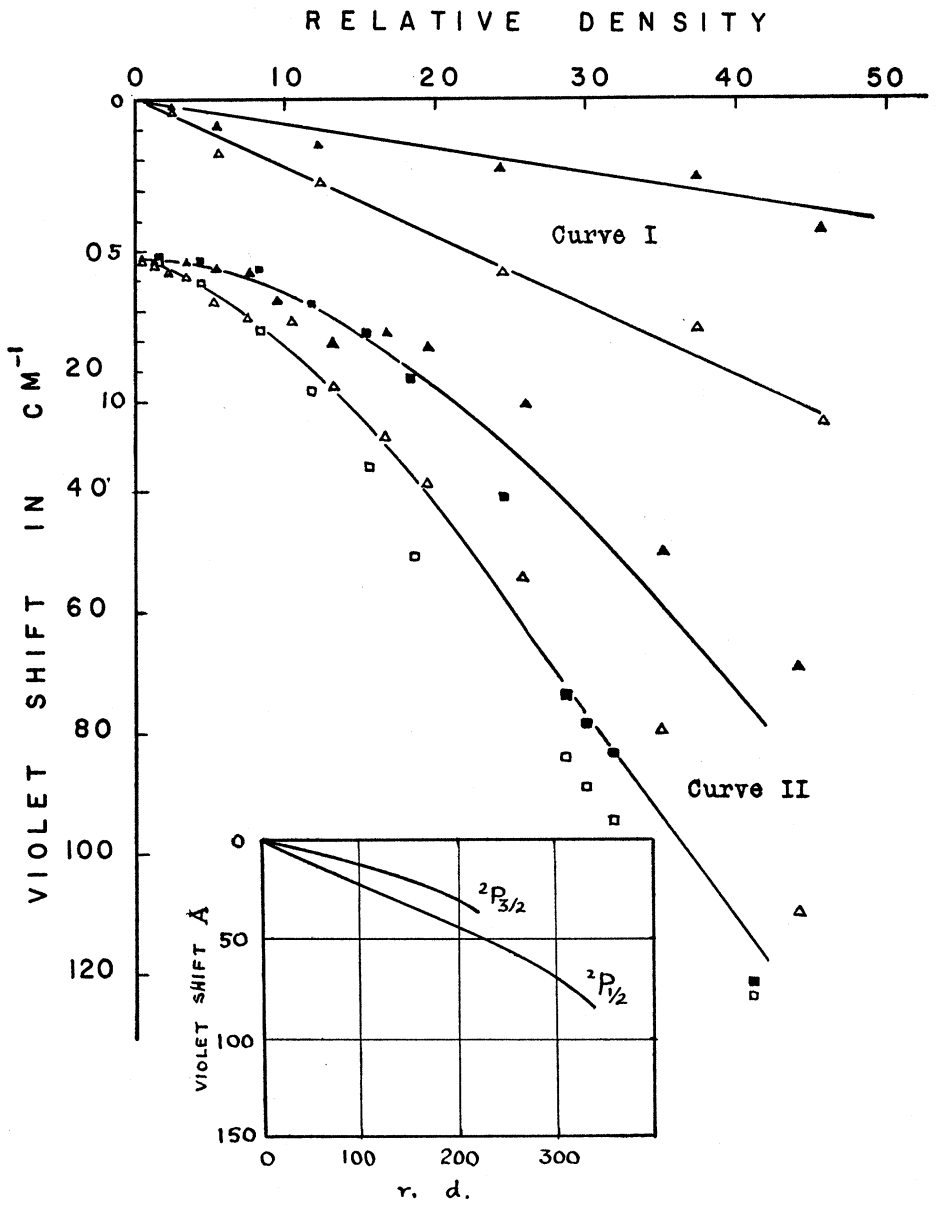

FIG. 6. The shift of the first doublet (Curve I) and of the second doublet (Curve II) of the absorption series of alkali atoms (Rb and Cs) produced by helium. The scale of the ordinate for Curve I is five times that for Curve II. The insert is the shift in A *vs* r.d. plot of the Rb resonance lines produced by He.

nance line first shifts towards *red*, then, at r.d. around 160, the shift swings back quite rapidly, and then, when the r.d. was over 270, the shift turns to *violet* with respect to the position of the line with no foreign gas pressure. This would lead us to believe that when the pressure is sufficiently high, say many thousand atmospheres, the shift will be toward violet for all gases, at least for all resonance lines. (For higher member lines, the potential curves of the excited states could cross each other at some magnitude of interactions. The distortion of levels due to crossing will prevent us from foreseeing, without detailed calculation, whether the shift will always be toward the violet at very high pressures.)

Helium produces a strong violet shift, as shown in Fig. 6 and Table I. The results are those observed by Ch'en and his associates[103,110,113] for Rb and Cs. The shift of the second doublet is about five times greater than that for the first doublet. Füchtbauer and Gössler observed that there was a switch from red to violet shift for Cs(1)/He to Cs(2)/He, and for Cs(2)/Ne to Cs(3)/Ne. The shift of Hg 2537 by helium was also toward violet with a value of $+0.031$ cm^{-1}/r.d.[86b] to $+0.079$ cm^{-1}/r.d.[86a] (-0.0051 A/r.d.).

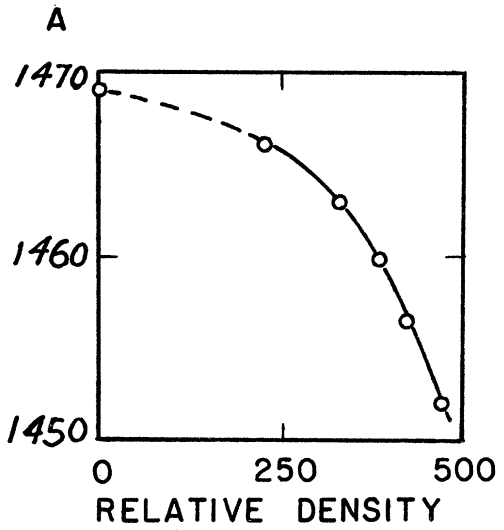

FIG. 7. The displacement of the resonance lines of xenon due to the presence of argon (after S. Robin and J. Romand[120]).

Observations for *neon* were made on the *second doublet* of the Rb principal series up to r.d. 8 by Ny and Ch'en.[117] The shift produced by Ne is very small. The $^2P_{\frac{1}{2}}$ component showed a weak shift toward violet while the $^2P_{\frac{3}{2}}$ component shifted slightly toward red.

Hydrogen produces a red shift for the Na−D lines[107,108] and Hg 2537 at low pressures,[85] but a violet shift at 120 atmospheres.[86,118] It gives a violet shift for the $^2P_{\frac{1}{2}}$ component and a red shift for the $^2P_{\frac{3}{2}}$ component of the first two absorption doublets[110,115] of Rb.

The effect of *temperature* on the broadening and shift of the resonance lines of K in the presence of nitrogen was studied by Hull.[119] An increase in shift and half-width due to increase in temperature was observed at low pressures (r.d.<7). The effect decreased with increased pressure, and is entirely negligible for r.d. higher than 9, in agreement with Margenau's theory. The last fact was also observed by Robin[83] with Na/A.

Robin and Romand[120] observed the shift of Xe 1469 as a function of the r.d. of argon compressed from 1 to 800 kg/cm² ($T=20°$C). Except for indications of a slight red shift at low pressures, the shift was about −3 A (toward the violet) for r.d. 200, and then increased rapidly as further pressure was added. The results are shown in Fig. 7. It is particularly interesting that argon produced *violet* shifts and *violet* asymmetry for Xe λ1469 in contrast to all other observations with argon. The different behavior in this case, in contrast to the effects observed with alkali atoms, may be due in part to the fact that both argon and xenon have completed electron shells in the ground states. Xenon is unfortunately opaque in the region of the absorption line of argon λ1048, preventing an otherwise interesting observation of the effect of xenon pressure on argon lines.

It is interesting to note that the ratio of shifts per r.d. of the first two member lines is nearly the same for argon, whether at low or high r.d., but the ratio is different for other perturbing gases.

2. Shift of the High Member Lines

The displacement of the high members of the principal series of Rb produced by He, Ne, and A[121] for pressures up to relative density 6 and that of Na, Rb, and Cs produced by H_2 and N_2[122] for pressures up to r.d. 5 were observed by Ny and Ch'en; that of K produced by He and that of Rb produced by neon, up to r.d. of about 20 were observed by Füchtbauer, Heesen, and Hansler.[123] Their results are summarized in Fig. 8.

Füchtbauer and Reimers[124] also observed the effect on the high terms of Cs of these gases and of paraffin vapors, but did not vary the pressure. The displacement was found to be proportional to the r.d., dependent on the nature of foreign gases but independent of the nature of the absorbing atoms, in agreement with the theoretical treatment by Fermi.[125] To illustrate how the shift/r.d. varies with various high member lines, Füchtbauer's[123] data for K/He is chosen. The slopes of the straight lines for the violet shift *vs* r.d. plots are 5.25, 6.20, 5.75, 6.2, 6.2, 5.63, 5.60, 5.50 cm^{-1}/r.d. for the 4th‡‡ up to the 11th members, respectively. Other gases that produced a violet shift, *viz.*, H_2, Ne, and N_2, had curves of shape similar to those for He, the shifts for Ne and N_2 being very small. Gases that produced a red shift are A, Kr, Xe, methane, ethane, and propane.[124] The shift of the high member lines of Na displaced by Cs vapor was alsome asured by Füchtbauer and Heimann[126] and was found to follow the same trend in the series as those produced by argon.

To summarize the results of observations, for gases that produce a violet shift, the shift decreases with the molecular weight (or polarizability) of the gas. The shift first increases with the ordinal number of the lines in the series, then attains a weak maximum at the 5th to 8th members, and finally approaches a constant value for lines higher than the 15th member up to the limit of the series.[121,122] For gases that produce a *red* shift, the shift *increases* with the molecular weight (or polarizability) of the gas. The shift *vs* series member plots have the same shape as those in the first case but there is *no* such weak maximum around the 5th–8th

[117] T. Z. Ny and S. Y. Ch'en, Phys. Rev. **52**, 1158 (1937).
[118] This change in direction of shift was also observed by J. Granier-Mayence and S. Robin, J. phys. radium **13**, 494 (1952), with the No band perturbed by A.
[119] G. F. Hull, Jr., Phys. Rev. **51**, 572 (1937).
[120] S. Robin and J. Romand, Compt. rend. **231**, 1455 (1950).
[121] T. Z. Ny and S. Y. Ch'en, Phys. Rev. **51**, 567 (1937).
[122] T. Z. Ny and S. Y. Ch'en, Phys. Rev. **54**, 1045 (1938).
[123] C. Füchtbauer and W. V. Heesen, Z. Physik **113**, (1939); and reference 130.
[124] C. Füchtbauer and H. J. Reimers, Z. Physik **97**, 1 (1935).
[125] E. Fermi, Nuovo cimento **11**, 157 (1934).
‡‡ There might be something erroneous about their[82] data on the shift of the $1s-5p$ line, as given on page 327 of that paper, if the line was not shifted towards red for r.d. less than 2.
[126] C. Füchtbauer and G. Heimann, Z. Physik **110**, 8 (1938).

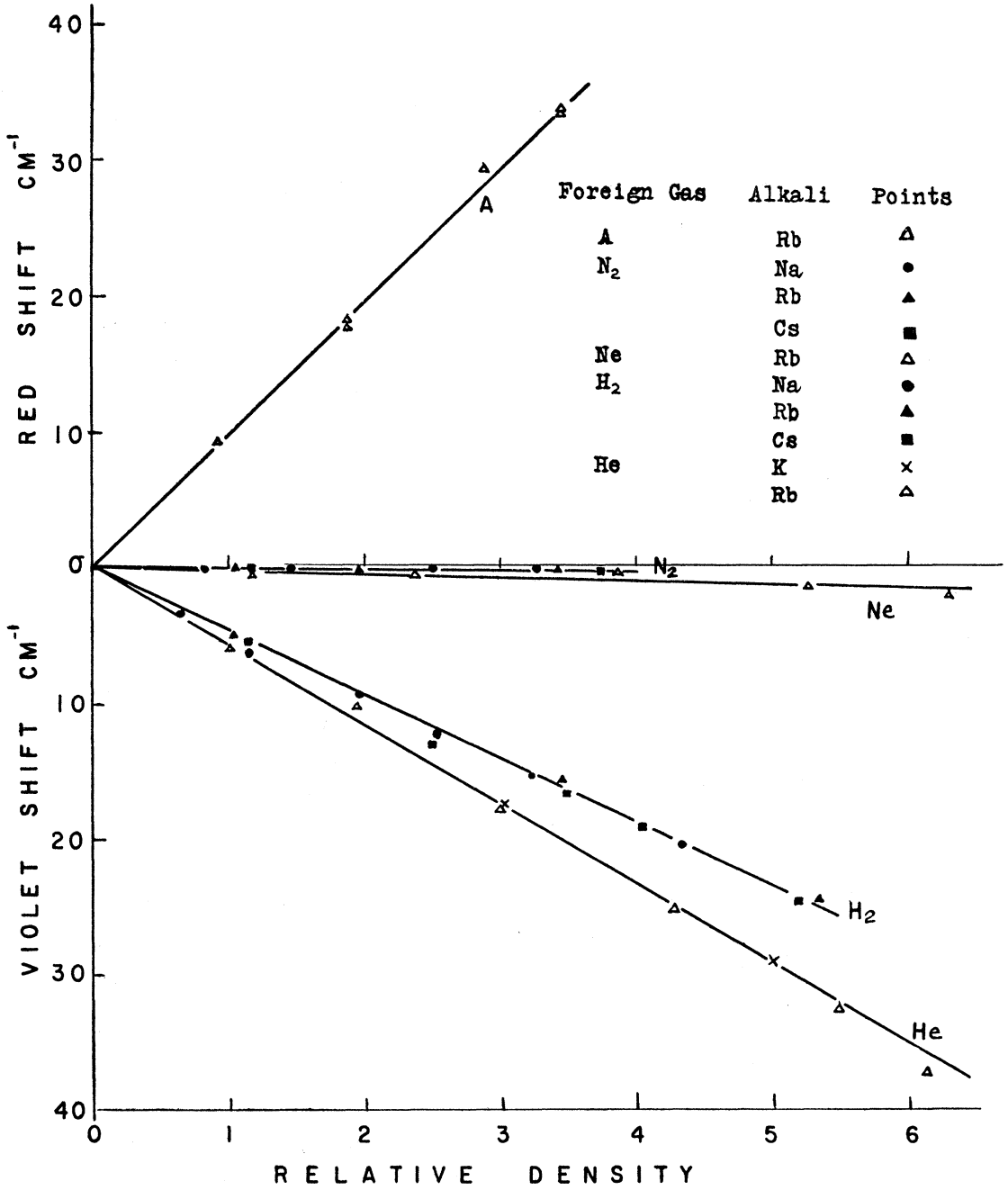

FIG. 8. The mean shift of the high members of the principal series of alkali atoms produced by various gases.

members. According to Fig. 8, the observed shift (in cm^{-1}/r.d.) for A, N_2, Ne, H_2, and He are -9.7, $+0.1$, $+0.2$, $+4.7$, and $+5.9$, respectively.

According to Fermi's theory§§ the effective collision cross section of single atoms of perturbing gases for electrons at very low relative velocity can be deduced from observation of the constant shifts of the high series lines of the alkalis at low pressure. The method is to take the difference between the observed shift Δ and the shift, Δ_ϵ, due to the polarization of the foreign atoms in the field of the core of the alkali atom to obtain Δ_σ, the shift caused by the perturbation of the valence electron by the foreign atoms.

$$\Delta_\epsilon = 20e^2(\epsilon_0-1)N^{4/3}/8\pi hcL_0$$
$$= 0.000922(\epsilon_0-1)N^{4/3}/L_0 \text{ cm}^{-1}, \quad (135)$$

§§ Sampson and Margenau have adapted this theory to the broadening of impurity levels in semiconductors, which arises from collisions between a hole and the phonons. D. Sampson and H. Margenau, Phys. Rev. **103**, 879 (1956).

TABLE II. The effective cross section of certain gases for electrons of very low velocity as measured by different authors.

Gas	By optical method, cm^2/cm^3	By electrical method, cm^2/cm^3 (kinetic energy of electron)
He	11.7[a], 15.5,[b] 15.5[c]	15.3 (0.03 ev)[i]
Ne	0.23,[b], 0.24[c]	3.13 (0.2 ev)[j]
A	42,[a] 25.2,[b] 23.7[c]	2.6 (0.03 ev)[i]
H_2	12.3,[a] 14.0[d]	24.4[k]
N_2	0.93,[a] 5,[b] 2.0[d]	10[k]
Kr	121.3[e]	20 (0.6 ev)[l]
Xe	412[f]	58 (0.2 ev)[l]
Hg	35–37.2[f]	250–300 (1 ev)[m]
CH_4	73[g]	
C_2H_6	120[g]	
Cs on Na	25.9×10^{3}[h]	1.1×10^{3}[n]

[a] E. Amaldi and E. Segrè, Nuovo cimento **11**, 145 (1934).
[b] Füchtbauer, Schultz, and Brandt, Z. Physik **90**, 403 (1934).
[c] See reference 121.
[d] See reference 122.
[e] C. Füchtbauer and H. J. Reimers, Z. Physik **95**, 1 (1935).
[f] C. Füchtbauer and F. Gössler, Z. Physik **93**, 648 (1935).
[g] See reference 124.
[h] See reference 126.
[i] See reference 127a.
[j] See reference 127b.
[k] See reference 114a.
[l] See reference 127c.
[m] See reference 127d.
[n] See reference 127e.

where L_0 is Loschmidt's number, ϵ_0 the dielectric constant of the foreign gas under normal conditions, and N the number of atoms per cm^3. Δ_σ is related to the effective cross section of a single atom of the perturbing gas, σ, by

$$\Delta_\sigma=\pm hN\sigma^{\frac{1}{2}}/4\pi^{\frac{3}{2}}mc=\pm1.09\times10^{-11}N\sigma^{\frac{1}{2}}\ cm^{-1}. \quad (136)$$

The Δ_σ values (in cm^{-1}) for He, Ne, A, Kr, Xe, H_2, and N_2 were found to be $+6.1$, $+0.7$, -7.95, -17.2, -31.6, $+5.85$, and $+2.2$, respectively. By multiplying σ by $L_0/760=3.54\times10^{16}$, the effective cross section for all atoms in 1 cm^3 at 1 mm pressure and 0°C is obtained as tabulated in the second column of Table II. The values tabulated in the last column were obtained by Wahlin and others[127] using a direct electrical method for the cross section at electron energies given in parentheses. The minimum energy of an electron attainable in the measurement is that of the thermal motion per electron (0.03 ev at room temperature).

Fermi's equations were derived for spherically symmetrical molecules. An extension of his treatment to axially symmetrical molecules as given by Reinsberg[128] showed that Fermi's equations can also be applied to them without any appreciable correction. Furthermore, Firsov[129] repeated the calculation in a more general way and found that Fermi's theory is good for shift. In view of the strong dependence of the cross section on electron velocity, Fermi's theory is satisfactory at low pressures and provides the only values at present available for the low-velocity limit of elastic collision cross section of different atoms and molecules.

The results of all authors indicate that when the relative density of the perturbing gas is high, namely above 5, the shift Δ_σ increases more rapidly than linearly with r.d. Thus, this gives the upper limit in pressure for the validity of Fermi's equations, as easily deduced from the assumption he made in the derivation. This validity can be clarified in another way. Namely, according to Fermi's equation, the shift should pass from violet to red with increasing relative density. This phenomenon is not observed, even when the Ne pressure is increased to a r.d. of 16, on the high series members of Rb.[130]

The continuous absorption of Cs vapor beyond its series limit was found to be reduced in intensity, and the maximum absorption shifted toward violet in the presence of all gases employed by Ditchburn and Harding,[131] *viz.* He, Ne, A, Kr, Xe, N_2, H_2, D_2, and C_6H_6.

3. The Broadening of the Low Member Lines

The broadening of the first and second doublets of the principal series of a number of alkalis produced by argon is given in Fig. 9. The curves are consistently linear for the resonance lines of Na[108] and Rb[110] with H_2, A, N_2, and He, A, respectively. For the resonance lines of K[109] the curve swings slightly upward for high relative densities. The slopes of these curves are given in the fourth column of Table III. These values are accurate only when the r.d. is low.|||| The strictly linear curves are indicated by "*L*" in column 4. Degrees of departure from linearity are indicated by *l* or *l*-. Robin, Robin, and Vodar[82] made a determination of the half-widths of the Na-D lines broadened by argon up to about 340 r.d. The half-widths, $\Delta\nu_{\frac{1}{2}}$, increase linearly with r.d. up to about 80 and then the curve swings upward gradually as shown in Fig. 10. The broadening of Hg 2537 produced by H_2 and He was measured recently by Robin.[86] The $\Delta\nu_{\frac{1}{2}}$ (in cm^{-1}) *vs* r.d. curve for both gases are nearly the same, and have a slope of 0.363 cm^{-1}/r.d. up to r.d. 430, then swing gradually upward.

The half-width *vs* r.d. curves obtained so far for the *second member* of the principal series of all alkalis are linear for low r.d., say up to 8, and for all gases. When the r.d. is high, the curve for argon still follows the linear relationship as before, while for helium the curve indicates a definite upward swing.[103,113] In plotting Curve II of Fig. 11, only readings for the $^2P_{\frac{1}{2}}$ component were used. The curve for the $^2P_{\frac{3}{2}}$ component was left

[127] (a) H. B. Wahlin, Phys. Rev. **37**, 260 (1931); (b) C. Normand, *ibid.* **35**, 1217 (1930); (c) C. Ramsauer and R. Kollath, Ann. Physik **3**, 536 (1929); **4**, 91 (1930); (d) R. B. Brode, Proc. Roy. Soc. (London) **A109**, 397 (1925); (e) R. B. Brode, Phys. Rev. **33**, 1069 (1929).
[128] (a) C. Reinsberg, Z. Physik **93**, 416 (1935); (b) C. Reinsberg, Z. Physik **105**, 460 (1937).
[129] O. B. Firsov, Doklady, Akad Nauk S.S.S.R. **61**, 357 (1949); Zhur. Eksptl. Theort. Fiz. **21**, 627 and 634 (1951).
[130] C. Füchtbauer and G. Hansler, Physik. Z. **41**, 555 (1940).
[131] R. W. Ditchburn and J. Harding, Proc. Roy. Soc. (London) **A157**, 66 (1936).
|||| When the r.d. was high, say above 10, the slopes were usually higher (see reference 116 and 117 in comparison with references 103 and 113).

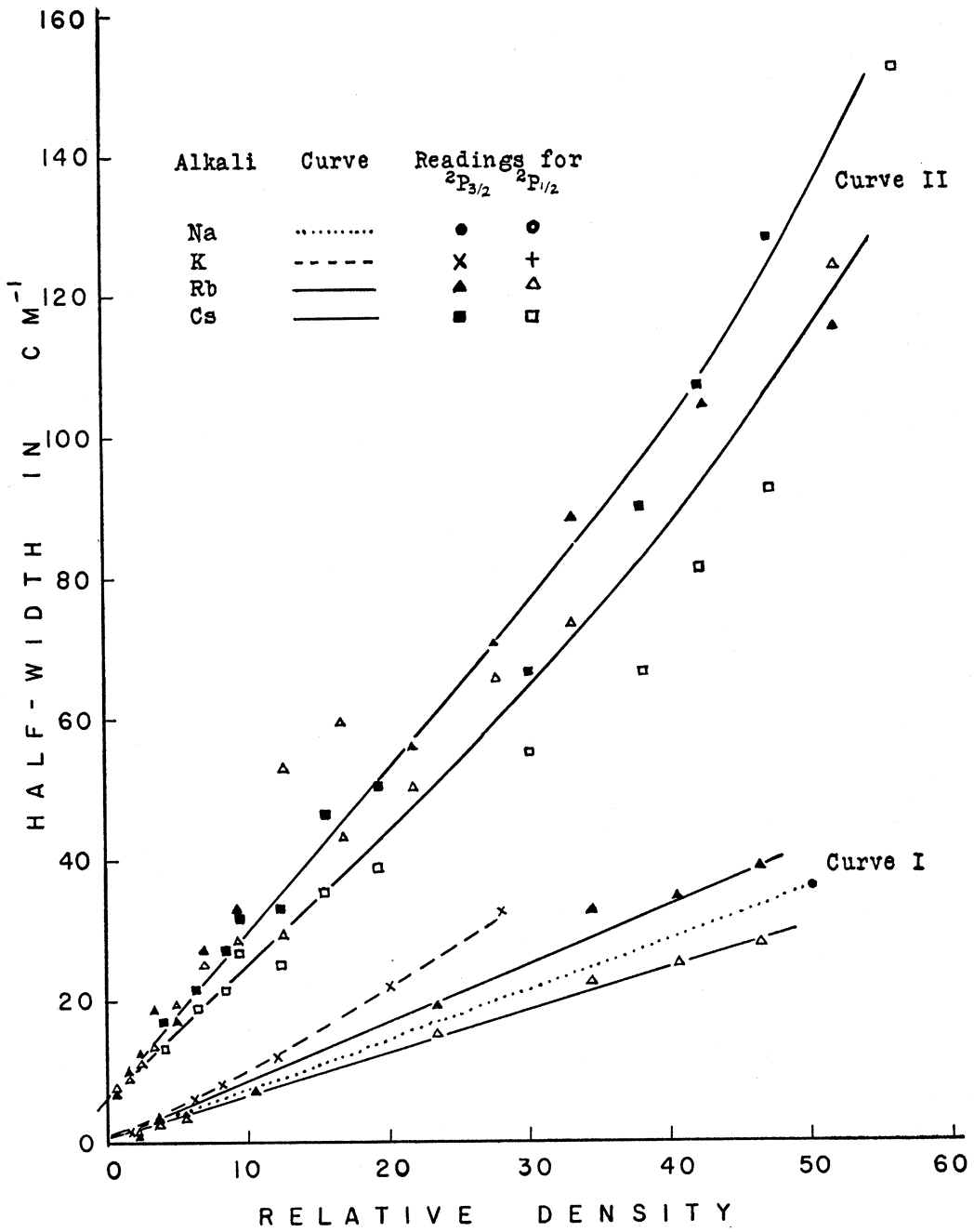

FIG. 9. Pressure broadening of the first (Curve I) and the second (Curve II) doublets of the principal series of alkali atoms produced by argon.

out because of its overlapping with the Rb—He diffuse band appearing at the short wavelength side.[103] The $\Delta\nu_{\frac{1}{2}}$ *vs* r.d. plot for Hg (2537)/He is[86b] linear up to r.d. 110 approximately.

The violet asymmetrical broadening of the resonance lines of K under the vapor pressure of Rb (150 mm Hg) was observed by Ch'en.[132] There is no measurable shift.

The temperature effect on line widths is much complicated. Theoretically, it is given by Eq. (37) (Lorentz) as $\sqrt{T}$ or by (57) as $T^{3/10}$ with N kept constant at low pressures. However, experimentally, the confirmation of either of them has not been established. Orthman[133] observed $\sqrt{T}$ effect with Hg 2537/H_2, while Horodoniczy and Jablonski,[134] very small T effect with Hg 2537/He

[132] S. Y. Ch'en, Phys. Rev. **73**, 1470 (1948).

[133] W. Orthman, Ann. Physik **78**, 601 (1925).

[134] H. Horodnicsy and A. Jablonski, Nature **142**, 1122 (1938); **144**, 594 (1939).

TABLE III. The shift ($\Delta\nu_m$) and the broadening ($\Delta\nu_{\frac{1}{2}}$) of various absorption lines of alkali atoms produced by unit relative density of foreign gases for low relative densities.

Gas	Lines	$\Delta\nu_m$ cm^{-1}/r.d.	$\Delta\nu_{1/2}$ cm^{-1}/r.d.	$\frac{\Delta\nu_{1/2}}{\Delta\nu_m}$	ρ Å	Authors
A	Na-5896	−0.196, −0.248	0.742 L, 0.72 L	3.79, 2.9	11.2	Kleman and Lindholm[a]
	Na-5890	−0.213	0.689 L	3.23		Margenau and Watson[b]
A	K-7699	−0.420	1.01 *l*	2.4	14.4	Hull[c]
	K-7665	−0.360		2.8		
A	K-4047	−0.92	2.20 *l*	2.4	22.2	Füchtbauer and Reimers[d]
	K-4044	−0.83	2.58 *l*	3.1		
A	Rb-7947	−0.51 ?	0.627 *L*	1.2	13.4	Ch'en[e]
	Rb-7800		0.855 *L*	1.7		
A	Rb-4216	−1.2	2.21 *L*	1.8	24.0	Ny and Ch'en[f]
	Rb-4202	−1.0	2.56 *L*	2.6		
A	Cs-4593	−2.69	1.63 *l*	0.6	22.2	Ch'en and Parker[g]
	Cs-4555		2.22 *l*			
A	Cs-4555	−0.53	1.27 *l*	2.4	18.0	Füchtbauer and Gössler[h]
	Cs-3876	−2.12	2.69	1.3	26.2	
N_2	Na-5896	−0.214	0.49 *L*	2.3	8.96	Margenau and Watson[b]
	Na-5890	−0.223	0.49 *L*	2.2		
N_2	K-7699	−0.277, −0.360	0.56 *l*-, 0.82 *l*-	2.0, 2.3	10.2, 12.3	Watson and Margenau,[i] Hull[c]
	K-7665	−0.261, −0.300	0.56 *l*-, 0.82 *l*-			
N_2	K-4047	−0.83, −0.81	1.65 *L*, 1.39 *L*	2.0, 1.7	17.5, 16.1	Füchtbauer and Reimers[d]
	K-4044	−1.02, −0.70	1.89 *L*	1.9, 2.0		Watson and Margenau[i]
N_2	K-3447	−0.57	...	...		Watson and Margenau[i]
	K-3446	−0.62	...	...		
N_2	Rb-4216	−0.52 ?	1.51 *l*-	2.9 ?	16.3	Ch'en and Pao[j]
	Rb-4202	−0.38 ?	1.01 *l*-	2.7 ?		
N_2	Cs-4555	−0.58	0.90 *l*	1.6	14.1	Füchtbauer and Gössler[h]
	Cs-3876	−0.50	1.53 *l*	3.1	18.4	
Ne	K-4044	−0.16	0.82	5.1	11.3	Füchtbauer and Reimers[d]
	K-4047		0.71	4.4		
Ne	Rb-4216	+0.22	1.30 *L*	5.9	13.8	Ny and Ch'en[f]
	Rb-4202	−0.16	0.73 *L*	4.5		
Ne	Cs-4555	−0.11	0.47	4.3	9.6	Füchtbauer and Gössler[h]
	Cs-3876	−0.33	0.91	2.8	13.3	
H_2	Na-5896	−0.189	0.82 *L*	4.3	7.16	Margenau and Watson[b]
	Na-5890	−0.186	0.82 *L*	4.4		
H_2	K-4047	−0.23	2.39	10	13.0	Füchtbauer and Reimers[d]
	K-4044	−0.33	2.88	8.5		
H_2	Rb-7947	+0.2 ?	0.65 ?	3.5 ?	7.01 ?	Ch'en[e]
	Rb-7800	−0.2 ?	0.87 ?	4.4 ?		
H_2	Rb-4216	+0.45 ?	1.87	4.1 ?	12.4	Ch'en and Pao[j]
	Rb-4202	−0.14 ?	2.86	20 ?		
He	K-4047	Small	1.45		12.3	Füchtbauer and Reimers[d]
	K-4044		2.02			
He	Rb-7947	+0.228	0.595 *L*	2.6	7.8	Ch'en[e]
	Rb-7800	+0.092	0.735 *L*	8.0		
He	Rb-4216	+0.93	2.77 *L*	3.0	14.5	Ny and Ch'en[f]
	Rb-4202	+0.43	1.88 *L*	3.4		
He	Cs-4555	+0.39	1.28 *l*	3.3	10.8	Füchtbauer and Heesen[k]
He	Cs-3876	+1.79	2.88 *l*	1.6	16.2	
He	Cs-3217	+5.25	4.7 ? *l*-	0.9	20.7 ?	
He	Cs-3102	+6.20	2.8 ? *l*	0.5		
He	Cs-3034	+5.75	1.6 *L*-	0.3		
He	Cs-2992	+6.2	1.6 *L*	0.3		
He	Cs-2963	+6.2	1.5 *L*	0.2		
He	Cs-2943	+5.63	1.5	0.3		
He	Cs-2928	+5.60	1.5	0.3		
He	Cs-2917	+5.50	1.6	0.3		
CH_4	K-4047	−1.02	1.77	1.7	13.7	Füchtbauer and Reimers[d]
	K-4044	−1.40	1.96	1.4		
C_2H_6	K-4047	−1.16	1.53	1.3	16.2	
	K-4044	−1.61	1.80	1.1		
C_3H_8	K-4047	−1.25	1.35	1.1	17.8	
	K-4044	−1.27	1.72	1.0		

[a] See reference 107.
[b] See reference 108.
[c] See reference 109.
[d] See reference 124.
[e] See reference 110.
[f] See reference 117.
[g] See reference 103.
[h] See reference 116.
[i] See reference 114.
[j] See reference 115.
[k] See reference 123.

and A. On the other hand, Hull[107] found very large T effect on the K resonance line perturbed by nitrogen, about twenty times larger than what the theories predict, at low pressures. Furthermore, Horodniczy and Jablonski observed a reduction of asymmetry with temperature, which has been confirmed by Gorodnichus[135] with Hg/A.

4. Broadening of the High Member Lines

The broadening of high member lines is found to be linearly proportional to the r.d. as is the shift, independent of the nature of absorbing atoms, but dependent on the nature of the foreign gas. The broadening of the higher series lines of K produced by He, and of Na produced by He, Ne, A, H_2, and N_2 were observed by Füchtbauer and Heesen[123] and Schulz.[136]

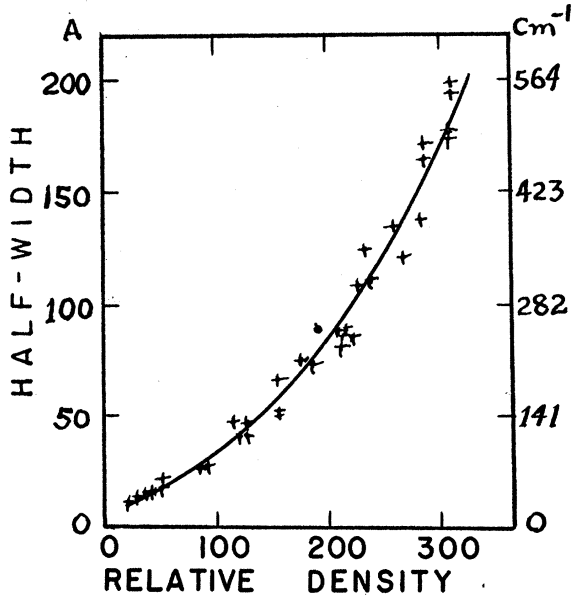

FIG. 10. Half-width of sodium D lines *vs* relative density of argon (after Robin, Robin, and Vodar[82]).

They found that the half-width *vs* series member curve had a broad maximum at the 3rd member for K/He and at the 5th member for Na/A and Na/He. Then the broadening turned back to a stationary value for high series members, *viz.* from the 11th to 12th member up for K/He (from the 9th or 10th member up for high r.d.), and from the 16th member up for Na/A, Na/He, Na/N_2, Na/Ne, and Na/H_2, as shown in Figs. 12 and 13. The broadening of the series end of the Na principal series in cm^{-1}/r.d. for He, Ne, A, Kr, Xe, H_2 and N_2 is 1.88, 1.42, 4.45, 8.12, 9.7, 6.16, and 6.16, respectively. A very large broadening of the sodium high member lines produced by Cs vapor was reported by Füchtbauer and Heimann.[126]

[135] G. A. Gorodnichus, Izvest. Akad. Nauk. S.S.S.R. Ser. Fiz. 18, 255 (1954).
[136] C. Füchtbauer and P. Schulz, Z. Physik 97, 699 (1935).

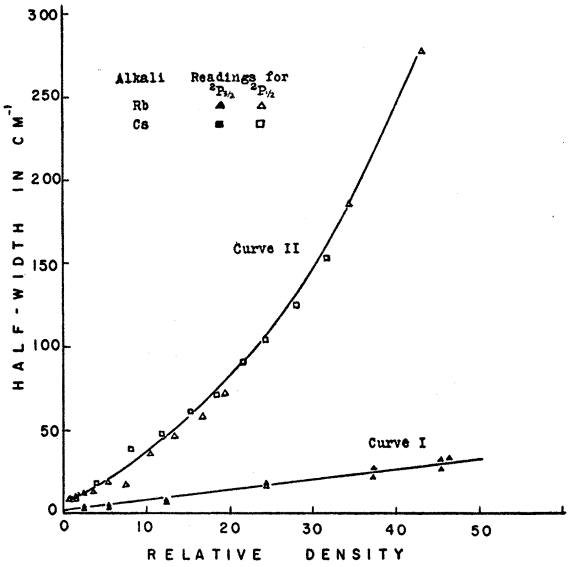

FIG. 11. Half-width *vs* relative density of He, as in Fig. 9.

The dependence of $\Delta\nu_{\frac{1}{2}}$ on r.d. for various members is shown in Fig. 14 for the case of K/He. The increase of broadening with r.d. (i.e., the slope of the curve) for the 4th and the 5th members of the K absorption series is greater for low densities than for high densities. The greater portions of the curve for the 6th and the 7th members become straight for higher densities. The readings for the 8th up to the 11th members are crowded together rather closely in some locations. The curves are linear or slightly concave upwards for high r.d.'s.

It is interesting to note in Table III that the average

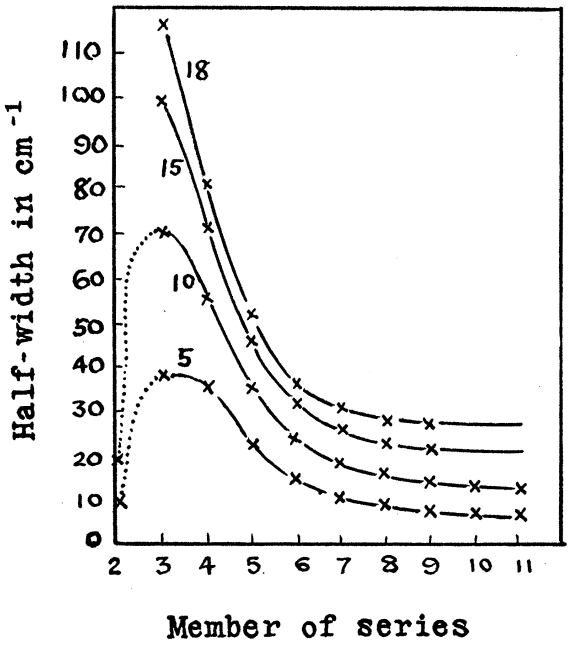

FIG. 12. Half-width *vs* members of the principal series of K for relative densities 5, 10, 15, and 18 of helium.

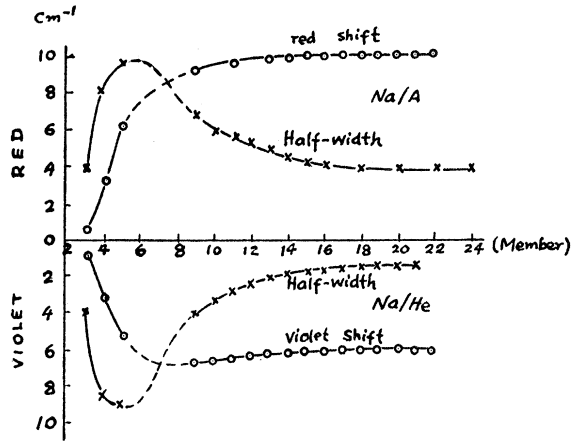

FIG. 13. Half-width and shift *vs* members of the principal series lines of Na in the presence of argon and helium. (r.d.=1, $P=762°K$) (after Füchtbauer and Schulz[136]).

of the ratio of half-width to shift for argon is 2.2 and that for N_2 is 2.3, which is in good agreement with Margenau's theoretical computation.[66] This ratio can be found easily also from Eqs. (97) and (98) to be 2.77, or from Eq. (58) to be 2.75, by taking $p=6$ for dispersion type interaction. Ne gave unexpectedly a rather large value of 4.4. The corresponding values for H_2, 4.1, and He, should not be included when comparison with theory is made.

Numerous cases have shown that for alkali atoms a line which undergoes greater broadening also undergoes a greater shift. But for certain lower member lines, where a switch of red shift to violet shift takes place, a small shift is usually accompanied by a large broadening. As an example, the broadening of K(2)/N_2 was 1.8 cm^{-1}/r.d. and that of K (2)/H_2 was 2.64 cm^{-1}/r.d. while the corresponding shifts were 0.93 cm^{-1} and 0.28 cm^{-1}, respectively. In these cases, forces of different signs are almost equally probable and as a limit no shift takes place.

Figure 13 illustrates how the shift and the broadening varies with the member of the series. For atoms other than alkali atoms, such as Hg[137] and Ag, the line broadening is always much greater than the shift. Nearly all lines are asymmetrically broadened. A red shift is usually accompanied by a red asymmetry and vice versa, with Cs 3876/N_2[116] the only exception. The asymmetry is, in general, larger for the doublet component that gives the larger shift. The theory of line breadth at the series limit has been discussed by Reinsberg[3,128b] with rather good agreement with experimental observations. Firsov[129] deduced an expression for the shift and the width of an energy level with high principal quantum number n in relation to the density of the perturbing gas N surrounding the atom. The shift is shown to be independent of the type of the atom and of n provided n is large. The half-width for large n and N is proportional to $N^{\frac{1}{2}}$ and n^{-3}. As a consequence, the width of spectral lines, for very high n, does not depend on n. His theoretical curves of the line width *vs* n relationship lie lower than the experimental one because the thermal motion of foreign gases is not taken into account.

[137] P. Schulz, Z. tech. Phys. **19**, 585 (1938).

5. The Evaluation of Some Physical Quantities

As described in Margenau and Watson's previous review article[2] the oscillator strengths f and transition probabilities A can be computed from the measurement of the amount of total absorption, $\int_0^\infty(n_k)d\nu$, by graphical integration of the line contours. n_k is the so-called index of absorption defined by the relation

$$n_k=\frac{\lambda}{4\pi l}\log i_0/i, \tag{137}$$

where l is the absorption path length. In practice, the line contours are often plotted with $\log_{10}i_0/i$ (or density) as ordinate and the distance in mm from the central maximum of the microphotometer curve as abscissa. The area under the line contour is measured by a planimeter in cm^2. Then it follows that:

$$\int_0^\infty n_k d\nu=\frac{2.303}{4\pi l\lambda}3\cdot10^{10}\int_0^\infty \log_{10}(i_0/i)\delta\lambda$$
$$=\frac{2.303}{4\pi l\lambda}3\cdot10^{10}\frac{B\cdot10^{-8}}{GMD}a, \tag{138}$$

where λ is taken as the wavelength of the central maximum, a the area under the contour in cm^2, D the density which corresponds to 1 cm in abscissa of the plot, and B/GM is the wavelength $\delta\lambda$ (in A) which corresponds to 1 cm in ordinate, M being the magnification ratio of the microphotometer trace, and G that on the graph.

According to radiation theory the oscillator strength of an atom is

$$f=\frac{4\nu m_a}{Ne^2}\int_0^\infty n_k d\nu=\frac{108\cdot10^2}{22.75}\cdot\frac{1}{\lambda N}\int_0^\infty n_k d\nu, \tag{139}$$

for $4\pi l\pi_k/\lambda\ll1$ and the transition probability per unit time, A,

$$A=\frac{4\pi}{cNh}\int_0^\infty n_k d\nu=\frac{\pi e^2}{chvm_e}f. \tag{140}$$

From such measurements Ch'en[110] computed the f values of the Rb resonance lines under different pressures of foreign gases up to r.d. 45.52 for helium and 46.44 for argon. The f values without the pressure of foreign gases were found by extrapolating to zero density of foreign gas. The results (0.33 and 0.66 for the $^2P_{\frac{1}{2}}$ and $^2P_{\frac{3}{2}}$ components, respectively) are in agreement

with Füchtbauer and Hofmann's determination[138] that the total oscillator strength is nearly unity. Although the precision of determination was not particularly high, it seems that the total absorption decreases with increasing r.d., so that f values decrease when the line is broadened. This was also true with Hg.[111] By means of exactly the same method, Michels and Kluiver[86b] obtained the oscillator strength of Hg 2537 as 0.0255 from their observations with He.

The transition probabilities, 6.93×10^9 and 3.53×10^9 for the Rb $^2P_{\frac{1}{2}}$ and the $^2P_{\frac{3}{2}}$ components, respectively, are in good accord with the results of the resonance lines of other alkalis.

The optical collision diameters can be computed from the observed half-widths, using the relation

$$\rho^2=[\pi\Delta\nu_{\frac{1}{2}}/2N(2\pi kT)^{\frac{1}{2}}]\cdot[mM/(m+M)]^{\frac{1}{2}}, \quad (141)$$

where m and M are the masses of the absorbing and of the perturbing atoms, respectively. The accuracy of the calculation depends greatly on that of the values of half-widths per unit r.d. As the slopes of these curves change with r.d. and are different for different doublet components, it is hard to assign a proper value. Although the average values of the 4th column of Table III were used, the figures listed in the 6th column can not be regarded as accurate. In spite of these limitations, the values of ρ for a given member of the absorption series and a given foreign gas are found to be very close for different alkalis. The mean values of ρ (in A) for the first member of the alkali absorption series in the presence of A, N_2, He, and H_2 are 13, 10, 8, and 7, respectively; and the mean values for the second member of the series in the presence of A, N_2, Ne, He, H_2, CH_4, C_2H_6, and C_3H_8 are, respectively, 21, 16, 12, 12, 12, 14, 16, and 18 A.

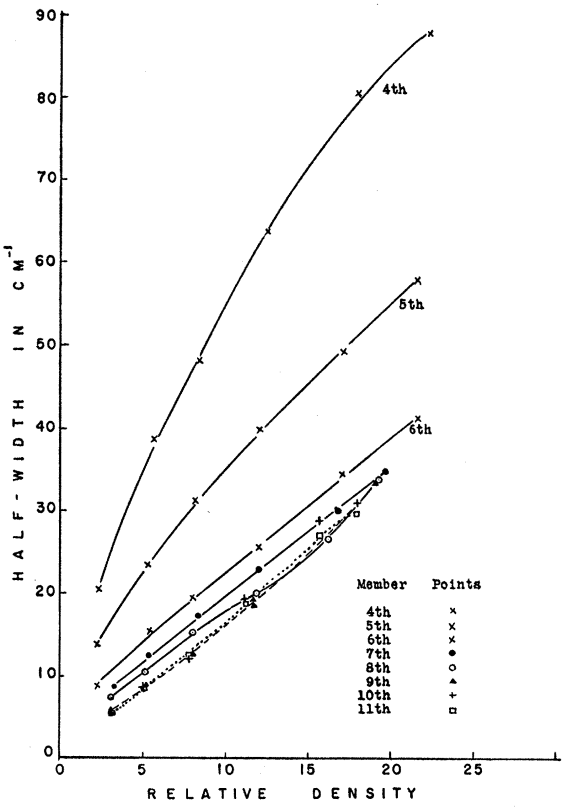

FIG. 14. Relationship of half-width and the relative densities of helium for high members of K principal series (after Füchtbauer and Heesen[123]).

B. FINE STRUCTURE PRESSURE EFFECTS

1. Pressure Effects Due to Identical Atoms

By direct measurement of the contours of the line wings, the broadening of the resonance lines of nearly all alkali atoms in absorption under various pressures of their own homogeneous vapor (resonance broadening) have been observed.[139–142] All observers reported that when the pressure was low (below 1 mm Hg) the line contours could be described nicely by the dispersion formula and the broadening was essentially symmetrical. The half-width varied linearly with the concentration of the vapor. All but the first, who used K, found that the half-width of the transition from the $^2P_{\frac{3}{2}}$ level was greater than that from $^2P_{\frac{1}{2}}$ level by a factor of about $\sqrt{2}$, quite in harmony with Foley's theoretical result[22] [see Eq. (131)]. Not only the ratios, but also the absolute values of half-widths given by Eq. (131), are found to be in accord with observations. However, when the thermal energy per perturber is comparable with the doublet separation, the theory will undergo some revision due to the fact that the J representation breaks down in such a case.[143]

Ch'en[140] and Gregory[142] observed also that indications of a violet and red asymmetry were present at high pressures for the $^2P_{\frac{3}{2}}$ and $^2P_{\frac{1}{2}}$ components, respectively, and a definite band on the red side of the $^2P_{\frac{3}{2}}$ and on the violet side of the $^2P_{\frac{1}{2}}$ component were observed. This strong asymmetry was also observed with Xe[144] and Hg.[76,77] Tomiser's observation shows that the broadening of Zeeman components are not a linear function of density.

This self-broadening has also been observed in a

[138] C. Füchtbauer and W. Hofmann, Ann. Physik **43**, 96 (1914).

[139] K: P. E. Lloyd and D. S. Hughes, Phys. Rev. **52**, 1215 (1937), at pressures up to 20 mm Hg. $\Delta\nu_{\frac{1}{2}}(J=\frac{3}{2})/\Delta\nu_{\frac{1}{2}}(J=\frac{1}{2})=1.0$. J. Tomiser, Acta Phys. Austriaca **8**, 325 (1954), observed up to 0.1 mm Hg with the result of ratio, 1.07–1.59 (mean: 1.41) (theor. 1.42).

[140] Rb: S. Y. Ch'en, Phys. Rev. **58**, 844 (1940), at pressures up to 152 mm Hg. $\Delta\nu_{\frac{1}{2}}(J=\frac{3}{2})/\Delta\nu_{\frac{1}{2}}(J=\frac{1}{2})=1.75$. J. Tomiser, reference 139, **9**, 18 (1954), up to 0.08 mm Hg with ratio 1.19–1.58 (mean: 1.26) (theor. 1.38).

[141] Na: K. Watanabe, Phys. Rev. **59**, 151 (1941), at pressures up to 70 mm Hg. $\Delta\nu_{\frac{1}{2}}(J=\frac{3}{2})/\Delta\nu_{\frac{1}{2}}(J=\frac{1}{2})=1.55$. J. Tomiser, reference 139, **8**, 198 and 276 (1954), up to 0.9 mm Hg with ratio 1.27–1.45 (mean 1.31) (theor. 1.42).

[142] Cs: C. Gregory, Phys. Rev. **61**, 465 (1942) at pressures up to 17.5 mm Hg. $\Delta\nu_{\frac{1}{2}}(J=\frac{3}{2})/\Delta\nu_{\frac{1}{2}}(J=\frac{1}{2})=1.72$ (theor. 1.52).

[143] M. Takeo, Bull. Am. Phys. Soc. Ser. II, **1**, 245 (1956).

[144] J. C. Madenann and R. Turnbull, Proc. Roy. Soc. (London) **A129**, 265 (1930); **A139**, 683 (1933).

discharge tube of mercury vapor on the lines Hg 10140 A ($2^1P_1-2^1S_0$) and Hg 5770 A ($2^1P_1-3^3D_2$). The broadening of the former line is purely due to self-pressure, while the latter was broadened proportionally to the electric current.[105] Thus, by extrapolating the latter broadening to zero current, the self-broadening of the line was obtained for each corresponding pressure.[145] Thus, the two lines were found to behave according to the impact theory with the same width. However, the experimental absolute width was 60% larger than the theoretical value.

2. Pressure Effects Due to Foreign Atoms

The difference in behavior of shift and broadening of the doublet components of the principal series lines of alkalis and of Ag was first emphasized by Ch'en and his collaborators.[110,112,113,117] For example, the shift of the first doublet of the Rb principal series produced by helium[110] was -6.88 A ($+10.88$ cm^{-1}) for the $^2P_{\frac{1}{2}}$ component and -2.68 A ($+4.40$ cm^{-1}) for the $^2P_{\frac{3}{2}}$ component for r.d. 45.52 as determined by a 21-foot grating. The corresponding figures for the half-widths were 16.9 A (27.8 cm^{-1}) and 20.2 A (33.2 cm^{-1}), respectively. The ratio of shifts for the two components is 2.5 and that of half-width is 0.84.

The shift of the Rb second doublet[113] produced by 43.9 r.d. of helium was -19.5 A ($+110$ cm^{-1}) for the $^2P_{\frac{1}{2}}$ component and -12.2 A ($+69.0$ cm^{-1}) for the $^2P_{\frac{3}{2}}$ component. The corresponding values for the half-width were 48.7 A (277 cm^{-1}) and 63.4 A (361 cm^{-1}), respectively. The ratios of shifts and half-widths are 1.60 and 0.766, respectively.

For argon, the difference of shifts of the two doublet components of all alkalis is very small, but the broadening of the $^2P_{\frac{3}{2}}$ component is slightly greater than that of the $^2P_{\frac{1}{2}}$ component by a factor of 1.12 on the average.

The line shift, as discussed in Sec. II.B.b, originates in the smaller phase shift in the oscillation of an absorber at a collision. The phase shift produced at a certain impact parameter depends strongly on the shape of the interatomic potential curves for various gases. For helium an impact parameter effective for line shift will be larger than the optical diameter, and the classical discussion of the shift may be adequate at rather high temperature by the following reason. Namely, for alkali resonance lines with helium as perturbers, the optical collision diameter happens in many cases to be nearly of the same order of magnitude as the sum of the atomic diameter of helium (3.5 A) and of the absorbing atom, both in the ground state. When the absorber is excited, the overlap integral will be appreciably larger than otherwise, and a repulsion will dominate the seond-order dispersion energy at the distances for line shift impact parameters. Thus, a violet shift with helium pressure may be expected. The shift for higher members should be larger, not because of the fact that the overlap integral is larger for higher states, but rather because of the fact that the number of collisions effective in line shift increases for higher states. However, this line shift is related to the shift of the center of gravity of the doublet.

The difference of shifts for doublet components must be found in the variation of the doublet separation, which is determined by the change of the wave function at the absorber's nucleus. The larger impact parameter, effective for higher-member line shift, is unlikely to change the doublet separation more than otherwise. Thus the ratio of shifts is smaller for higher members. On the other hand, observation shows that for alkali resonance lines with argon pressures the optical collision diameter is about 1.5 times larger than the sum of atomic diameters concerned and lies well inside the region dominated by dispersion forces. In this case, the ratio of shifts for the doublet components will be constant for different members. The same kind of argument may follow for the ratio of half-widths for doublets. But the phase shift most effective for broadening would be larger than that produced at the optical collision diameter. For helium, the impact paramerer lies inside a quantum-mechanical region, although for argon the classical picture is still applicable, using the result in Sec. II.A.b, that the ratio of half-widths for doublet components perturbed by argon should be nearly constant for different members.

Peterman and Füchtbauer[124] noticed that the half-width of K(2)/N_2 and of K(2)/He was greater for the $^2P_{\frac{3}{2}}$ component. Ch'en[110,115] also observed that hydrogen produced a violet shift on the $^2P_{\frac{1}{2}}$ component and a red shift on the $^2P_{\frac{3}{2}}$ component for both the resonance and the second doublets of the rubidium principal series. More illustrations are given in Figs. 3, 5, 6, and 9. It is also apparent in Fig. 15 that the separation between the narrow peak and the broadened peak is different for different doublet components. Kleman and Lindholm's precise measurement of the shift and half-width of the Na$-$D lines produced by argon[107] revealed that the $^2P_{\frac{1}{2}}$ component had a smaller shift and a larger half-width than the $^2P_{\frac{3}{2}}$ component.

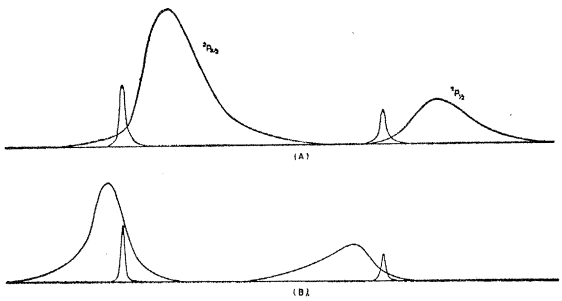

FIG. 15. (A) Microphotometer traces of the doublet components of the second member of the Rb principal series broadened by argon at pressures 0.1 atmos (narrow peaks) and 12.18 atmos (broad peaks). (B) Corresponding traces for helium at pressures of 0.12 and 10.92 atmos, respectively. Note the difference in shift and broadening of the two components (after Ny and Ch'en[117]).

[145] P. Gerthsen, Z. Physik **138**, 515 (1954).

Recent observations by Robin and Robin[85] showed that the shift of the $^2P_{\frac{1}{2}}$ component of Rb resonance lines when perturbed by A, He, and N_2 up to several hundred r.d. was nearly linear with r.d., while that of the $^2P_{\frac{3}{2}}$ component reversed its direction of shift for r.d. equal to 180 for N_2 and 260 for A. Because of the fact that the $^2P_{\frac{3}{2}}$ component was broadened more rapidly than the $^2P_{\frac{1}{2}}$ component, the relative intensities of the two lines varied very much with pressure. The less intense $^2P_{\frac{1}{2}}$ component at low pressure became more intense at high pressures.

From the results of observations obtained so far one can make the following general empirical statements:

(1) The difference in shift (when expressed in cm^{-1}) of the multiplet components depends on the member of the series and the nature of foreign gases, but is independent of the nature of the absorbing atom.

(2) For gases that produce a violet shift, the longer wavelength component ($^2P_{\frac{1}{2}}$) exhibits a greater violet shift than the shorter wavelength component ($^2P_{\frac{3}{2}}$), as predicted at the end of Sec. II.C.b, and the ratio for the first doublet is larger than that for the second doublet.

These two statements are supported by all available data, such as Rb(1)/He, Rb(2)/He, Cs(2)/He, and Ag(1)/He without exception. For Rb(2)/Ne, the $^2P_{\frac{1}{2}}$ component produced a violet shift while the $^2P_{\frac{3}{2}}$ component produced a red shift. For a given r.d. of He, the differences of shift (in cm^{-1}) of the doublet components for the second member of Rb and Cs principal series are the same within experimental error.

(3) The difference in shift of the double components for gases that produce a red shift is usually small as shown in Sec. II.C.b. There is no apparent indication as to which component should show a stronger red shift. For Rb(1)/*A*, Rb(2)/A, Cs(2)/A, K(1)/A, Ag(1)/A, K(1)/N_2, and K(2)/N_2 the $^2P_{\frac{1}{2}}$ component shows a slightly stronger red shift; while for Na(1)/A Rb(2)/N_2, and Robin's high pressure observations of Rb(1)/A and Rb(1)/N_2 the $^2P_{\frac{3}{2}}$ component has a slightly stronger red shift.

(4) The broadening of the short wavelength ($^2P_{\frac{3}{2}}$) component is greater than that of the longer wavelength ($^2P_{\frac{1}{2}}$) component. Observations confirming this statement are Cs(2)/H_2, K(2)/H_2, Rb(1)/He, Rb(2)/He, Rb(1)/A, Rb(2)/A, and Ag(1)/A. Robin and Robin[85] proved indirectly, from the variation with pressure of the ratio of the optical densities of the maxima of the resonance lines of K and Rb, that the $^2P_{\frac{3}{2}}$ is broadened more than the $^2P_{\frac{1}{2}}$ component.

Exceptions to this are Na(1)/A, Rb(2)/Ne, and Rb(2)/He only when the r.d. is low. As shown in reference 113, when the r.d. of He is above 19, the half-width of the short wavelength component becomes greater than that of the longer wavelength one.

It is to be noted that in this and the following sections there is demonstrated very strikingly the important fact that there exists a conspicuous difference in the interactions at close distances for the two fine structure levels. There is no doubt that this phenomenon will be useful in interpreting certain detailed phenomena of various basic observations.

Many research problems dealing with these effects can be suggested, such as the pressure effect on high multiplicity components, the fine-structure pressure effects of multiplet components in relation to different couplings of the angular momenta of the optical electrons, etc.

C. NARROW DIFFUSE BANDS OF VARIOUS METALS PRODUCED BY CLOSE ENCOUNTERS WITH FOREIGN PARTICLES

The most intense part of a broadened spectra line should come from the majority of the perturbers and corresponds to distant collisions. The shapes of the wings, however, will depend on the phenomena occurring close to the absorber where spectral lines are affected most strongly. This phenomenon is manifested as narrow diffuse bands which appear as faint wings of the atomic lines if they are not resolved. They have been observed very conspicuously as separate bands or diffuse lines in the neighborhood of certain atomic lines. These bands which are often called "satellites," are present at foreign gas pressures even as low as a few milimeters of Hg.

1. Observations in Emission Spectra

This phenomenon was probably first observed by Oldenberg,[146] who obtained a narrow continuum of this sort on both sides of Hg 2536.7 in fluorescence by the irradiation of the mercury resonance line in a mixture of mercury and a few cm pressure of helium. When heavier rare gases were used one or two diffuse intensity maxima were found on the short wavelength side, lying closer to the atomic line the greater the atomic weight of the rare gas used. Kuhn and Oldenberg[147] interpreted the bands as due to loosely bound molecules or space quantization.

Krefft and Rompe[148] observed similar diffuse bands in the positive column of electric discharges in mixtures of Tl, In, Zn, Na, K, Rb, and rare gases. The vapor pressure of the metal was about 1 mm and the gas pressure about 2–10 mm. They found that the characteristics of the bands depend upon the rare gas used and also upon the atomic levels of the metal. These bands were classified according to visual judgment of their shape, and a number of empirical relations were suggested, such as the proportionality of the separation of certain violet bands to $1/\sqrt{M}$, M being the atomic weight of the rare gas used.

Preston[149] made an extensive study of these bands in

[146] O. Oldenberg, Z. Physik **47**, 184 (1928); **55**, 1 (1929).
[147] H. Kuhn and O. Oldenberg, Phys. Rev. **41**, 72 (1932).
[148] H. Kreft and R. Rompe, Z. Physik **73**, 681 (1932).
[149] W. M. Preston, Phys. Rev. **51**, 298 (1937).

a simple capillary discharge tube of Hg, Cd, or Tl in the presence of 10 cm of He or A. He used a Hilger medium quartz spectrograph, and found that the intensity of the band was of the order of a few hundredths to two thousandths of the intensity of the accompanying metal line. The Hg 2537 band at 2526.0 A was not changed within a limit of error of about 0.3 A for three different temperatures, 55, 130, and 400°C. Also, no observable shift was reported when argon pressure was varied from 1 mm to 10 cm, although the band may be visible, with much less intensity, even with 0.1 mm of argon. He identified the collision-induced spectra near 13 lines of the spectrum of Hg, 12 of Cd, and 6 of Tl. The majority of these spectra had roughly defined edges at the shorter wavelength side and no resolved maximum. Only three definite cases of maxima on the short wavelength side of lines were encountered, all lying fairly close to and definitely associated with an atomic line. Several examples were also found of maxima at varying distances on the long wavelength side of lines, some at such great distances that they could not be definitely connected with any particular line. He pointed out that the bands associated with the lines of a particular spectral multiplet are much more alike in form and width than those belonging to unrelated lines.

It should be noted that the conditions for the appearance of the bands in emission, such as the presence of ions, electron impacts, inhomogeneity in temperature distribution and in concentration of emitting atoms, etc. in the source, could hardly be neatly defined for theoretical analysis.

2. Observations in Absorption Spectra

a. Observations with Low Foreign Gas Pressures

Although the appearance of a new band of Hg at 2528 A due to the presence of foreign gases was first known to Moore[150] and Oldenberg[146] systematic observations of the structureless alkali-foreign-gas absorption bands were perhaps first started by Ch'en and collaborators.[151–153,78,79] With the Bausch and Lomb or the Hilger large Littrow spectrograph the band appearing on the short wavelength side of the second member of the principal series of rubidium in the presence of foreign gases (H_2, He, N_2, and Ne) was first observed, and then the observation was extended to the second member of cesium and potassium, and the third member of the sodium principal series.[152] In the presence of helium, bands were observed near the fourth through the seventh member of the lithium principal series.[78] Recently, with infrared plates and more careful technique, the bands appearing in the neighborhood of the resonance lines and the third or higher members of the rubidium principal series were also observed with a number of other gases,[79] *viz.*, A, Kr, and Xe. Most recently Ch'en and Jefimenko[153] first confirmed that the narrow bands exist simultaneously both on the red and on the violet side of the first few principal series lines of Rb and Cs, with the red bands having a higher intensity. In addition to the well-defined series of rare gases (also N_2 and H_2), fourteen different kinds of paraffin molecules, whose physical properties are very well known, were employed as a series of perturbing particles. Over two hundred more new bands of this kind were obtained.[153] For details one should refer to these original papers.

Only with heavy foreign gases, such as xenon and krypton, and saturated hydrocarbon vapors heavier than propane, was the narrow diffuse band resolved on the *red side* of each component of the absorption doublets of Na, Rb or Cs. Figure 16 is a set of sample spectra for the Rb/Xe and Cs/Xe "red" bands. The red

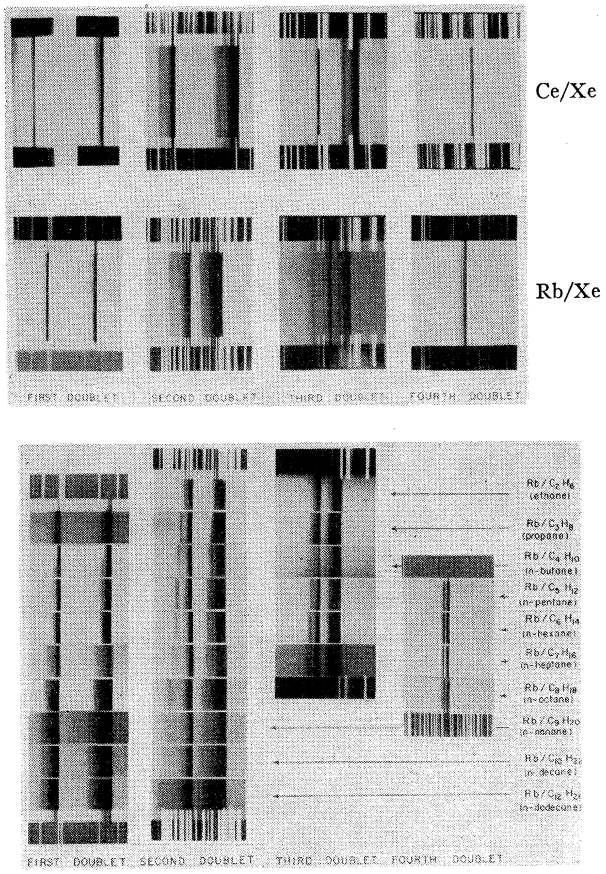

FIG. 16. (a) The red bands of Rb and Cs in the presence of xenon (1) for the resonance lines, (2) for the second doublet, (3) for the third doublet, and (4) for the fourth doublet of the principal series. The corresponding pictures for the fifth doublet showed only some red asymmetry (after Ch'en and Jefimenko[153a,b]). (b) The red bands of Rb in the presence of various paraffin vapors (after Ch'en and Jefimenko[153b]).

[150] H. R. Moore, Science **66**, 543 (1927).
[151] T. Z. Ny and S. Y. Ch'en, Nature **138**, 1055 (1936); J. phys. **9**, 169 (1938).
[152] S. Y. Ch'en, Phys. Rev. **65**, 338 (1944).
[153] (a) S. Y. Ch'en and O. Jefimenko, J. Chem. Phys. **26**, 256 (1957) (results for Rb). (b) O. Jefimenko and S. Y. Ch'en, J. Chem. Phys. (to be published) (Cs).

TABLE IV. The $\Delta\nu_m$ (in cm^{-1}) values for alkali-foreign gas red bands for the various members of the principal series.

	$\Delta\nu_m$ (1st member)		$\Delta\nu_m$ (2nd member)		$\Delta\nu_m$ (3rd member)		$\Delta\nu_m$ (4th member)	
	$^2P_{\frac{1}{2}}$	$^2P_{\frac{3}{2}}$	$^2P_{\frac{1}{2}}$	$^2P_{\frac{3}{2}}$	$^2P_{\frac{1}{2}}$	$^2P_{\frac{3}{2}}$	$^2P_{\frac{1}{2}}$	$^2P_{\frac{3}{2}}$
Na/Xe	−26.6[a] cm^{-1}	...	−76 cm^{-1}	...	−47 cm^{-1}	...	−16 cm^{-1}	...
Rb/Xe	−17.4	−33.3	−45.2	−43.5	−34.4	−21.0	−10.7	−9.5
Cs/Xe	−11.7	−31.4	−37.7	−52.7	−29.3	−29.4	−6.1	−9.4
Rb/*n*-octane	−64[a]	−76[a]	−53.0	−46.5	−21.9	−20.9	−10.5	−10.6
Cs/*n*-octane	−47[a]	−69[a]	−46.7	−49	−19.8	−19.9	−8.2	−9.7

[a] The accuracy determination is low, because the absorption maxima could not be definitely established or resolved from the atomic line.

bands become perceptible when the vapor pressure of Rb or Cs is of the order of 10^{-3} mm Hg or higher (temperature of absorption tube = 120−150°C) and the pressure of foreign gas is higher than 20 cm Hg.¶¶ When the vapor pressure is increased (by increasing the temperature of the absorption tube to 200–270°C) the red bands and the absorption lines of Rb or Cs overlap, and the bands are no longer resolved from the broadened absorption line. Under these conditions the violet bands become intense enough for observation. When the temperature of the absorption tube is still increased (400–500°C) a number of additional bands are observed between the doublet components of the resonance lines. Owing to the fact that the appearance and the regularities of occurrence of these types of bands are quite different. They are described in separate sections.

(*i*) *The Red Bands.*—As shown in Fig. 16 the red bands appear in general close to the atomic line as a single absorption maximum. No red bands are produced by light gases, H_2, D_2, He, Ne, and N_2. Argon and methane merely give a red asymmetry of the atomic lines. A definitely resolved red band is observed for each component of the first four doublets of the principal series of Na, Rb, and Cs for all the other heavier rare gases and saturated hydrocarbons employed.

Observations connected with the *red bands* associated with the principal series lines of alkali atoms may be summarized as follows: (1) The separation (in cm^{-1}) between the band and the associated absorption line, $\Delta\nu_m$, varies strongly with the member of the principal series. For Kr and Xe, the largest values of $\Delta\nu_m$ are those associated with the second member of the series, while for all paraffin molecules the highest value of $\Delta\nu_m$ falls on the first member, and $\Delta\nu_m$ decreases rapidly with the increase in the ordinal number of the member of the series, as illustrated in Table IV. No bands were resolved from the atomic lines of fifth and higher doublets of the series. (2) The values of $\Delta\nu_m$ are different for the two doublet components. For both rare gases and saturated hydrocarbons all values of $\Delta\nu_m$ associated with the short wavelength ($^2P_{\frac{3}{2}}$) component of the resonance lines are considerably greater than that associated with the long wavelength ($^2P_{\frac{1}{2}}$) component. For the second member of the Rb principal series the foregoing statement holds for Kr, and light hydrocarbons (propane and butane), but is reversed for Xe, butane, and all heavier paraffin molecules. The difference becomes small for the third and the fourth member of the Rb principal series. (3) Red bands are resolved only for heavy gases. As shown in Figs. 17 (a) and (b) for any given doublet, $\Delta\nu_m$ increases linearly with the polarizability, α, of the gases (with possibly a saturation for very large particles). The slopes of the curves are almost the same for both Rb and Cs, *viz.*, 0.31 and 0.27 in cm^{-1}/α (α being expressed in 10^{25} cm^3) for the $^2P_{\frac{1}{2}}$ and the $^2P_{\frac{3}{2}}$ components of the second doublet, respectively. The corresponding values for the third doublet are both 0.11. (4) Although there are no sufficient data, the values of $\Delta\nu_m$ for $^2P_{\frac{1}{2}}$ component for a given foreign gas appears to be a little higher for lighter alkalis. (5) The positions of the maxima of the bands is not appreciably changed by either a variation of pressure from $\frac{1}{2}$ to 2 atmospheres, or a change of temperature from 120° to 190°C. (6) The widths of bands decrease with the ordinal member of the doublets and are roughly of the same order of magnitude as those of the associated

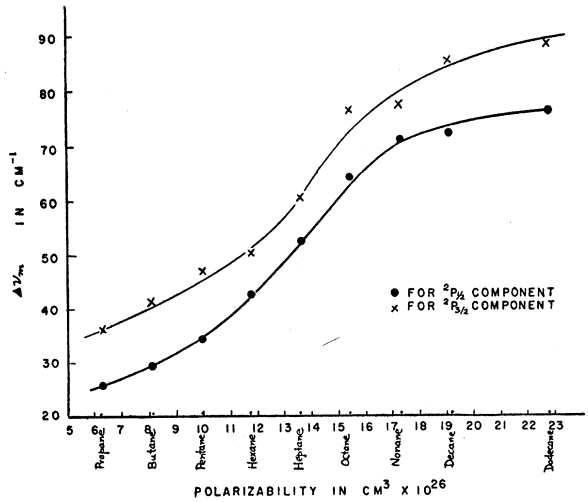

FIG. 17. (a) $\Delta\nu_m$ *vs* the polarizability of paraffin molecules for the 1st member of the Rb principal series (after Ch'en and Jefimenko[153a]).

¶¶ If the foreign gas pressure is much lower than this value, the vapor pressure of Rb must be increased to make the band intense enough for observation.

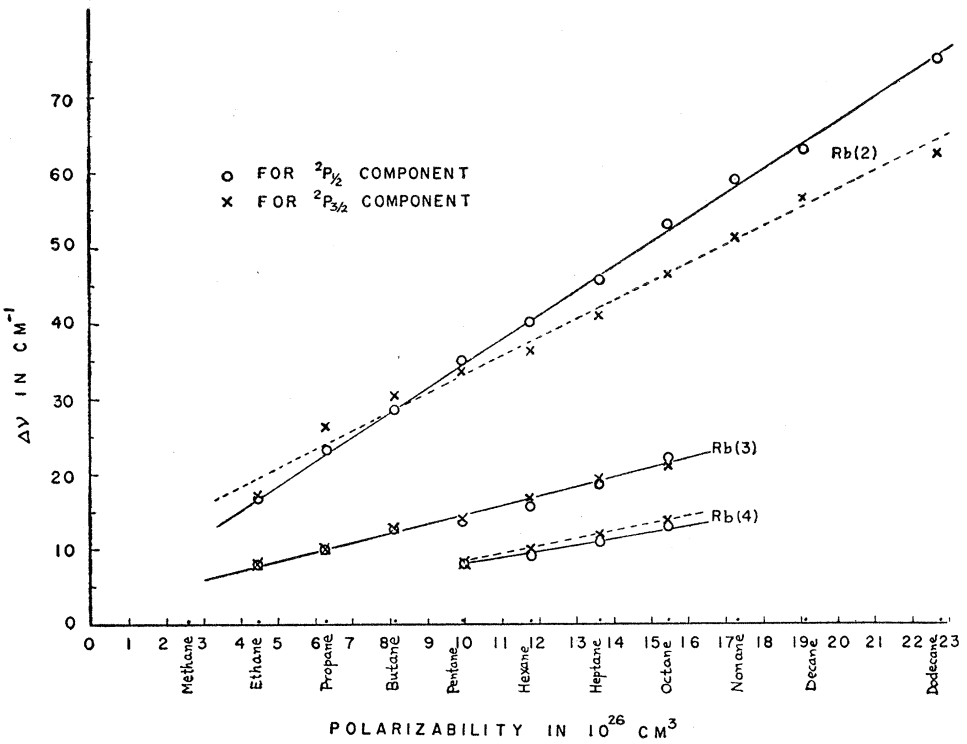

FIG. 17. (b) $\Delta\nu_Q$ *vs* the polarizability of paraffin molecules for the second, the third and the fourth members of the Rb principal series (after Ch'en and Jefimenko[153a,b]).

absorption line. (7) The intensity of the bands relative to that of the associated atomic line is higher for bands with smaller $\Delta\nu_m$ or smaller widths. When the pressure of foreign gas is low, say below 3 cm of Hg, the intensity depends strongly on both the concentration of the absorbing atom and that of the foreign gas. (8) The red bands are observed only for those gases which produce a red shift in pressure effects.

(*ii*) *The Violet Bands.*—The violet bands, i.e., the bands on the short wavelength side of the absorption doublet, appear usually when the temperature of the absorption tube is appreciably higher than that at which the red bands are first perceptible. The behavior and appearance of the violet bands are entirely different from those of the red bands. Several points can also be singled out with regard to observations of the violet bands: (1′) The violet bands are considerably fainter than the red bands. Although no direct measurement of the relative intensities of the red with respect to the violet bands is made yet, one can make a rough estimation, from the lowest vapor pressure at which the bands are first perceptible, to be around 100. (2′) Violet band or bands are observed near the resonance lines of the alkalis for all gases employed, while red bands are observed only for heavy gases that produce a red shift. (3′) The bands are located at the short wavelength side of the entire doublet. The values of $\Delta\nu_m$ given in Table V are measurements from the short wavelength component ($^2P_{\frac{3}{2}}$) of the doublets. (4′) Several maxima may be observed near the resonance lines. The values of $\Delta\nu_m$ for the violet bands near the resonance lines are very much greater than those of the red bands, but decrease much more rapidly towards higher members of the principal series than in the case of the red bands. For Rb, the values of $\Delta\nu_m$ for the second member of the series are decreased by 8, 12, and 20-fold relative to those for the first member, for He, Ne, and A, respectively. If one followed this trend of decrease, the values of $\Delta\nu_m$ for the second member would be 11 and 8 cm^{-1} for Kr and Xe, respectively, so, experimentally, the band is never resolved. For the third member of the Rb absorption series, the violet bands are never observed

TABLE V. The $\Delta\nu_m$ (in cm^{-1}) values for various alkali-foreign gas violet bands.

Alkali \ Foreign gas	H_2	He	N_2	Ne	A	Kr	Xe
Na(1)	1203	1200	1201	1086	1069	906	893
Na(2)	...	...	...	136	50	...	...
Na(3)	52	50	55	53	...	...	...
K(2)	230	174	174	62	...	...	...
Rb(1)	921	778	718	448	433	342	334
Rb(2)	133	98	112	38	22	...	...
Rb(3)	...	...	18	...	...	...	...
Cs(1)	428	356	408	231	213	151	134
Cs(2)	78	64	60	29	...	...	...
Cs(3)	...	...	12	...	...	...	...

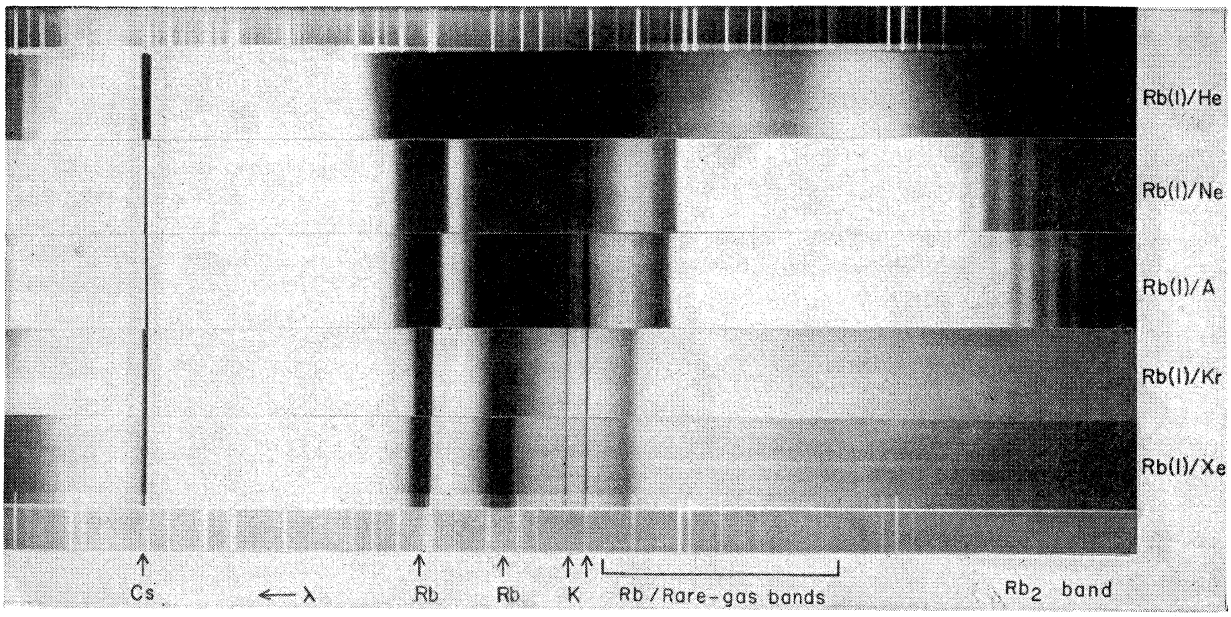

FIG. 18. The violet bands of Rb resonance lines in the presence of rare gases. The lines marked with K and Cs are the respective potassium resonance lines and the shorter wavelength component of cesium resonance lines which appeared as impurities (after Ch'en and Jefimenko[153a]).

for heavy gases; for light gases they are so close to the atomic line that only violet asymmetry was observed. (5′) As shown in Table V, the values of $\Delta\nu_m$ for violet bands (in contrast to red bands) decrease with increases in the mass of the absorbing atom. As an illustration, for a given foreign gas the $\Delta\nu_m$ values for Na(1) range from 1.5 to 2.6 times greater than those for Rb(1); the $\Delta\nu_m$ values for Rb(1) are again twice those for Cs. (6′) The most profound difference between the violet and the red bands manifests in the dependence of $\Delta\nu_m$ on the type of colliding particles. In contrast to the red bands, the $\Delta\nu_m$ values decrease with increasing mass of foreign gas particles, or remain essentially constant for paraffin series ones. This point is further detailed in next paragraph. (7′) The width of the bands is greater for those with a greater $\Delta\nu_m$. (8′) The position of the bands is not appreciably changed by a smaller variation of pressure from $\frac{1}{2}$ to 10 atmospheres, and point (7) for red bands is also true for violet bands. The effect at very high pressures for (8′) is discussed in the subsequent subsection.

As shown in Fig. 18, for a given absorbing alkali the violet bands produced by various rare gases near the resonance lines can be classified into three groups according to the magnitude of $\Delta\nu_m$: (a_1) the alkali (1)/He band which is very broad and stretched very far from the resonance lines, (b_1) alkali(1)/Ne and alkali (1)/A bands with two similar maxima: $\Delta\nu_{m1}$*** is much closer to the atomic line concerned than that for the case of (a_1) and $\Delta\nu_{m2}$ lies between them, and (c_1) alkali (1)/Kr and alkali (1)/Xe bands, in the same manner, with two maxima. $\Delta\nu_{m1}$ is still smaller than that for case (b_1). This effect may be correlated with the electron density at the surface of a perturber. The electrons having nearly the same energy associated with the atomic surface are s^2 for He, s^2p^6 for Ne and A, and $s^2p^6d^{10}$ for Kr and Xe. Since their atomic radii are nearly the same, Kr and Xe are most unlikely affected at a close encounter by whether the alkali atom is in the ground state or in the excited state.

Likewise, the violet alkali-paraffin bands near the resonance lines can be divided into three groups: (a_2) the bands in the presence of methane. They are characterized by a $\Delta\nu_m$ smaller than that for any other hydrocarbons studied, and by $\Delta\nu_{m2}$ smaller than $\Delta\nu_{m1}$. The bands resemble very closely those of (b_1)[79] in their appearance and positions. (b_2) the bands in the presence of ethane and propane. These bands have only one maximum with a $\Delta\nu_{m1}$ of apparently the same magnitude for both hydrocarbons. (c_2) the bands due to butane and heavier paraffin series. These always have two maxima, with essentially the same $\Delta\nu_{m1}$. They decrease slightly with the increase in the molecular weight of hydrocarbons; however, $\Delta\nu_{m2}$ is greater than $\Delta\nu_{m1}$ and increases slowly with the increase in the weight of the hydrocarbon. These bands resemble in appearance the violet bands in the presence of N_2.[79]

A test of the dependence of the values of $\Delta\nu_m$ on the mass of the foreign gas could only be made by employing H_2 and D_2. The positions and the appearance of the Cs/H_2 and Cs/D_2 bands are identical, within experimental errors, although the latter bands are somewhat slightly sharper.[153b]

*** The subscript "1" in $\Delta\nu_m$ refers to the value of separation for the intense maximum in the band; while subscript "2" to the much fainter maximum in the same band.

The appearance of new bands near the absorption lines of alkali atoms due to collisions with its own vapor were also observed.[78,151,154]

b. Observations with High Foreign Gas Pressures

Robin and Robin[84,86] observed a violet band near Hg 2537 in the presence of argon, nitrogen, and helium. The fusion of the band with the broadened line made the points of maxima deviate, and rendered it impossible to measure the broadening of the line. (A similar situation occurred with the observation of the broadening of Rb 4201 by helium.[103]) The intensity of the band increased rapidly with argon pressure and became greater than that of the principal line at about 300 atmospheres. As the argon or nitrogen pressure was increased, the maximum of the violet band of Hg first displaced toward the red, then seemed to be very little displaced between r.d. 250 and 400 for argon (with the band located at 2530 A) or between r.d. 150 and 350 for nitrogen (with the band located at 2531±1 A), and then displaced readily toward the violet. The authors regard this change of the maximum position as due to the change in polarizability of both absorbers and perturbers due to pressure. It has been pointed out[155] that for spherical nonpolar molecules the polarizability increases first with pressure up to about several hundreds atmospheres and then decreases. As the pressure was increased to 5000 kg/cm² with N_2 and 6000 kg/cm² with argon (temperature 95°–160°C) a second satellite band was observed by Robin and Vodar[156] at the short wavelength side of the first satellite. For helium as the pressure was increased the violet band (which appeared at 250 kg/cm² and was located at 2522±1 A at 600 kg/cm²) displaced toward the violet (2516±1.5 A at 1400 kg/cm²).

A faint (broad) violet band was also observed for Na at 5565±10 A[72] when the pressure of argon was very high (at 1000 atmos and 400°C). The Na(1)/A band observed by Ch'en and Stauffer at low pressure was at 5543.5±5 A, showing that the band was shifted towards red at high pressures. Also, the Rb(1)/A band was reported[85] as displaced toward the red (7575±10 A to 7630±20 A) up to r.d. 120, then returned toward blue (7480±30 A at r.d. 390). The Rb(1)/He band at r.d. 100, displaced toward the blue (it was at 7250±30 A at r.d. 300, 260°C). Two K(1)/A bands were observed (7370 and 7670±30 A) at r.d. 300 and 280°C, the last being only visible at high density.

So far the effect of high foreign gas pressure on the bands which appear on the violet side of the atomic line can be outlined in four points: (1) For gases which produce a red shift of the atomic line, the band will displace first toward the red and then will gradually turn back to displace toward the violet as the pressure is increased. (2) For gases which produce a violet shift, the band will displace toward the violet when the pressure is increased. (3) The intensity of the band increases with increase in pressure. (4) For gases that produce a red shift of spectral lines the intensity of the violet band is much lower than that for gases that produced a violet shift.

No observation has been made yet on the pressure shift of the recently observed "red band" of the alkali metals.[79,153] It is to be noted that the pressure shift of the violet band as stated in points (1) and (2) of the previous paragraph are in harmony with the observation of the pressure shift of spectral lines.

Interpretations of these effects have never advanced beyond a qualitative level. A simple mechanism which accounts roughly for the presence of both the red and the violet bands can be formulated by means of the very versatile potential curves following the ideas of Kuhn,[146] Oldenberg,[147] and Preston.[149] These correspond strictly to the statistical theory for the line edges described in Sec. II.C. The frequency of the light absorbed is given by the difference between the interatomic potentials for the upper and lower states concerned, since it is assumed that the energy of thermal motion of the system does not change during the electronic transition. Hence, the frequency of the absorbed light observed should be confined within the region defined by the minimum and the maximum appearing in the potential difference curve. The potential difference usually changes very slowly at the minimum and the maximum, so that rather pronounced bands will appear at the line edges corresponding to them. Thus, the minimum of the potential difference gives rise to the red band and the maximum to the violet band. If there are several minima and maxima in the potential difference curve related with an atomic line, several such resolved bands could be expected.

Red bands are not observed for light gases, such as He, H_2, and Ne, because their polarizabilities are too small to give rise to any striking minimum. Since the maximum of the potential difference appears at small interatomic distances and the radial distribution of perturbers falls off rapidly with decreasing distances, the intensity of the violet bands at low pressures are usually very weak. However, it increases enormously at high pressures,[84] probably because of the smaller mean interatomic distances.

The difference of the values of $\Delta\nu_m$ of the red bands for the two doublet components may correspond to the conspicuous variation of doublet separations at the intermediate (red band) distances of interaction according to the state of the absorber. The observed linear dependence of $\Delta\nu_m$ of the red bands with hydrocarbons on their polarizabilities certainly deserves a discussion. For a small region at intermediate distances, the R-dependent part of the potential difference curve may be approximated by $U\{(6/p-6)(R_0/R)^p$

[154] H. Kuhn, Z. Physik **76**, 782 (1932); T. Z. Ny and W. P. Wong, Compt. rend. **202**, 1428; **203**, 429 and 860 (1936); D. K. Bhattacharyya and J. Murari, Indian J. Phys. **19**, 20 (1945).
[155] L. Jansen and P. Mazur, Physica **21**, 193 and 208 (1955).
[156] J. Robin and B. Vodar, Compt. rend. **242**, 2330 (1956).

$-(p/p-6)(R_0/R)^6\}$ (as suggested by the Lennard-Jones potential function), where U is the minimum energy difference giving approximately the red band maximum $\Delta\nu_m$. p and R_0 are adjustable parameters, independent of the $\Delta\nu_m$. If R_0, the position of the energy minimum, is nearly the same for all perturbers, U will be proportional to the polarizability and $\Delta\nu_m$ will vary linearly with it. Also, the rapid decrease in $\Delta\nu_m$ of the red bands for higher member lines may be due to a rapid increase of R_0 with the total quantum number. Thus, the relative intensity of the band to that of the associated atomic line should increase with the ordinal number of members. This has not yet been experimentally verified.

The fact that the positions of the alkali-paraffin violet bands are essentially the same for all paraffins ($\Delta\nu_m$(Rb(1)]$\sim$480$-$450 cm^{-1}) except for methane ($\Delta\nu_m$[Rb(1)]$\sim$390 cm^{-1}) is considered to be due to the effect of collisions localized at a colliding part of the molecular surface, instead of with the whole molecule. Considering that intermolecular repulsion comes from electrostatic interaction between slightly bared nuclei due to distortions of the electronic distribution, $\Delta\nu_m$ may be roughly inversely proportional to the charge density [roughly$\sim(2n+2)/n^{\frac{2}{3}}$] at the contour surface and to the curvature (roughly $\sim 1/n^{\frac{1}{3}}$), where n is the number of carbon atoms in the paraffin molecule. Thus, $\Delta\nu_m \sim n/(2n+2)$, which predicts the smallest $\Delta\nu_m$ for methane. Although this calculation would predict a larger $\Delta\nu_m$ for large n, this effect is presumably suppressed by the larger dispersion energy of the heavier molecule. Actually, when molecules are approaching each other, the valley of potential minimum may tend to orient towards the colliding pair in spite of thermal rotations. This effect would be also one of the reasons for the same value of $\Delta\nu_m$ with butene-2 as with those of normal hydrocarbons.

Although Preston's idea could be used to account for some observed phenomena as described above, one should note that his picture is still far from complete. Several bands associated with an atomic line require several minima and maxima in the potential difference curve, which is hardly to be expected, although the potential curve at close distances must be very complicated. The rapid decrease in $\Delta\nu_m$ of the red and the violet bands for higher member lines and the usual expectation of less steep repulsive potentials for higher excited states may indicate that the potential difference curves tend to have less and less pronounced minima and maxima for higher members, resulting in a monotone curve such as Eq. (52). Then, for highly excited states the potential well may be deep and wide enough for easier molecular formation, which is not observed. Furthermore, the quantum number J may not be good any more, since an angular momentum originated in thermal motion of a perturber, including both translational and, in the case of hydrocarbons, rotational, should be added. The intermolecular field deviates from the spherically symmetric one at close distances when an alkali atom is in the state $^2P_{\frac{1}{2}}$, so that the angular wave function for thermal motion in the ground and excited states are not orthogonal to each other. The angular momentum of thermal motion may be required to change at an electronic transition although this is not obvious without calculation. Red and violet bands are modifications of atomic lines due to thermal motion of perturbers. But why is it possible to broaden the line several times larger in energy units than the energy of the thermal motion per particle? Although generally the statistical theory does not lead to large errors, even when it is not obviously applicable, it has not been considered quantum-mechanically for the case of close encounters. The WKB method[98] loses its validity, when the potential varies rapidly over the wavelength for the motion of a perturber. Also the representation of perturbers as points, instead of wave packets, used in the impact theory becomes worse. The interatomic region responsible for the red and violet bands may be largely affected by quantum-mechanical effects due to the noncommuting properties involved, including the radial distribution function of perturbers at close distances. Thus, this region has been excluded, as a quantum-mechanical region, in the discussion of II.B., C, and D.

D. PRESSURE BROADENING OF MOLECULAR BANDS IN THE INFRARED REGION

The effect of transparent foreign gases in increasing the infrared absorption of a given amount of absorbing gas has been known since 1889.[157a] Beer's law,[157b] however, states that each molecule of a gas absorbs independently and the absorption coefficient is proportional to the concentration of the absorbing gas molecules. This discrepancy has been attributed to molecular collisions in the gas mixture[158] and, later, to collision broadening of individual absorption lines.[159]

A quantitative measurement of the effect of various transparent gases on the intensity of the absorption maximum of N_2O at 4.5 μ and of CO at 4.66 μ ($T=298°$K) was made by Cross and Daniels[160] with instruments of medium resolution. The effective cross sections of foreign gases for increasing infrared absorption thus found are linearly related to the gas kinetic diameters. Likewise the effect was also studied for methane at 7.65 μ, CO_2 at 4.3 μ, and isobutylene at 14.8 μ by Coggeshall and Saier,[161] as shown in Fig. 19. They found that the pressure broadening effects of certain gases on one absorber were characteristic of

[157a] K. Angström, Öfversigt af K. Vetensk. Akad. Förh. **46**, 549 (1889); W. W. Watson, J. Phys. Chem. **41**, 61 (1937).
[157b] A. v. Beer, Pogg. Ann. **86**, 78 (1852).
[158] Eva v. Bahr, Ann. Physik **33**, 585 (1910).
[159] C. Füchtbauer, Physik. Z. **12**, 722 (1911).
[160] P. C. Cross and F. Daniels, J. Chem. Phys. **2**, 6 (1934).
[161] N. D. Coggeshall and E. L. Saier, J. Chem. Phys. **15**, 65 (1947).

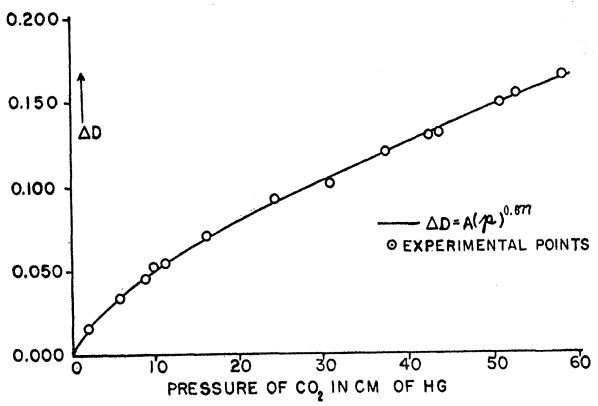

FIG. 19. Increase in optical density of constant pressure of methane as a function of foreign gas pressure (after Coggeshall and Saier[161]).

the nature of the absorber and the wavelength studied, just as the pressure effects on atomic lines.

Usually the absorption coefficient is measured by observing transmittance T_i, when a spectrometer is set to transmit radiation of a certain frequency ν_i. But it actually transmits a frequency band of finite width given by a spectrometer transmission function $f(|\nu-\nu_i|, a)$, where a is the width of the entrance slit. T_i is defined by I_i/I_{0i}, where I_{0i} is the intensity of the radiation transmitted by absorption cell and spectrometer when the cell is empty and I_i is the intensity of the radiation transmitted when the cell is filled with the absorbing gas. If I_ν represents the energy distribution in the radiation reaching the slit through the empty cell,

$$T_i=\frac{I_i}{I_{0i}}=\frac{\int_0^\infty I_\nu \exp(-k(\nu)/l) f(|\nu-\nu_i|, a)d\nu}{\int_0^\infty I_\nu f(|\nu-\nu_i|, a)d\nu}, \quad (142)$$

where l is the absorption length and $k(\nu)$ the absorption coefficient under collision damping, which is given by a general expression summing all single absorption lines m,

$$k(\nu)=\sum_m k_m(\nu)=\sum_m \alpha_m/2\pi^2\tau\left[(\nu-\nu_m)^2+\left(\frac{1}{2\pi\tau}\right)^2\right]. \quad (143)$$

ν_m is a center frequency of a single line and α_m is the total absorption coefficient of the line m.

For simplicity, if lines are assumed to appear quite isolated and when the frequency interval transmitted is so narrow that I_ν may be considered to be constant over this interval, Eq. (142) leads to

$$T_i=\frac{\int_0^\infty \exp\{-\alpha_m l/2\pi^2\tau[(\nu-\nu_m)^2+(1/2\pi\tau)^2]\} f(|\nu-\nu_i|, a)d\nu}{\int_0^\infty f(|\nu-\nu_i|, a)d\nu}. \quad (144)$$

For further calculation, a detailed knowledge of the function $f(|\nu-\nu_i|, a)$ is required. Landenberg and Reiche[162] took $f(|\nu-\nu_i|, a)$ to be constant in the frequency interval ν_i-a, ν_i+a and zero outside. Dennison[163] used a Gaussian function of the form, $\exp[-2.77(\nu-\nu_i)^2/a^2]$. Nielsen, Thornton, and Dale[164] assumed a triangular form, with maximum at $\nu=\nu_i$ and extending from ν_i-a to ν_i+a. With one of these assumptions, expansion of the exponentional function in Eq. (144) and integration term by term give, at $\nu=\nu_i$, when $(1/\tau^2)\ll(\alpha l/\tau)<2(\pi a)^2$,

$$T_m=1-2\frac{(\alpha_m l/2\pi\tau)^{\frac{1}{2}}}{a}+\cdots \simeq\exp[-2(\alpha_m l/2\pi\tau)^{\frac{1}{2}}/a], \quad (145)$$

for a rectangular form and

$$T_m=\exp[-1.879(\alpha_m l/2\pi\tau)^{\frac{1}{2}}/a], \quad (146)$$

for a Gaussian form. Thus, the result is essentially insensitive to the form of the transmission function. These expressions have been successfully used to account for measurements on individual strong lines. But to get over-all dependence on α_m, τ, l, and a of T_m, Eq. (144) must be numerically integrated.[164]

In infrared bands of polyatomic molecules, the individual lines generally lie so close together that a considerable number of them have their centers in the narrow frequency range transmitted by the spectrometer. The idealized case of an absorption band consisting of an infinite sequence of equidistant identical absorption lines, of which many fall in the frequency band transmitted by the spectrometer, has been treated by W. M. Elsasser.[165] Starting from Eqs. (142) and (143) with $\alpha_m=$ const (α) and $\nu_m=md$ because ν_m distributes with equal spacing d in frequency, he obtained, for small values of $1/d\tau$ (low pressure),

$$T=1-\Phi\left(\frac{(\alpha l/2\tau)^{\frac{1}{2}}}{d}\right). \quad (147)$$

[162] R. Landenburg and F. Reiche, Ann. Physik **42**, 181 (1913).
[163] D. M. Dennison, Phys. Rev. **40**, 81 (1932).
[164] Nielsen, Thornton, and Dale, Revs. Modern Phys. **16**, 307 (1944).
[165] W. M. Elsasser, Phys. Rev. **54**, 126 (1938).

Φ is the probability integral. For large values of $1/d\tau$ (high pressure),

$$T=\exp\left[-\frac{\alpha l}{d}\tanh\frac{1}{d\tau}\right]\cdot J_0\left(i\frac{(\alpha l/d)\tanh(1/d\tau)}{\cosh(1/d\tau)}\right). \quad (148)$$

J_0 is the Bessel function of zeroth order.

The above calculations are only for limiting cases and actual lines are neither quite isolated nor equally spaced in an infinite sequence, but rather are between them. Extensions to more general types of vibration-rotation bands have been given by Matossi and collaborators.[166] However, the above results for idealized cases lead to the correct functional relations between absorption, pressure, and optical density.

The discussion above has been limited to the case of Lorentz broadening. With strongly polar or reactive gases, larger deviation from a simple absorption expressed by Eqs. (147) and (148) may be expected.

When instruments of high resolving power are used, the half-widths of the individual rotational lines can be measured instead of the total band absorption. Herzberg and others[167] investigated the self-broadening of the rotational lines in HCN. The same problem was studied by Kortüm and Verleger[168] for both self-broadening and pressure broadening due to the addition of different foreign gases. The line widths of both the P and the R branch of the 0–3 vibration-rotation band of HCN at $1.0380\,\mu$ were measured. The self-broadening of the HCN band over the pressure range 75 to 550 mm Hg is shown in Fig. 20. It is to be noted that the half-widths for both branches reach a maximum at the density maximum of the band ($J\simeq 8$), and decrease with both decreasing and increasing J's.

The broadened lines of linear polar molecules are somewhat less well understood because of the difficult calculation of the interaction energy involved. One

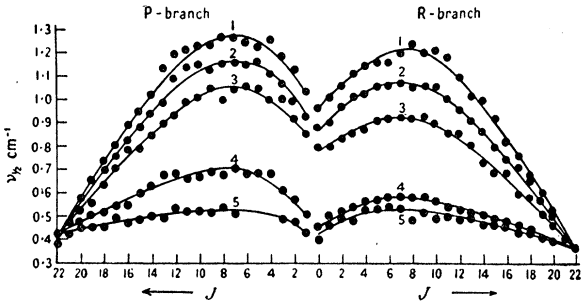

FIG. 20. The half-width values of the absorption lines of the 0–3 band of HCN in relation to the rotational quantum number J of the P and R branch for different pressures of the absorption gas (after Kortüm and Verleger[168]). 1: $p=550$ mm; 2: $p=450$ mm; 3: $p=300$ mm; 4: $p=150$ mm; 5: $p=75$ mm.

[166] Matossi, Mayer, and Raucher, Phys. Rev. **76**, 760 (1949).
[167] G. Herzberg and J. W. T. Spinks, Proc. Roy. Soc. (London) **A147**, 434 (1934); S. D. Cornell, Phys. Rev. **51**, 739 (1937); E. Lindholm, Z. Physik **109**, 223 (1938); **113**, 596 (1939).
[168] G. Kortüm and H. Verleger, Proc. Phys. Soc. (London) **63**, 462 (1950).

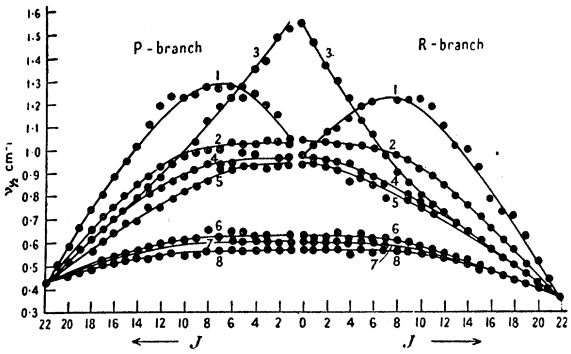

FIG. 21. The half-width values of the absorption lines of the 0–3 band of HCN in relation to the J's of P and R branches when various foreign gases are added (after Kortüm and Verleger[168]).

1: HCN/HCN
2: HCN/DCN
3: HCN/C_2H_5Cl
4: HCN/SO_2
5: HCN/$(CH_3)_2O$
6: HCN/H_2S
7: HCN/N_2O
8: HCN/N_2

should expect at least two types of interactions between HCN molecules, rotational and dipole-dipole, although the rotating dipoles should not have any permanent dipole moment on the average. As described in Sec. II. A. 2.b.i, the dipole-dipole interaction for lower rotational levels must obey the R^{-3} law, since the interaction between molecules due to the thermal motion is easily larger than the level spacing $\hbar^2 J/I$ for such levels, I being the moment of inertia. Thus, a permanent dipole moment may appear. Under these considerations, the interaction energy difference in the transition $J-1\rightarrow J$, will be $0.2\,\mu\mu'/JR^3$, as given in Eq. (17), for lower rotational levels. Hence, through Eq. (55), a larger half-width is expected for lines with smaller J values. In addition, for self-pressure, the two interacting molecules, with $\Delta J=\pm 1$ either before or after absorption, undergo resonance, according to Eq. (13), either before or after absorption respectively. This resonance causes another half-width which depends on J through Eq. (13) and on its statistical population, giving a maximum around $J=8$. The total half-width will be given approximately by combining the effects due to rotational resonance and dipole-dipole interaction.

The rate of decrease in half-width for increasing J is greater for higher pressures, and the absolute value of half-width for the R branch is smaller than those for the P branch, as theoretically predicted by Lindholm[167] through London's formula.[36] The average half-width values for all band lines were strictly proportional to the pressure for the pressure range studied. The slope was about $9.1\cdot 10^{-4}$ cm^{-1}/mm Hg.

Figure 21 gives the half-width values of the absorption lines of the 0–3 band of HCN in relation to J of the P and R branches when various foreign gases were added. The HCN partial pressure was kept at 75 mm and the total pressure at 550 mm. It is to be noted that, under the pressure of foreign gases, the half-widths were not greatest at the intensity maximum of

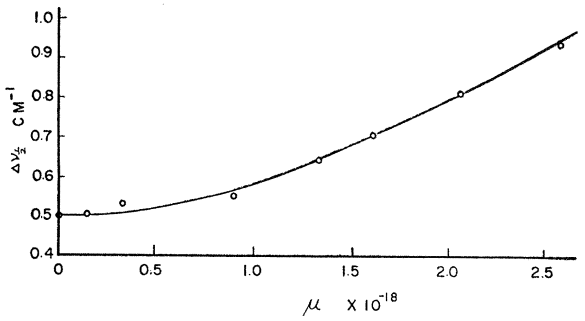

FIG. 22. Mean values of the half-width values of all the rotational lines of the HCN O–3 band in relation to the dipole moment of the added gas (after Kortüm and Verleger[168]).

the band, but reached a maximum for lines which resulted from transitions between energy states of low J values. This is to be expected from Eq. (17) and the discussion in the previous paragraph, since no resonance energy is assigned in this case. The effect that the broadening decreases in both branches for increasing J was particularly apparent for ethyl chloride. The effect that the half-width due to DCN (with the largest dipole moment of all) is smaller than that due to ethyl chloride was considered possibly due to the fact that the hydrogen bonds had a strong affinity for chain association. In particular, the resonance effect predominant for the HCN case should be reduced for DCN, because of the different magnitudes of moments of inertia. Figure 22 is a plot of the average half-width of all the lines of a band *vs* $\mu\mu'$, where μ is the dipole moments of the added gases and μ' that of HCN. It follows from the curve that the half-widths first changed slowly for small μ and then the variation was amost linear with $\mu\mu'$ when $\mu > 0.75$.

The rotational lines of the near infrared band of HCl, H_2O and CO_2 were broadened to about the same extent and the line width could be accounted for by Lorentz theory, *viz.*, approximate proportionality between the width and the pressure and with intensity distributions of the dispersion form.

Coulon[169,170] examined the perturbation of the infrared fundamental bands of HCl (3000 cm^{-1}) by N_2, A, He, H_2 and O_2 and of the 2100 cm^{-1} band of CO by N_2 and A compressed up to 1000 atmospheres, using a Perkin-Elmer spectrometer with LiF prism. With He, H_2, or argon the rotational structure was still visible for the P branch of HCl at r.d. 350. The two maxima for the P and the R branches were obvious even when the argon r.d. was 450, the highest attained. With nitrogen the rotational structure disappeared around r.d. 170. The perturbation grew stronger in the order He, H_2, A, O_2, N_2. An absorption maximum very close to the forbidden Q branch of HCl was observed as induced by the nitrogen pressure. The intensity of this Q maximum increased rapidly with pressure. As is characteristic of collision-induced absorption,[171,172] the total intensity of the band, $I = \int \alpha(\nu) d\nu$, increased linearly with the density of the gases beyond 50 r.d. (but more rapidly with N_2 than with a spherical atom A). For CO (with a smaller dipole moment than that of HCl) the changes in intensity are smaller than for HCl.

In the case of the vibration-rotation bands of some other polystomic molecules such as NH_3, no J dependence of this line broadening could be established, although there was a definite increase in line width with pressure. Other molecules such as CH_4 gave sharp lines under similar conditions.[173]

When the rotational half-width of molecules were very small, so small that the direct measurement of the line shape was beyond the resolving power attainable with most spectrographic instruments, it could be estimated indirectly by studying the dependence of apparent absorption on total pressure.[174] From Eq. (147) $T \sim 1 - 2(\alpha l/2T)^{\frac{1}{2}}/d$ or $-dT/d(p)^{\frac{1}{2}} = 2(\alpha l/2\tau_0)^{\frac{1}{2}}/d$ where $1/\tau = (1/\tau_0)p$, p being a total pressure and $1/\tau_0$ a number of optical collision per unit time at a unit pressure. Thus, the last expression, i.e. the slope of a T *vs* $p^{\frac{1}{2}}$ plot can be used to determine half-width $1/2\pi\tau_0$ at unit pressure. Thus, Penner and Weber showed that the rotational half-width of the fundamental line of CO in the presence of H_2 or A was 0.077 cm^{-1} per atmosphere or 0.040 cm^{-1} per atmosphere, respectively. Similarly for H_2 the first overtone of CO showed a half-width of 0.063 cm^{-1} per atmosphere. These results are somewhat smaller than the values 0.10 cm^{-1} atmos^{-1} and 0.12 cm^{-1} atmos^{-1} for the fundamental and first overtone line with air.[175]

The pressure broadening of individual pure rotational lines, *viz.*, the $J = 2 \rightarrow 3$ line of the HCl band at 3.4 μ and the $J = 4 \rightarrow 5$ line of the CH_4 band at 3.25 μ, was studied by Benesch and Elder[176] using a matching method to establish a comparison between line widths. An absorption line was broadened by the same amount for each broadening (foreign) gas. The quantity of broadening gas necessary to produce this predetermined line width for a fixed number of absorbers was an inverse measure of the relative efficiencies for broadening by these gases. The experimentally determined information on broadening ability was used to compute the relative optical collision diameters obtained from pressure broadening of an infrared line of HCl against the values of absolute collision diameters obtained from

[169] Coulon, Oksengorn, and Robin, Compt. rend. **236**, 1481 (1953).
[170] Coulon, Galatry, Oskengorn, Robin, and Vodar, J. phys. radium **15**, 58 (1954).
[171] Crawford, Welsch, and Locke, Phys. Rev. **75**, 1607 (1949); M. Mizushima, Phys. Rev. **76**, 1268 (1949); **77**, 149 (1950).
[172] Kiyama, Minomura, and Ozawa, Proc. Japan Acad. **30**, 758 (1954).
[173] H. Verleger, Physik. Z. **38**, 83 (1937).
[174] For instance, A. M. Thorndike, J. Chem. Phys. **16**, 211 (1948); S. S. Penner and D. Weber, *ibid.* **19**, 1351 (1951).
[175] L. A. Matheson, Phys. Rev. **40**, 813 (1932).
[176] W. Benesch and T. Elder, Phys. Rev. **91**, 308 (1953).

pressure broadening of a microwave absorption line of NH_3 (by Smith and Howard[42] and Hill and Smith[177]) using the same foreign gases, as shown in Fig. 23. The correlation indicated in the figure emphasizes the fundamental similarity of pressure broadening results in the two distinct spectral regions. In this particular case, not only the frequency (3000:1) was enormously different (leading to a corresponding disparity between the duration of collision and the period of the absorbed radiation) but the dipole moments were different, and, furthermore, one line (HCl line) originated in molecular vibration-rotation and the other (NH_3 line) resulted from the inversion of the ammonia molecule.

To show the effect of a dipole moment in the absorbing molecule Benesch and Elder[176] also used nonpolar CH_4 as absorber. The relative collision diameters obtained for HCl absorption were plotted against those for CH_4 absorption as shown in Fig. 24. The points fall nearly along two straight lines, except for HCl which displayed a higher collision cross section due to resonance interaction. The lower lines belong to points for molecules with a high degree of symmetry, *viz.*, the five rare gases and SF_6. This line, like that of Fig. 23, nearly passes through the origin, showing that the interaction is probably dependent on the polarizability of the perturbing molecules. The strength of interaction was not constantly enhanced by the dipole moment in the absorbing molecule.

The much greater slope of the upper line indicates that the ratio of the interaction strength between the same molecules and CH_4 is much greater, due to the influence of the dipole moment of HCl. So additional

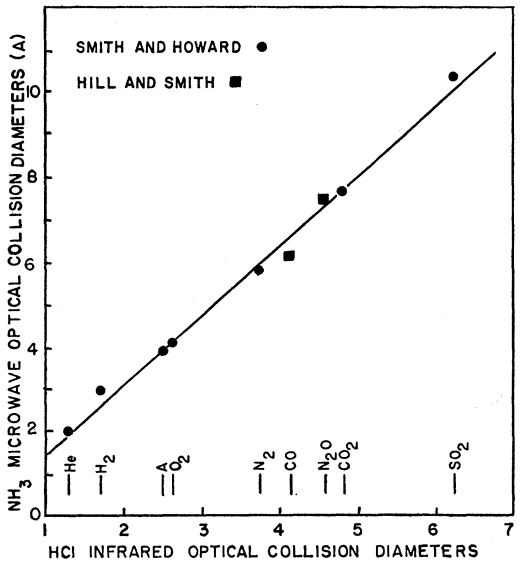

FIG. 23. Optical collision diameters obtained from broadening of a microwave absorption line of NH_3 compared with relative optical collision diameters obtained from broadening of an infrared line of HCl (after Benesch and Elder[176]).

[177] R. M. Hill and W. V. Smith, Phys. Rev. 82, 451 (1951).

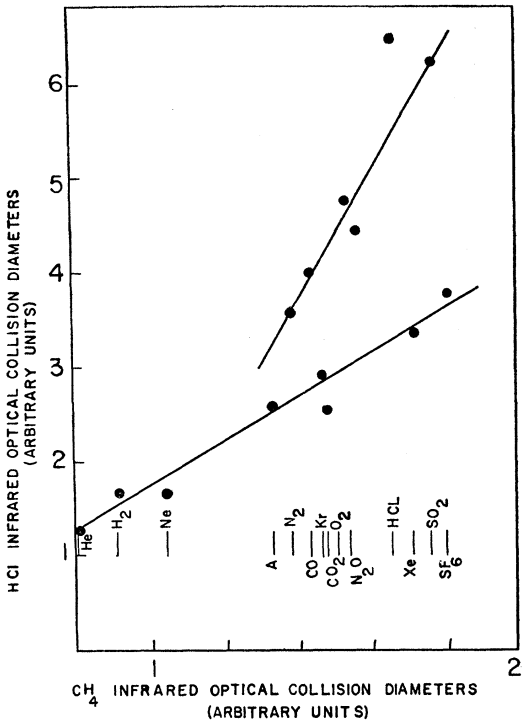

FIG. 24. Relative optical collision diameters obtained by pressure broadening of an HCl infrared absorption line compared with those obtained by pressure broadening of a CH_4 infrared absorption line with the same gases (after Benesch and Elder[176]).

interaction strength due to this dipole moment was added to the common value shown in the lower line. This investigation pointed out the source of difficulty inherent in previous interpretations of experimental data. While a single type of long range interaction between dipole moment, induced dipole moment and quadrupole moment of the absorber and the perturber may be capable of explaining the behavior of one particular group of molecules, at least two different types of interactions were involved in the pressure broadening of a dipole absorber when a variety of perturbers was used.

E. PRESSURE BROADENING OF LINES IN THE MICROWAVE REGION

More accurate measurements of the absorption intensities can be made in the centimeter wave region than in the optical or the infrared regions. Thus, the shape of the spectral lines and the variation of their widths have been studied over a range of pressures from atmospheric down to 0.01 mm Hg or less. For low pressures, effects due to multiple encounters can be neglected and the Van Vleck-Weisskopf expression (36a) will be applicable, but the theoretical analysis is not yet refined well enough to give a complete interpretation of experimental data.

Considerable work has been done on self-broaden-

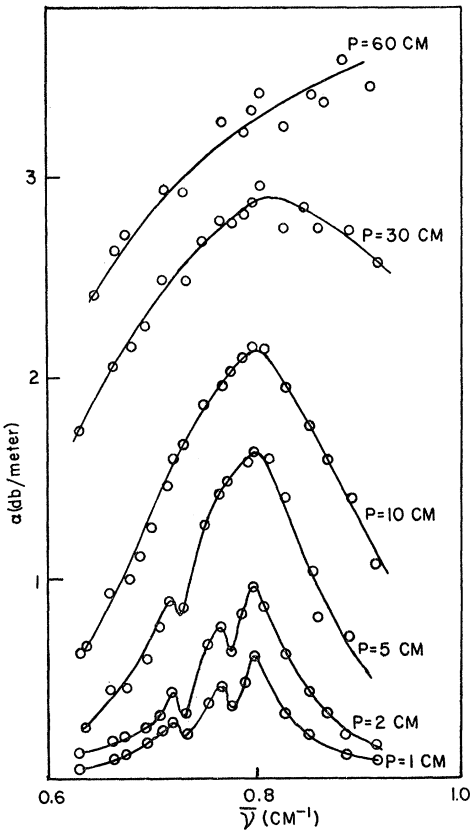

FIG. 25. Absorption curves for ammonia at various pressures (after Bleaney and Penrose[179]).

ing[178] such as the broadening of the inversion spectrum of ammonia[42,177,179] ($\rho\sim$14 A for (3.3) line), oxygen[180] ($\rho\sim$5 A for $J=6\rightarrow 8$ line), water[181] ($\rho\sim$10 A for $J=5_{-1}\rightarrow 6_{-5}$ line), methyl halides[182] ($\rho\sim$8 A) and of rather simple linear molecules[183] ($\rho\sim$10–20 A). The values of ρ, the collision diameter, is indicated in each case. Figure 25 is a sample curve for ammonia at various pressures. The lines become sufficiently broad to obscure the fine structure at a pressure of 10 cm Hg.

At low pressures, say, between 0.5 mm and 10 cm Hg, all results obtained by various investigators confirm that the line widths vary linearly with pressure, and there is no observable shift. For ammonia, however, when the pressure is high (above 30 cm Hg) the experimental curve[179] shows a definite shift to lower frequencies as shown in Fig. 26, and the resonance frequency becomes substantially zero for pressures above two atmospheres. The line width no longer increases linearly with pressure but rather decreases with pressure, but above four atmospheres, again, it increases linearly with pressure.

This pressure variation for ammonia, particularly of the shift, has been explained in a semiquantitative way.[184] Margenau,[35] applying the variational method, calculated the shift of and the transition probabilities between energy levels of two and three NH_3 molecules under dipole-dipole interaction in a simple model. He showed that the inversion line split, due to the perturbation, into respectively two or three lines. In either case, only one line appears with decreasing frequency but with increasing intensity with perturbation at the expense of the rest. Thus, the shift is obvious and the presence of two or more frequencies with changing intensities will destroy the proportionality of line widths with pressure and narrowing may take place, although no rigorous theoretical treatment about this effect has appeared. If the pressure becomes high, the most intense line component will accentuate its frequency reduction. The frequency of this line component changes as for a binary collision,

$$\nu_0'=\nu_0[(1+\lambda^2)^{\frac{1}{2}}-\lambda], \tag{149}$$

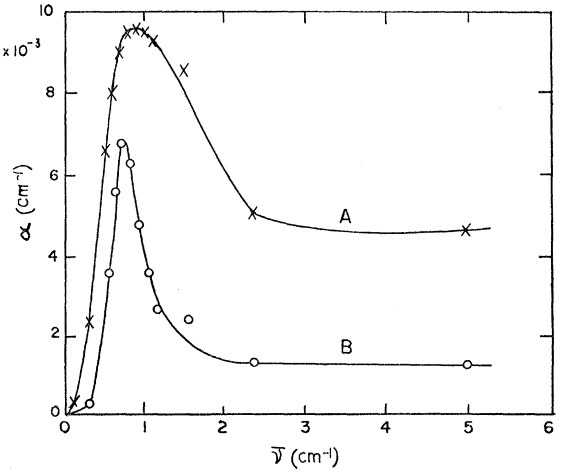

FIG. 26. Absorption coefficient *vs* frequency for ammonia *A*: 90 cm Hg; *B*: 30 cm Hg (after Bleaney and Loubser[179]).

[178] Gordy, Smith, and Trambarulo, *Microwave Spectroscopy* (John Wiley and Sons, Inc., New York, 1953), p. 185; C. H. Townes and A. L. Schawlow, *Microwave Spectroscopy* (McGraw-Hill Book Company, Inc., New York, 1955).

[179] C. H. Townes, Phys. Rev. **70**, 665 (1946); B. Bleaney and R. P. Penrose, Proc. Phys. Soc. (London) **59**, 418 (1947); Proc. Roy. Soc. (London) **A189**, 358 (1947); B. Bleaney and J. H. N. Loubser, Nature **161**, 522 (1948); Proc. Phys. Soc. (London) **A63**, 483 (1950); D. F. Smith, Phys. Rev. **74**, 506 (1948); I. R. Weingarten, thesis, Columbia University (1948), and reference 47.

[180] Anderson, Smith, and Gordy, Phys. Rev. **82**, 264 (1951); R. Beringer, Phys. Rev. **70**, 53 (1946); J. H. Van Vleck, Phys. Rev. **71**, 413 (1947); Strandberg, Meng, and Ingersoll, Phys. Rev. **75**, 1524 (1949); H. R. L. Lamont, Phys. Rev. **74**, 353 (1948); J. O. Artman and J. P. Gordon, Phys. Rev. **87**, 277 (1952), and reference 191.

[181] (a) G. E. Becker and S. H. Autler, Phys. Rev. **70**, 300 (1946); (b) C. H. Townes and F. R. Merritt, Phys. Rev. **70**, 558 (1946).

[182] B. Bleaney and J. H. N. Loubser, reference 179; Gillam, Edwards, and Gordy, Phys. Rev. **75**, 1014 (1949).

[183] ICI, Townes, Merritt, and Wright, Phys. Rev. **73**, 1334 (1948); OCS, Townes, Holden, and Merritt, Phys. Rev. **74**, 1113 (1948); C. M. Johnson and D. M. Slager, Phys. Rev. **87**, 677 (1952); and references 47 and 192; ICN, ClCN, BrCN, Smith, Gordy, Simmons, and Smith, Phys. Rev. **75**, 260 (1949); and reference 193; CH_2O, R. B. Lawrence and M. W. P. Strandberg, Phys. Rev. **83**, 363 (1951).

[184] P. W. Anderson, Phys. Rev. **75**, 1450 (1949); H. Margenau, Phys. Rev. **76**, 121 (1949).

where $\lambda \sim 2\mu^2 N/h\nu_0 c$, ν_0 being the unperturbed frequency of the inversion line. μ is the permanent dipole moment, and N the number of molecules per cc. For $\lambda \gg 1$, ν_0' equals substantially zero and the absorption should change from the resonant absorption to that of the Debye type.

The experimental confirmation of Eq. (149) may be attributed to the work by Birnbaum and Maryott.[185] The completely deuterated ammonia ND_3 is expected to behave in the same manner as NH_3 under pressure. However, since the resonance frequency ν_0 of the ND_3 inversion line is near 1600 Mc/sec[186] and 14.8 times less than that of NH_3, the shift in the inversion frequency should occur at pressures about 15-fold lower than in the case of NH_3 according to Eq. (149). They observed this relationship with a good agreement using the results for NH_3 by Bleaney and Loubser.[179] At higher pressures (above 6 cm Hg) the resonance frequency of ND_3 drops to zero more rapidly than predicted by Eq. (149).

Measurement of the half-widths of 14 resolved magnetic absorption[187] lines in the 5-mm wavelength region for oxygen were made by Anderson, Smith and Gordy[188] and others.[189]. Line-breadth parameters††† obtained ranged from 0.0319 to 0.0516 cm^{-1}/atmos with a population weighted mean of 0.0475 cm^{-1}/atmos. On the other hand, the half-width for the rotational transition at 2.5 mm wavelength was found by Hill and Gordy[190] as $\Delta\nu_{\frac{1}{2}}' = 0.064$ cm^{-1}/atmos at $T = 300°K$ and 0.09 cm^{-1}/atmos at 195°K.

The difference between these half-width parameters can be understood as caused by the temperature difference. In this case, $\Delta\nu_{\frac{1}{2}}$, in units of cm^{-1} $atmos^{-1}$, will vary approximately as T^{-1} according to their measurement, although Beringer and Castle[191] observed that it varied as $T^{-\frac{3}{4}}$ to T^{-1}. Equation (56) predicts its variation as $T^{-\frac{3}{4}}$ for constant $\Delta\gamma$, since N is proportional to pressure divided by T. But since the populations of rotational levels J of perturbers change with temperature, $\Delta\gamma$ changes its value with T. Hence, this temperature dependence is extremely complex when rotational levels are involved. However, its observation offers one of the important methods of finding the nature of interaction forces. The temperature dependence of the optical collision diameters, $T^{-0.2}$ for OCS[192] and $T^{-0.5}$ for BrCN,[193] has been theoretically analyzed by Smith, Lackner, and Volker.[43] They find that the T dependence requires the introduction of a quadrupole-dipole interaction in addition to the first-order dipole-dipole, and have determined the quadrupole moment of BrCN as $Q/e = 5.7\times10^{-16}$ cm^2. For ammonia, Bleaney and Penrose[179,194] obtained the T^{-1} law. Then, with Eq. (35), the absorption at wings is proportional to T^{-3}, which has been confirmed experimentally by Birnbaum and Maryott.[195]

Because of the special origin of a spectral line (magnetic absorption), oxygen, like ammonia[194] (inversion spectra), is one of the rare cases which has microwave spectral lines in the significantly populated rotational states K. Since Eqs. (23) and (56) give[37]

$$\Delta\nu_{\frac{1}{2}} = 1.33\times10^{15} Q(1/K \pm \tfrac{3}{8}K^2)^{\frac{1}{2}} \text{ cm}^{-1} \quad \text{for} \quad \begin{matrix} K+1\to K \\ K-1\to K \end{matrix}$$

for high K values and the dispersion force gives the same type of K dependence,[64] the variation of the observed line width as a function of K may reveal again a rotational resonance interaction, with its maximum at the largest population predicted by the Boltzmann statistics, as mentioned before for the infrared lines of HCN (Fig. 20). This indication of resonance interation might be checked by changing the temperature of the gas, since the change in K value for maximum population thus resulting could cause the shift of the K value corresponding to the maximum half-width.

Pressure broadening due to foreign gases in the microwave region has been studied experimentally with ammonia, water and oxygen. Bleaney and Penrose[194] and, later, Smith and Howard[42] and Hill and Smith[177] measured the collision cross sections of the $(J,K) = (3,3)$ line at 0.796 cm^{-1} of the inversion spectrum of ammonia for binary mixtures of seventeen different nonpolar and polar gases. The results are tabulated in Table VI, showing larger collision cross sections for polar gases than otherwise. The ammonia partial pressure was between 0.2 to 3 mm Hg (0.02 to 0.04 mm Hg for Howard and Smith[42]) and the concentration of foreign gas to ammonia was about 10:1. The collision cross section was computed from the measurement of the absorption coefficient α at the center of the line, which is related to half-width $\Delta\nu_{\frac{1}{2}}$ by Eq. (36a), neglecting effects[178] of saturation[50,51] given by Eq. (36b) and collisions with the walls. With $\nu = \nu_0$, Eq. (36a) leads to

$$\alpha = \frac{8\pi^2 |\mu_{JK}|^2 \nu_0^2 N_{JK}}{3kT\Delta\nu_{\frac{1}{2}}} \text{ cm}^{-1}, \tag{150}$$

[185] G. Birnbaum and A. A. Maryott, Phys. Rev. **89**, 895 (1953); **92**, 270 (1953).

[186] Nuckolls, Rueger, and Lyons, Phys. Rev. **89**, 1101 (1953).

[187] Oxygen molecule has no electric dipole moment, but it does have a magnetic moment of two Bohr magneton and gives rise to magnetic absorption. R. Schlapp, Phys. Rev. **51**, 342 (1937).

[188] Anderson, Smith, and Gordy, Phys. Rev. **87**, 561 (1952).

[189] B. V. Gokhale and M. W. P. Strandberg, Phys. Rev. **84**, 844 (1951).

††† Line-breadth parameter is defined as the half-width measured at half-intensity (the half-intensity *half-width*), and will be indicated as $\Delta\nu'_{\frac{1}{2}}$. The half-width, $\Delta\nu_{\frac{1}{2}}$ (without a prime) as used in Sec. III(1) is half-intensity *width*, and is, therefore, twice larger.

[190] R. M. Hill and W. Gordy, (unpublished).

[191] R. Beringer and J. G. Castle, Jr., Phys. Rev. **81**, 82 (1951).

[192] Feeney, Lackner, Moser, and Smith, J. Chem. Phys. **22**, 79 (1954).

[193] Trambarulo, Lackner, Moser, and Feeny, Phys. Rev. **95**, 622(A) (1954).

[194] B. Bleaney and R. P. Penrose, Proc. Phys. Soc. (London) **60**, 540 (1948).

[195] G. Birnbaum and A. A. Maryott, J. Chem. Phys. **21**, 1774 (1953).

TABLE VI. Optical collision diameters for mixtures of various gases in the microwave region.

Absorber and line	Perturber	$\mu(\bar{\mu})$[a] Debye	Molecular weight of perturber	Optical collision diameter A Exp.	Theor.[b]	Kinetic collision diameters[c]	Reference
NH_3 (3,3)	HCN(2.59)[d]	2.96(0)	27.0	9.95			
	ClCN(−)	2.80(0)	61.5	11.9			
	CH_3Cl(4.56)	1.87(0.47)	50.5	11.3			g
	SO_2(3.72)	1.6(0)	64.1	10.4			
	CH_2Cl_2(6.48)	1.59(0)	85.0	10.3			
	NH_3(2.26)	1.44(0.78)	17.0	13.8[e]	14.0[f]	4.43	h
	$CHCl_3$(8.23)	0.95(0.57)	119.0	13.7			g
	OCS(−)	0.71(0)	60.1	7.54			
	N_2O(3.00)	0.25(0)	44.0	7.32		4.35	i
	CS_2(8.74)	0(0)	76.1	7.5–7.72			g, h
	CO_2(2.65)	0(0)	44.0	7.59		4.51	g
	CCl_4(10.5)	0(0)	154.0	7.20			
	O_2(1.60)	0(0)	32.0	4.85–3.86	3.35	4.02	
	N_2(1.76)	0(0)	28.0	6.4–5.54	3.39	3.4	
	H_2(0.79)	0(0)	2.0	3.50–2.95	2.57	3.58	g, h
	A(1.63)	0(0)	39.9	4.6–3.73	3.42	4.04	
	He(0.22)	0(0)	4.0	2.35–2.00	2.15	3.20	
H_2O ($J=5_{-1}\rightarrow 6_{-5}$)	Air	0(0)		5.4		3.5	j
	H_2O(1.5)	1.94	18.0	10.0		10.2	
O_2 ($J=8\rightarrow 9$)	NH_3(2.26)	1.44(0.78)	17.0	4.3		4.02	
	N_2O(3.00)	0.25(0)	44.0	4.4		4.15	
	O_2(1.60)	0(0)	32.0	3.5–5		3.61	k
	N_2(1.76)	0(0)	28.0	2.8–4.5		3.68	
	A(1.63)	0(0)	39.9	3.6		3.63	

[a] μ: Static dipole moment of a perturber. $\bar{\mu}$: Weighted average of dipole moment over population of rotational levels.
[b] See reference 41.
[c] E. H. Kennard, *Kinetic Theory of Gases* (McGraw-Hill Book Company, Inc., New York, 1938).
[d] Polarizability (in $cm^3\times10^{-24}$) averaged over three directions See Landolt-Börnstein (Springer-Verlag, 1951), I. Band, 3. Teil, p. 511.
[e] For low pressure (7.7 A for pressures more than 4 atmos).
[f] See reference 52.
[g] See reference 176.
[h] See reference 194.
[i] See reference 177.
[j] See reference 181b.
[k] See reference 188.

for relatively sharp lines as are commonly observed in the microwave region. Here,

$|\mu_{JK}|^2$ = square of dipole moment associated with the line (J,K).
ν_0 = wave number of the line in cm^{-1}.
N_{JK} = number of ammonia molecules per cc in rotational level (JK).
$\Delta\nu_{\frac{1}{2}}$ = the half-width in $cm^{-1}=f_{12}/\pi c$, f being the collision frequency between the foreign gas and an ammonia molecule in state (3,3); c, velocity of light.

$$f_{12}=2N_2S_{12}\left(\frac{2RT}{\pi}\right)^{\frac{1}{2}}\left(\frac{1}{M_1}+\frac{1}{M_2}\right)^{\frac{1}{2}},$$

N_2 being the number of foreign gas molecules, M_1 and M_2 the molecular weights, and S_{12} the cross sections for ammonia-foreign gas collisions, which is equal to $\pi\rho_{12}^2$ where ρ_{12} is the collision diameter. Since S_{12} is proportional to f_{12}, which is in turn proportional to $\Delta\nu_{\frac{1}{2}}$,‡‡‡ S_{12} is also a measure of the effect of collision broadening of the (3,3) line produced by various gases. If the order of efficiencies for broadening by these foreign gases is that shown in Fig. 23, the result is in perfect agreement with that obtained with infrared spectra. No shifts of absorption line frequency were observed. These results show that the impact theory is a good approximation under low pressures, as seen in Table VI. However, it might be noticed here that although the idea of the collision diameters is very often useful, for instance, for the determination of the force law, the force laws in many cases are so complicated that the collision diameters are hardly meaningful without detailed discussion.

Becker and Autler[181] made accurate measurements on the broadening of the water vapor line at 0.742 cm^{-1} for mixtures of water vapor and air at 45°C. The half-width $\Delta\nu_{\frac{1}{2}}'=0.087\pm0.001$ cm^{-1} for zero concentration of water in air and, $\Delta\nu_{\frac{1}{2}}'=0.107\pm0.001$ cm^{-1} at a concentration of 50 g/m^3 of water. The values of collision diameter are shown in Table VI. The value of the half-width is much smaller than for NH_3 because a water

‡‡‡ The relation between $\Delta\nu_{\frac{1}{2}}$ and collision diameters is $\Delta\nu_{\frac{1}{2}}=\sqrt{2}n_1v_1\rho_1^2+n_2v_{12}\rho_{12}^2$ where n_1 is the molecular density (no. of absorbers per cc) $v_{12}=(v_1^2+v_2^2)^{\frac{1}{2}}$, the root-mean-square velocity of the perturbing molecule with respect to the ammonia molecules, and ρ_{12} the collision diameter of the perturbing gas.

molecule is an asymmetrical top. Its dipole moment will have a fairly small steady component in the two rotational levels between which the transition takes place.

Beringer and others[180] measured the integrated high pressure absorption band of oxygen at 2 cm^{-1} mixed with nitrogen and showed that the half-width at atmospheric pressure should be around 0.04 cm^{-1}, giving a collision diameter 3.8 A.

The effect of various concentrations of foreign gases on the width of the oxygen absorption lines was studied by Anderson, Smith and Gordy[188] by measuring the half-widths of the rotational line ($J=8\rightarrow9$) at a fixed oxygen partial pressure (1.5 mm Hg) and variable total pressure of the mixtures of gases, as shown in Fig. 27. The chosen foreign gases NH_3, N_2O, N_2, and A, represent, respectively, large dipole moment, small dipole moment, large quadrupole moment and electrical inactivity. Since the half-width in Mc of O_2 with O_2 is larger than that with N_2, whose quadrupole moment is expected to be three times larger than that of O_2, the nonresonant quadrupole-quadrupole moment seems to be relatively ineffective in broadening spectral lines.

In general, since the strong long-range forces give an optical collision diameter larger than a kinetic collision diameter with momentum transfer for the corresponding system, we may conclude that collisions take place at most without deflections of flying path. The

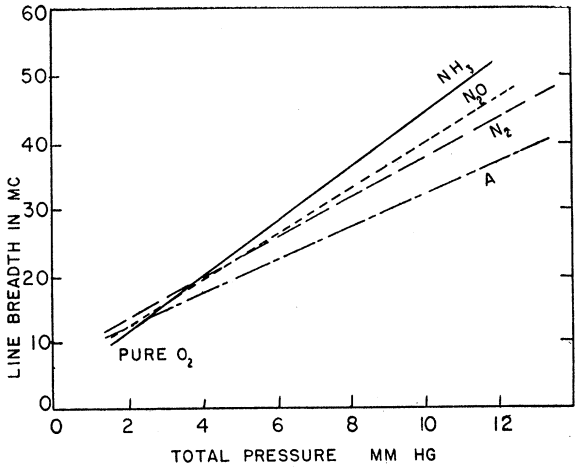

FIG. 27. The broadening of an oxygen line by various foreign gases. $J=8\rightarrow9$. The partial pressure of O_2 is 1.5 mm Hg (after Anderson, Smith, and Gordy[188]).

theory seems to be satisfactory for the system under interactions of such forces. The relations have been used to obtain force constants or quadrupole moments[42,66] as stated in Sec. II. A.2.d.

The authors take great pleasure in acknowledging the encouragement and very valuable criticism of Dr. Henry Margenau, Professor at Yale University, and Dr. R. T. Ellickson, Professor at the University of Oregon, during the preparation of the manuscript.

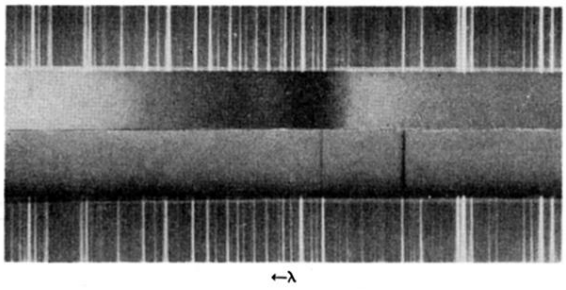

FIG. 1. The red shift and broadening of the blue doublet of Cs produced by argon (after Ch'en and Parker[103]).

Upper spectrum: Argon pressure = 128 atmospheres
Temperature = 262°C
Lower spectrum: Argon pressure = 1.09 atmospheres
Temperature = 150°C.

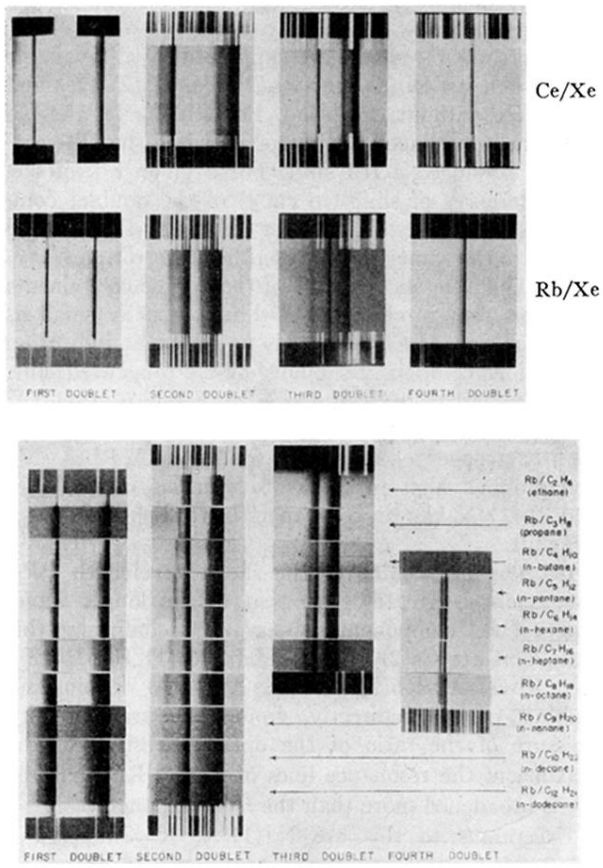

FIG. 16. (a) The red bands of Rb and Cs in the presence of xenon (1) for the resonance lines, (2) for the second doublet, (3) for the third doublet, and (4) for the fourth doublet of the principal series. The corresponding pictures for the fifth doublet showed only some red asymmetry (after Ch'en and Jefimenko[153a,b]). (b) The red bands of Rb in the presence of various paraffin vapors (after Ch'en and Jefimenko[153b]).

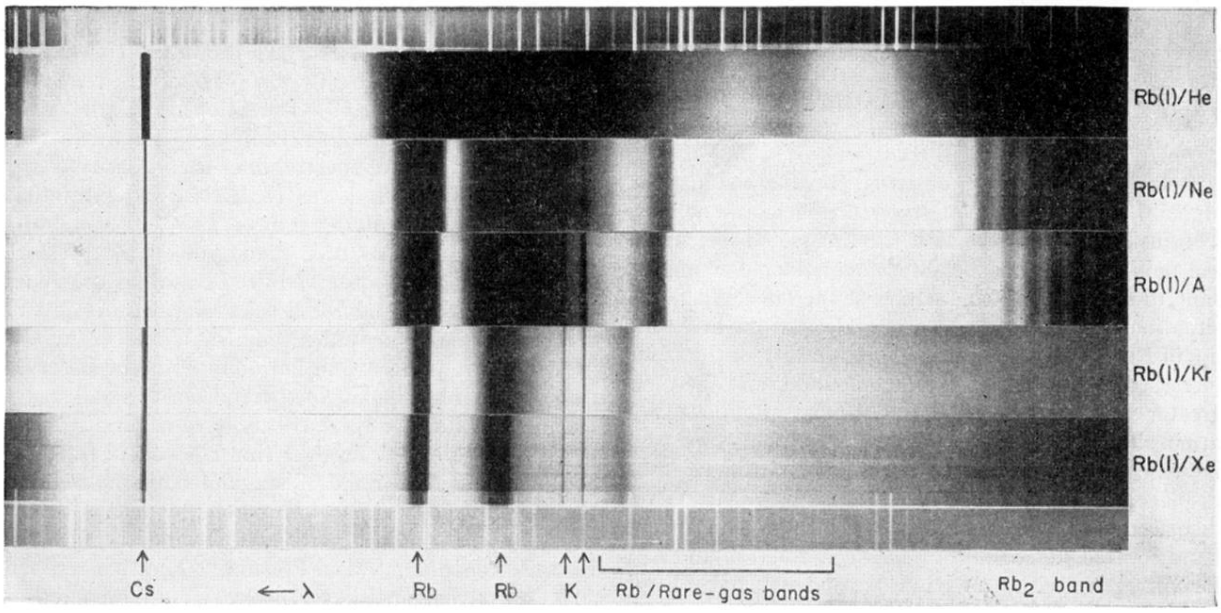

FIG. 18. The violet bands of Rb resonance lines in the presence of rare gases. The lines marked with K and Cs are the respective potassium resonance lines and the shorter wavelength component of cesium resonance lines which appeared as impurities (after Ch'en and Jefimenko[153a]).